https://doi.org/10.15388/vu.thesis.810
https://orcid.org/0000-0001-8478-1294

VILNIUS UNIVERSITY
STATE RESEARCH INSTITUTE CENTER FOR PHYSICAL SCIENCES AND TECHNOLOGY

Touqeer Gill

Characterization and Source Apportionment of Carbonaceous Aerosol in Rural, Urban and Coastal Environments

DOCTORAL DISSERTATION

Natural Sciences,
Physics (N 002)

VILNIUS 2025

This dissertation was written between 2020 and 2024 at State Research Institute Center for Physical Sciences and Technology (Lithuania).

Academic supervisor – Dr. Kristina Plauškaitė-Šukienė, (State Research Institute Center for Physical Sciences and Technology, Natural sciences, physics,N 002)

This doctoral dissertation will be defended in a public meeting of the Dissertation Defence Panel:

Chairman – Dr. Evaldas Maceika (Center for Physical Sciences and Technology, Natural sciences, Physics – N 002).

Members:

Dr. Galina Lujanienė (Center for Physical Sciences and Technology, Natural sciences, Physics – N 002),

Assoc. Prof. Dr. Pauli J. Paasonen (University of Helsinki, Finland, Natural sciences, Physics – N 002),

Dr. Rita Plukienė (Center for Physical Sciences and Technology, Natural sciences, Physics – N 002),

Assoc. Prof. Dr. Vaida Šerevičienė (Vilnius Gediminas Technical University, Technological sciences, Environmental Engineering – T004).

The dissertation shall be defended at a public meeting of the Dissertation Defence Panel at 13 p.m. on 16th September 2025 in meeting room D401 of the Center for Physical Sciences and Technology.

Address: Saulėtekio av. 3, LT-10257 Vilnius, Lithuania

Phone.: +37064515550; e-mail: office@ftmc.lt

The text of this dissertation can be accessed at the libraries of Center for Physical Sciences and Technology and Vilnius University, as well as on the website of Vilnius University: *www.vu.lt/lt/naujienos/ivykiu-kalendorius*

https://doi.org/10.15388/vu.thesis.810
https://orcid.org/0000-0001-8478-1294

VILNIAUS UNIVERSITETAS
VALSTYBINIS MOKSLINIŲ TYRIMŲ INSTITUTAS FIZINIŲ IR TECHNOLOGIJOS MOKSLŲ CENTRAS

Touqeer Gill

Anglingų aerozolio dalelių charakterizavimas ir šaltinio kilmės nustatymas kaimo, miesto ir pakrantės aplinkose

DAKTARO DISERTACIJA

Gamtos mokslai,
Fizika (N 002)

VILNIUS 2025

Disertacija rengta 2020 – 2024 metais Valstybiniame mokslinių tyrimų institute (VMTI) Fizinių ir technologijos mokslų centre (Lietuva).

Mokslinė vadovė – dr. Kristina Plauškaitė-Šukienė (VMTI Fizinių ir technologijos mokslų centras, gamtos mokslai, fizika, N 002).

Gynimo taryba:

Pirmininkas – dr. Evaldas Maceika (VMTI Fizinių ir technologijos mokslų centras, gamtos mokslai, fizika – N 002).

Nariai:

dr. Galina Lujanienė (VMTI Fizinių ir technologijos mokslų centras, gamtos mokslai, fizika – N 002),

asoc. prof. dr. Pauli J. Paasonen (Helsinkio universitetas, Suomija, gamtos mokslai, fizika – N002),

dr. Rita Plukienė (VMTI Fizinių ir technologijos mokslų centras, gamtos mokslai, fizika – N 002),

doc. dr. Vaida Šerevičienė (Vilniaus Gedimino technikos universitetas, technologijos mokslai, aplinkos inžinerija – T 004).

Disertacija ginama viešame Gynimo tarybos posėdyje 2025 m. rugsėjo mėn. 16 d. 13 val. Fizinių ir technologijos mokslų centro D401 auditorijoje. Adresas: Saulėtekio al. 3, LT-10257 Vilnius, Lietuva. Tel.: +37064515550; el. paštas: office@ftmc.lt

Disertaciją galima peržiūrėti Fizinių ir technologijos mokslų centro bei VU bibliotekose ir VU interneto svetainėje adresu:
https://www.vu.lt/naujienos/ivykiu-kalendorius

CONTENTS

ABBREVIATIONS

AAE – Absorption Angstrom exponent coefficient
ACSM – Aerosol Chemical Speciation Monitor
AE31 – Aethalometer
APS – Aerodynamic particle sizer
b_{abs} – light absorption coefficient
BBOA – Biomass burning organic aerosol
BC – Black carbon
BrC – Brown carbon
BC_{TR} – Transport related black carbon
BC_{WB} – Wood burning related black carbon
BC_{FF} – Fossil fuel related black carbon
BC_{BB} –Biomass burning related black carbon
COA – Cooking related organic aerosol
CWT – Concentration-weighted trajectory
EPA – Environmental Protection Agency
eBC – Equivalent black carbon
GAW – Global Atmosphere Watch
HYSPLIT – Hybrid Single-Particle Lagrangian Integrated Trajectory
IA – Inorganic aerosol
LOA – Local organic aerosol
m/z – Mass to charge ratio
$NO_{3(Org)}$ – Organic nitrates
$NO_{3(Inorg)}$ – Inorganic nitrates
NR-PM_1 – Non-refractory submicron particulate matter
OA – Organic aerosol
OOA – Oxygenated organic aerosol
PM – Particulate matter
PMF – Positive matrix factorization
POA – Primary organic aerosol
PMC – Particle mass concentration
PNC – Particle number concentration
QCG – Quezon City Government
RH – Relative humidity
SOA – Secondary organic aerosol
TOF – Time of flight
WCCAP – World Calibration Centre for Aerosol Physics
WMO – World Meteorological Organization's

INTRODUCTION

The Earth's climate system is influenced in complex ways by aerosol particles, including organic, inorganic and carbonaceous components. Higher concentrations of these aerosol particles have a significant impact on the climate in rural, urban and coastal areas. These various aerosols play a crucial role in atmospheric processes that influence weather and affect air quality. To address uncertainties, it is crucial to comprehensively understand the chemical composition, sources, formation, transformations, and dynamic interactions of aerosol particles within the Earth's climate system. Recent studies in Western and Southern Europe have comprehensively characterized aerosol sources, especially in urban and rural areas. Despite this extensive knowledge, the Baltic region, particularly Eastern Europe, has seen limited studies, marking a significant gap in our understanding. The present study aims to fill this gap by presenting a comprehensive, long-term approach focusing on the chemical composition of organic, inorganic and carbonaceous aerosol particles in the rural environment of boreal forests (North-Eastern part) and the urban environment of Lithuania. This includes leveraging local studies and datasets to provide a regional perspective that enhances our understanding of aerosol dynamics in these areas. The objective is to enhance knowledge about pollution seasonality, source variability, and their implications for decision-makers. Similarly, in the Philippines, the research focuses on the critical issue of black carbon (BC) pollution in urban and coastal areas. While previous research has made significant progress in characterizing aerosol particles in terms of size distribution, concentration, and spatial variability, knowledge gaps persist, particularly in understanding BC sources other than road activity and the impact of the Manila Port on aerosol levels. This research aims to provide new insights into these areas, contributing to our understanding of the complex atmospheric mechanisms that regulate aerosol composition and distribution as well as their influence on climate change.

THE MAIN AIM AND TASKS

The objective of this study was to identify the main sources of organic, inorganic, and carbonaceous aerosol particles and compare their properties across rural, urban, and coastal environments.

To achieve this objective, the following tasks were established:

- Characterization of organic, inorganic and carbonaceous aerosol particles in rural, urban and coastal environments.

- Source apportionment of carbonaceous aerosol particles in rural, urban and coastal environments.
- Evaluation of the impact of meteorological conditions on organic, inorganic and carbonaceous aerosol particles in rural, urban and coastal environments.

NOVELTY

A key novelty of this study lies in the comparative analysis carried out in the urban environments of Northern Europe and South Asia, which allowed identification of a consistent relative contribution of brown carbon to carbonaceous aerosol across geographically and climatically distinct regions, despite differences in biomass burning sources driven by seasonal and socioeconomic factors, i.e. domestic heating in Lithuania and agricultural residue burning in the Philippines.

DEFENSIVE STATEMENTS

1. Organic aerosols (OA) were the dominant component across rural, urban, and coastal environments (53 – 80%). Inorganic aerosols (SO_4^{2-}, NO_3^-, NH_4^+, and Cl^-) remained lower than OA throughout the study, indicating a consistent dominance of organics in the composition of atmospheric aerosol particles regardless of environmental differences.

2. Black carbon (eBC) originating from fossil fuel combustion and the transport sector was the dominant source (contributing 80 – 90%) in rural, urban, and coastal environments. In contrast, biomass burning accounted for a significantly lower share (10 – 20%), confirming the larger impact of traffic and fossil fuel sources on eBC levels across different environments.

3. In rural, urban and coastal environments, brown carbon (BrC) accounted for only 14 – 22% of the total composition of carbonaceous aerosol. Biomass burning is the main source of BrC and has a relatively smaller impact on air quality comparing to other dominant of eBC, such as fossil fuel combustion and transport emissions.

4. eBC and BrC concentrations in Northern European urban environment is 14 – 15 times lower than in South Asian urban environments, but the relative contribution of fossil fuel and biomass combustion sources remains similar (4% difference) regardless of geographical location and season of the year.

WORK RELEVANCE

Characterizing the chemical components of atmospheric submicron aerosols in rural, urban, and coastal environments is important due to their adverse effects on human health and their significant influence on the Earth's climate system. Therefore, it is crucial to deepen our understanding of aerosol chemical composition and the pathways of their formation. The results of this study could enhance our understanding of atmospheric chemistry at both local and global scales. Additionally, it highlights the persistent black carbon (BC) pollution in developing regions and calls for scientifically based strategies to mitigate the air quality crisis.

CONTRIBUTION OF THE AUTHOR

The research presented in the original publications 1–4 is an outcome of the author's own ideation and discussions between the author, supervisor, and coauthors. The author had a leading role in designing and performing the analysis of measurement data. The separation of organic and inorganic nitrates, determination of the Absorption Ångström exponent, and application of corrections and interpretations of Aethalometer measurements data were mainly conducted by the author. For these tasks, MATLAB was utilized for its powerful suite of tools suitable for statistical analysis and handling large datasets, particularly useful for matrix operations and visualization. Python was employed for its extensive libraries and frameworks tailored for data science, including NumPy for numerical data processing, Pandas for data manipulation, and Matplotlib and Seaborn for advanced data visualization. R was specifically used for creating open-air plots, leveraging its strong graphical capabilities to effectively communicate complex environmental data patterns. This combination of tools enabled detailed and efficient analysis of aerosol data to uncover patterns and correlations within the dataset. The source apportionment using the PMF model (2) and the analysis of meteorological data by the HYSPLIT model (1, 2, and 4) were performed by co-authors. The findings presented at scientific conferences, publications and dissertation were written by the author in collaboration with the supervisor and other co-authors.

LIST OF PUBLICATIONS

Research results are published in 4 articles:

1. S. Byčenkienė, **T. Gill**, A. Khan, A. Kalinauskaitė, V. Ulevicius, K. Plauškaitė (2023). "Estimation of Carbonaceous Aerosol Sources under

Extremely Cold Weather Conditions in an Urban Environment", Atmosphere 14(2), 310 (IF: 3.11, Q3), https://doi.org/10.3390/atmos14020310.

2. **T. Gill**, J. Pauraitė, A. Kalinauskaitė, S. Byčenkienė, K. Plauškaitė (2024). "Long-term study of chemical characteristics of aerosol compositions in the rural environment of Rūgšteliškis (Lithuania)", Atmospheric Pollution Research, 15(4), 102048, (IF: 4.5, Q2), https://doi.org/10.1016/j.apr.2024.102048.

3. **T. Gill,** S. Kecorius, K. Kandrotaitė, V. Dudoitis, L. Madueño, A. Wiedensohler, L. Poulain, E. A. Vallar, M. Cecilia, D. Galvez, S. Byčenkienė and K. Plauškaitė (2025). "Carbonaceous aerosol particle sources in Manila North Port and urban environment", Oceanologia, (IF: 2.6, Q2), https://doi.org/10.5697/TQCH9343

4. **T. Gill**, A. Kalinauskaitė, V. Dudoitis, S. Kecorius, S. Byčenkienė, K. Plauškaitė (2025). "A 4-Year study of carbonaceous aerosol particle sources in a rural environment of Northern Europe, Lithuania", Atmospheric Pollution Research, 16 (2025), 102428 (IF: 4.5, Q2), https://doi.org/10.1016/j.apr.2025.102428.

OTHER PUBLICATIONS

1. S. Byčenkienė, D. Pashneva, I. Uoginte, J. Pauraitė, A. Minderyte, L. Davuliene, K. Plauškaitė, M. Skapas, V. Dudoitis, **T. Gill**, J. Andriejauskiene, V. Araminiene, E. Dzenajaviciene, P. Sicardd, V. Gudynaitė-Franckeviciene, I. Varnagirytė-Kabasinskiene, N. Pedišius, E. Lemanas, T. Vonžodas (2021). "Evaluation of the anthropogenic black carbon emissions and deposition on Norway spruce and silver birch foliage in the Baltic region", Environmental research, 207, 1 – 10, (IF: 8,431; Q1),https://doi.org/10.1016/j.envres.2021.112218.

LIST OF CONFERENCES

The dissertation material was presented at 15 conferences:

1. **Touqeer Gill**, Simonas Kecorius, Kamilė Kandrotaitė, Vadimas Dudoitis, Leizel Madueno, Alfred Wiedensohler, Steigvilė Byčenkienė and Kristina Plauškaitė, Chemical Characterization of Submicron Aerosol In Metro Manila, Philippines, 67th International Conference for Students of Physics and Natural Sciences, Open Readings 2024, 23-26th of April, 2024, Vilnius, Lithuania. Poster presentation.

2. **Touqeer Gill**, Simonas Kecorius, Kamilė Kandrotaitė, Vadimas Dudoitis, Leizel Madueno, Alfred Wiedensohler, Steigvilė Byčenkienė and

Kristina Plauškaitė, Characterizing carbonaceous aerosol origins in Metro Manila, Philippines: A Comparative Study at Two Sites, 45th Lithuanian National Physics Conference (LNFK-45 2023) National center for physical sciences & technology, 25-27th October, 2023, Vilnius, Lithuania, Poster presentation.

3. **Touqeer Gill**, Simonas Kecorius, Kamilė Kandrotaitė, Vadimas Dudoitis, Leizel Madueno, Alfred Wiedensohler, Steigvilė Byčenkienė and Kristina Plauškaitė, Carbonaceous aerosol particle sources In Manila North Port and Urban Environment, (FizTech 2023) 18-19th October 2023, Vilnius, Lithuania. Oral presentation.

4. **Touqeer Gill**, Julija Pauraitė, Steigvilė Byčenkienė and Kristina Plauškaitė, A 5-Year correlation study of submicron organic aerosols and temperature in rural-forestry environment. European Aerosol Conference (EAC 2023), 3-8th September, 2023, Malaga, Spain, Poster presentation.

5. **Touqeer Gill**, Simonas Kecorius, Kamilė Kandrotaitė, Vadimas Dudoitis, Leizel Madueno, Alfred Wiedensohler, Steigvilė Byčenkienė and Kristina Plauškaitė, Estimation of carbonaceous aerosol particle sources at two locations In Metro Manila, Philippines, 66th International Conference for Students of Physics and Natural Sciences, (Open Readings 2023), 18-21st April, 2023, Vilnius, Lithuania. Poster presentation.

6. **Touqeer Gill**, Vadimas Dudoitis, Abdullah khan, Kamilė Kandrotaitė, Agnė Minderytė, Simonas Kecorius, Julija Pauraitė, Steigvilė Byčenkienė and Kristina Plauškaitė, Evaluation of the aerosol chemical composition at two Manila mega-city sites, Philippines. (FizTech 2022) 19-20th October 2022, Vilnius, Lithuania. Oral presentation.

7. **Touqeer Gill**, Julija Pauraitė, Steigvilė Byčenkienė and Kristina Plauškaitė, A 5-Year correlation study of submicron organic aerosols and temperature in rural-forestry environment. International Aerosol Conference (IAC 2022), 4-9th September, 2022, Athens, Greece. Poster presentation.

8. Abdullah Khan, Muhammad Afzaal, Steigvilė Byčenkienė, **Touqeer Gill**, and Muhammad Bilal Concentrations of airborne PM_{10} and lead in major bus terminals of Lahore and Peshawar, Pakistan, 65th International Conference for Students of Physics and Natural Sciences, (Open Readings 2022), 15-18th March, 2022, Vilnius, Lithuania. Poster presentation.

9. **Touqeer Gill**, Julija Pauraitė, Steigvilė Byčenkienė and Kristina Plauškaitė, Correlation study of 5-Years submicron organic aerosols with temperature in the rural environment, 65th International conference for students of physics and natural sciences, (Open Readings 2022), 15-18th March, 2022, Vilnius, Lithuania. Oral presentation.

10. **Touqeer Gill**, Julija Pauraitė, Steigvilė Byčenkienė and Kristina

Plauškaitė, Investigation of 5-Years submicron organic aerosol composition in Rūgšteliškis (Lithuania) rural environment. (FizTech 2021), 20-21st October 2021, Vilnius, Lithuania. Oral presentation.

11. **Touqeer Gill**, Julija Pauraitė, Steigvilė Byčenkienė and Kristina Plauškaitė, Variability of aerosol main chemical components in Lithuanian rural environment: a 5-years study, American Association for Aerosol Research (AAAR 2021) Albuquerque Convention Center. 18-21st October 2021, Albuquerque, New Mexico, Poster presentation.

12. **Touqeer Gill**, Julija Pauraitė, Steigvilė Byčenkienė and Kristina Plauškaitė, Chemical composition of submicron organic aerosol in rural environment: a long-term study, 44th Lithuanian National Physics Conference (LNFK44 2021) National center for physical sciences & technology, 6-8th October, 2021, Vilnius, Lithuania, Poster presentation.

13. **Touqeer Gill**, Julija Pauraitė, Steigvilė Byčenkienė and Kristina Plauškaitė, Submicron organic aerosol composition in a rural environment: 5-years study of high temporal-resolution chemical composition measurements. European Aerosol Conference (EAC 2021), 30th August to 3rd September, 2021, Birmingham, UK, Poster presentation.

14. **Touqeer Gill**, Julija Pauraitė, Steigvilė Byčenkienė and Kristina Plauškaitė, 5-Years ACSM data of aerosol main chemical Components in Rūgšteliškis (Vilnius) rural Environment, 17th International Conference of Young Scientists on Energy and Natural Sciences Issues (CYSENI 2021), 24-28th May, 2021, Vilnius, Lithuania, Poster presentation.

15. **Touqeer Gill**, Julija Pauraitė, Steigvilė Byčenkienė and Kristina Plauškaitė, Long term submicron aerosol chemical characterization in Rūgšteliškis (Lithuania) rural environment, 64th International Conference for Students of Physics and Natural Sciences, (Open Readings 2021), 16-19th March, 2021, Vilnius, Lithuania, Poster presentation.

1 LITERATURE REVIEW

1.1 Causes of climate change in rural, urban and coastal environment

Climate change is one of mostly pressing global crises of our time and has profound impacts on rural, urban and coastal environments, and organic, inorganic and carbonaceous aerosol particles are one of the main players (Kantamaneni et al., 2023). The impacts of atmospheric pollution are diverse and include shifts in weather patterns, sea level rise, and disruption to biodiversity and human settlements (Pathak et al., 2023; Pal et al., 2022). Understanding how aerosols affect atmospheric processes in different geographical locations is crucial for developing effective mitigation and adaptation strategies. However, despite the increasing number of studies on regional climate effects, there is still uncertainty regarding the regional impacts of aerosols, particularly in North-Eastern Europe and Southeast Asia, where data availability is limited. In rural regions, climate change is often reflected in changes in agricultural productivity and water resources. Shifts in temperature and precipitation patterns have a direct impact on crop yields, biodiversity and the occurrence of pests and diseases (Atkinson et al., 2023). Rural areas are highly dependent on natural resources, and disruptions to these resources can lead to severe socio-economic consequences. Biomass burning, fossil fuel combustion, deforestation, and livestock grazing are major contributors to atmospheric pollution and radiative forcing in rural areas. Biomass burning, in particular, releases large amounts of carbonaceous aerosols, including black carbon and organic carbon, which can significantly alter atmospheric radiation balance (Rusmayandi et al., 2023). Additionally, long-distance transportation of air pollutants affects even remote rural areas, contributing to atmospheric degradation. Soil degradation, largely driven by deforestation and unsustainable agricultural practices, also reduces the soil's ability to act as a carbon sink, further exacerbating greenhouse gas emissions. Despite extensive research on these climate drivers, there is still limited knowledge on the long-term impact of rural aerosols on climate dynamics and their interaction with regional meteorology. This study seeks to address this gap by investigating the seasonal variations of organic and carbonaceous aerosols in rural environments and their potential influence on climate processes. Urban areas experience the "urban heat island" effect, a prime example of how built environments alter local climate and energy balance (Pathak et al., 2023). This occurs when cities experience significantly higher temperatures than nearby rural areas due to human activities and the prevalence of surfaces that absorb and retain heat. Factors such as increased energy use, high greenhouse gas emissions and extensive deforestation

contribute to this warming trend. Research indicates that the thermal characteristics of urban materials can influence local microclimates, impacting both energy equilibrium and weather patterns within cities (Morais et al., 2019). Urban air pollution worsens the effects of atmospheric changes and poses health risks to the public, including heat related illnesses and respiratory problems caused by poor air quality (Tewari et al., 2023). Pollutants such as aerosols, nitrogen oxides, and volatile organic compounds from industrial and transportation sources not only degrade air quality but also influence cloud formation and weather patterns. For example, aerosols can impact the planet's reflectivity (albedo), resulting in either cooling or warming effects depending on their properties (Christensena et al., 2020). Although numerous studies have been carried out on urban air pollution in highly industrialized regions, less attention has been given to North-Eastern Europe and developing countries in Southeast Asia, particularly regarding black carbon emissions from traffic, industrial activities, and biomass burning. The role of black carbon in urban warming is still debated, with uncertainties surrounding its radiative forcing and contribution to extreme weather events. This research seeks to improve understanding of urban black carbon emissions, their seasonal variations, and their contribution to air quality deterioration and climate-related impacts. Coastal areas are dealing with specific challenges caused by environmental changes, such as the increasing sea levels, stronger storms and saltwater intrusion into freshwater systems (Pathak et al., 2023; Pal et al., 2022). These changes pose threats to the infrastructure, ecosystems and communities along the coast. The increasing sea levels are linked to melting ice caps and warmer ocean temperatures, directly impact lower lying areas through floods and erosion (Grases et al., 2020). Furthermore, anthropogenic emissions from ships, boats, cranes and cargo trucks have a significant impact on coastal environments by contributing to air and water pollution that adds pressure on these delicate ecosystems (Karl et al., 2023; Jang et al., 2023; Schwarzkopf et al., 2022). Additionally, coastal ecosystems like mangroves, coral reefs and salt marshes are particularly at risk due to climate change. These ecosystems play vital roles in capturing carbon dioxide and act as barriers against storm surges and erosion (Segaran et al., 2023; Hulsen et al., 2023). However, their decline due to rising sea temperatures and salinity changes reduces their ability to sustain marine biodiversity and protect coastal communities (Röthig et al., 2023). Despite ongoing conservation efforts, there is a lack of quantitative data on how aerosol pollution from shipping and industrial activities affects these fragile ecosystems. This study will investigate black carbon concentrations in coastal areas and their potential role in modifying regional climate and air quality. Although previous studies

have investigated the impact of aerosols on atmospheric processes, significant uncertainties remain regarding the role of carbonaceous aerosols in climate forcing. The extent to which black carbon contributes to warming or cooling remains debated, particularly in coastal and urban areas where multiple pollution sources interact. Additionally, while urban air pollution has been extensively studied in Western cities, fewer studies focus on Eastern Europe and Southeast Asia, where biomass burning, traffic, and ship emissions contribute significantly to black carbon levels. Carbonaceous aerosols play a significant role in climate forcing, making it essential to study their spatial and seasonal variations across different environments. This study aims to address existing knowledge gaps by providing long-term observational data on black carbon and brown carbon in rural, urban, and coastal regions. By analysing aerosol composition, seasonal trends, and meteorological impact, this research will contribute to a better understanding of how aerosols impact climate and air quality in regions that have been underrepresented in previous studies.

1.2 Atmospheric particulate matter

The emergence of aerosol science as a distinct field can be traced back to the post-World War II period. This interdisciplinary science draws on the expertise of scientists hailing from diverse research domains including meteorology, physics, engineering, chemistry, mathematics, and more. The collaborative efforts of these experts have laid the foundation for the evolution of aerosol science over time. Within the sphere of atmospheric sciences, the term 'aerosol' originates from the Greek 'aero', meaning air, and 'solution' (solutio, -onis), referring to suspension. It pertains to solid and/or liquid particles suspended within an air mass, excluding clouds and precipitation droplets (Lushnikov et al., 2010), commonly categorized as hydrometeors. Both natural and anthropogenic sources release primary particulate matter into the atmosphere, shaping aerosol attributes like size, density, and surface properties (Table 1 and Table 2). This assortment of primary sources and the diverse mechanisms of secondary aerosol formation yield particulate matter (PM) composed of distinct origin particles with varying compositions and granulometric distributions. The chemical composition, size, and number of the particles can change due to different processes (Pöschl et al., 2005). Some of these include nucleation (homogeneous and heterogeneous), coagulation, and adsorption/desorption. Following their evolution, they can be removed out of the atmosphere through either dry or wet deposition or through heterogeneous chemistry (in-cloud scavenging or below-cloud scavenging). These removal mechanisms are critical in determining the atmospheric

lifetime of aerosols, which can range from a few hours for coarse particles to several weeks for fine particles. Particles can vary in size, spanning from a few nanometres to several tens of microns (Fig. 1 and Table 3). Size plays a pivotal role in defining how aerosols behave. The majority of features related to aerosols, along with the mechanisms that control these features and their effects, are closely tied to the size of the particles (Seinfeld and Pandis, 2012). The lognormal function is commonly used to characterize size distributions, providing a suitable match for a diverse range of real-world data (Castro et al., 2010; and Calvo et al., 2013). Aerosols' chemical, microphysical, and optical characteristics wield influence over a range of consequences, encompassing effects on human health, global climate, occurrence of acid rain, ecosystems equilibrium, visual clarity, and the durability of building materials (Costa et al., (2009); Katul et al., (2011); Schleicher et al., (2011); Yuan et al., (2011)). Due to the diverse fields affected by particulate matter, it becomes imperative to manage aerosol concentrations and establish thresholds, particularly to safeguard human well-being and the broader environment. Consequently, numerous governments worldwide have implemented maximum standards. In the European context, the prevailing regulation 2008/50/CE introduced the regulation of $PM_{2.5}$ fraction (particles with an aerodynamic diameter < 2.5 μm), acknowledging its health implications. Despite existing regulations, many regions, especially in developing countries, continue to experience PM concentrations that exceed safe limits, emphasizing the need for stronger emission controls and regional air quality assessments. Significant gaps persist in understanding aerosol radiative effects, source attribution, and aerosol-cloud interactions, which hinder accurate climate projections. A comprehensive understanding of aerosols including their sources, composition, and transport is crucial for developing effective mitigation strategies. This study addresses these gaps by analysing carbonaceous aerosols in diverse environments, providing insights to improve air quality management and climate models in underrepresented regions.

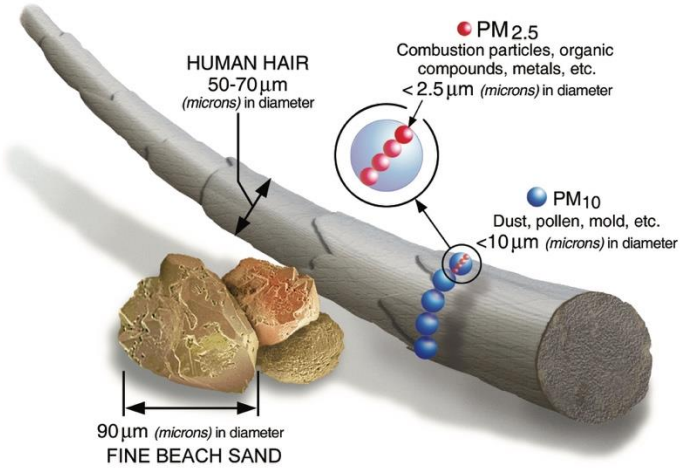

Fig. 1. Illustration that puts the size of PM_{10} and fine particulate matter, $PM_{2.5}$, into perspective (Morris, 2022).

Table 1. Inorganic marker elements associated with various emission sources or processes (Calvo et al., 2013).

Secondary aerosols		SO_4^{2-}, NO_3^-, NH_4^+
Sea salt		C1, Na, Na^+, Cl^-, Br, I, Mg and Mg^{2+}
Crustal or geological tracers		Elements associated with feldspars, quartz, micas and their weathering products (mostly clay minerals), i.e. Si, Al, K, Na, Ca, Fe and associated trace elements such as Ba, Sr, Rb, and Li. In addition, there will be accessory silicates (notably zircon, titanite and epidote), and representatives from the minority non-silicate mineral groups, namely carbonates, sulphates, oxides, hydroxides and phosphates.
Technogenic tracers	Steel industry	Cr, Ni and Mo
	Copper metallurgy	Cu and As
	Ceramic industries	Ce, Zr and Pb
	Heavy industry (refinery, coal mine, power stations)	Ti, V, Cr, Co, Ni, Zn, As and Sb
	Petrochemical industry	Ni and V
	Oil burning	V, Ni, Mn, Fe, Cr, As, S and SO_4^{2-}
	Coal burning	Al, Sc, Se, Co, As, Ti, Th, S, Pb and Sb
	Iron and steel industries	Mn, Cr, Fe, Zn, W and Rb
	Non-ferrous metal industries	Zn, Cu, As, Sb, Pb and Al
	Cement industry	Ca
	Refuse incineration	K, Zn, Pb and Sb
	Biomass burning	K and Br
	Firework combustion	K, Pb, Ba, Sb and Sr
	Vehicle tailpipe	Platinum group elements, Ce, Mo and Zn
	Automobile gasoline	Ce, La, Pt, SO_4^{2-} and NO_3^-
	Automobile diesel	S, SO_4^{2-} and NO_3^-
	Mechanical abrasion of tyres	Zn
	Mechanical abrasion of brakes	Ba, Cu and Sb

Table 2. Main organic aerosol constituents and their associated sources and formation pathways. Symbol "✓" indicates confirmed associations, and "?" indicates potential or uncertain associations (Calvo et al., 2013).

	Primary					**Secondary**		
	Fossil fuel Combustion (e.g Vehicles)	Other anthropogenic process (e.g. manufacturing, cooking)	Biogenic (e.g. vascular waxes and bioparticles (e.g. spores)	Biomass burning	Soil	Gas particle partition (adsorption and absorption)	Reactive condensation (e.g. acid catalysed reactions)	In-cloud processing
Alkanes, alkenes, alkanals, alkanoic acids, diacids	✓	✓	✓	✓	✓	✓		**?**
Aromatics, PAHS	✓	✓		✓	✓	✓	**?**	**?**
Hopanes, steranes, unresolved complex mixture (UCM)	✓							
Photochemical products (e.g. carbonyls, methyl tetrols, carboxylic acids, organo sulphates)						✓	✓	✓
Sugars, polyols, polysaccharides			✓	✓	✓			
Levoglucosan				✓				
HULIS					**?**		**?**	**?**

Table 3. Size classification of some typical atmospheric particles by diameters (Tasić et al., 2006).

Diameter	Examples
Very small (0.01 to 5 μm)	Paint pigments, Tobacco Smoke, Dust, Sea-Salt particles.
Larger (5 to 100 μm)	Cement dust, wind-blown soil dust, Foundry dust, Pulverized coal, Milled Flower.
Liquid Mist (5 to 10,000 μm)	Fog, Smog, Mist, Raindrops.
Of Biological Origin (0.001 to 0.01 μm)	Viruses, Bacteria, Pollen, Spores.
Of Chemical Formation (0.001 to 100 μm)	Atmospheric sulphur dioxide oxidizes producing sulfuric acid; the acid attracts Atmospheric water forming small droplets (haze). Metal oxides form when Fuels that contain Metals are burned.

1.3 Chemical composition of aerosols

1.3.1 Organic aerosols

Particulate matter (PM) consists primarily of organic compounds that were adsorbed onto particles. Airborne particles contain a diverse range of organic chemical molecules (olefins, aldehydes, ketones, nitro-compounds, quinones, etc.). Quinones (1,2- and 1,4-napthoquinones, 9,10-anthraquinone, etc.) are toxicologically significant because they can produce reactive oxygen species (ROS) by redox cycling (Ciarelli et al., 2019). According to Marmureanu et al., (2020) soot particles retain the characteristic organic species associated with their sources (e.g., benzoquinone, phenolic groups); however, ageing processes such as ozone reaction can rapidly erase these fingerprints. Heikkinen et al., (2020) investigated the possibility that the oxidation of primary volatile organic species may also produce low-volatility chemicals, which condense on the surfaces of primary particles. The secondary organic aerosol (SOA) species may account for the majority of carbonaceous PM mass in both urban and rural areas (Keskinen et al., 2020).

1.3.2 Inorganic aerosols

1.3.2.1 Nitrates

The majority of nitrogen compounds are secondary in origin, resulting from the reactivity of both naturally occurring and man-made gaseous precursors. The two primary nitrogen compounds found in atmospheric particulate matter are NH_4^+ and NO_3^-. Nitric acid is the principal by product of atmospheric oxidation, and the principal precursor gases released by human and natural sources are NO, NO_2, N_2O, and NH_3 (Huang et al., 2021). In cities, traffic is the primary source of nitrogen oxides, which serve as the molecular building blocks for nitrogen compounds (Crippa et al., 2013). According to Seinfeld and Pandis., (2012), the primary sources of natural nitrogen compounds include electrical discharges (NO), wildfires (NO_2, NO), soil emissions (nitrification, N_2O), and biogenic emissions (NH_3). In normal conditions, the ammonia in the atmosphere combines with the gaseous nitric acid dissolved in liquid microparticles to generate particulate ammonium nitrate (Bauer et al., 2007). Due to the greater vapour pressure of NH_3 and HNO_3^- (Crippa et al., 2013), ammonium nitrate is unstable and essentially volatilizes at temperatures over 20°C, reverting to gaseous nitric acid.

Organic nitrates can be formed by the oxidation of volatile organic compounds (VOCs) by hydroxyl radicals in the presence of NO and sunlight during the day and by nitrate radicals during the night (Fig. 2) (Scharr et al.,

2016; Sobanski et al., 2017). The products of these reactions include peroxynitrates ($RO2NO_2$) and alkyl and multifunctional nitrates ($RONO_2$) (Eq.1) (Retama et al., 2019). Peroxynitrates are thermally unstable and decompose back to NOx within minutes to days at warm temperatures (Eq.2) (Huang et al., 2020; Lee et al., (2016)).

Inorganic nitrates primarily form through distinct pathways influenced by diurnal variations. The predominant pathways include the hydroxyl radical-mediated oxidation of nitrogen dioxide (NO_2) during the day and the heterogeneous reactions involving dinitrogen pentoxide (N_2O_5) during the night (Ayres et al., 2015); Calvo et al., 2013). Other pathways leading to the formation of inorganic nitrate include the hydrolysis of organic nitrate, heterogeneous reactions between N_2O_5 and particulate chloride (Cl^-), direct oxidation of NO to HNO_3 by HO_2, and the hydrogen-abstraction of hydrocarbons by nitrate radicals (NO_3) (Eq.3) (Alexander et al., 2020); Vieno et al., 2014). The relative partitioning of inorganic nitrate depends on temperature, aerosol chemical composition, aerosol abundance, and aerosol liquid water content. It divides into the gas $HNO_{3(g)}$ and particle (NO_3) phases. The formation of inorganic nitrate, occurring as both HNO_3(g) and particulate NO3, serves as the predominant sink for NOx globally. High-resolution aerosol mass spectrometry facilitates the calculation of inorganic nitrates (Yan et al., 2019).

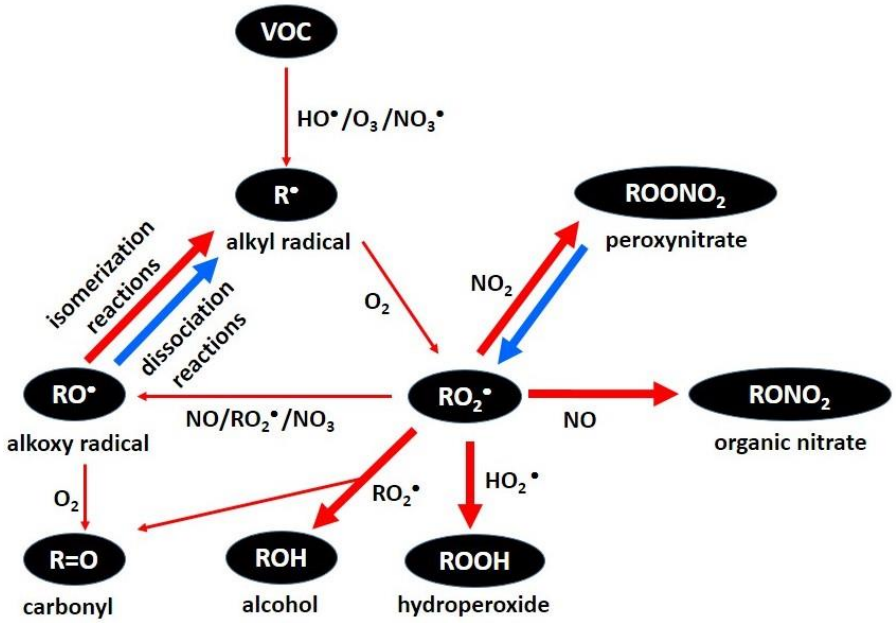

Fig. 2. A simple non-photochemical oxidation mechanism for a typical volatile

organic compound (VOC) (Pillar et al., 2018).

$$NO_3 + BVOC \longrightarrow RONO_2 + \text{Other products} \quad (1)$$

$$NO_3 + O_3 \longrightarrow NO_3 \longrightarrow \text{Organonitrates} \longleftrightarrow \text{Organonitrates nitrates} \quad (2)$$

$$NO_3 + OH \longrightarrow HNO_3 \xrightarrow{\text{Aerosol surface}} \text{Inorganic nitrates} \quad (3)$$

1.3.2.2 Ammonium

Ammonia (NH_3), emitted in large quantities from industry and agriculture, can partly neutralize particulate sulphuric acid, forming ammonium sulphate, which is acknowledged to be one of the main contributors to submicrometric aerosol mass. Agricultural activities such as land fertilization are the main source of atmospheric ammonia. In addition, ammonium nitrate, formed from the reaction between ammonia and nitric acid, is a common inorganic PM constituent (Heikkinen et al., 2020). In recent years, several studies focused on the origin of ammonium in the atmosphere. Jiang et al., (2019) and Drugé et al., (2019) investigated that ammonium aerosols such as ammonium nitrate (NH_4NO_3) and ammonium sulphate ($(NH_4)_2SO_4$) are produced by the neutralization of nitric acid (HNO_3) and sulphuric acid (H_2SO_4) with ammonia (NH_3) (Allen et al., 2019).

1.3.2.3 Sulphur

Sulphate particles, consisting of sulphur-containing airborne particles, form from gas-phase precursors, ranging in size up to 0.1μm (Saliba et al., 2020). These particles, primarily secondary pollutants, originate from the oxidation of sulphur dioxide (SO_2) emitted mainly by coal-fired power plants. In the atmosphere, sulphur dioxide transforms into sulphate (SO_4) at a rate of 0.1 – 5% per hour, a process expedited by higher temperatures, solar radiation, and oxidants (Huang et al., 2020). Further interactions with water vapour may produce sulphuric acid (H_2SO_4), a corrosive acid that is harmful to ecosystems and humans, as well as ammonium sulphate $(NH_4)_2SO_4$, which is especially effective at obstructing visibility. Fossil fuels combustion, which releases sulphur dioxide (SO_2) and nitrogen oxides (NO_x), by-products of the conversion of sulphur and nitrogen, respectively. Sulphuric acid, nitric acids, and peroxyacetyl nitrates (PANs) are produced when these species react with

OH radicals (during the day) and ozone (at night) in the atmosphere (Hao et al., 2014; Wang et al., 2016). Sulphate particles have a long residence life in the atmosphere, 2 – 10 days, allowing for them to travel hundreds or thousands of kilometres at a regional or continental scale. Acid rain occurs when relatively soluble sulphate particles are washed out by precipitation (Zhao et al., 2015). Sulphate concentration in rural areas of Europe is generally below 5 $\mu g/m^3$ (Kanawade et al., 2020).

1.3.2.4 Chloride

Chloride aerosols are a large component of atmospheric particulate matter and play essential functions in the chemistry of the troposphere. They are widely distributed in different chemical variations, as well as having different sizes and geographical locations (Crippa et al., 2013). In oceanic and seaside regions, sea salts, which are dominated by sodium chloride (NaCl), contribute a large concentration of chloride aerosols. In woodland, grassland, and agricultural areas, chloride aerosols come from potassium chloride (KCl) and are released by biomass burning. Chloride aerosols participate in tropospheric chemistry via reactions with strong acids or acid anhydrides (Wang et al., 2017). Earlier field experiments by Ng et al., (2017) have shown that particulate phase chlorides such as sodium chloride and potassium chloride react with sulfuric acid and/or nitric acid to generate gas-phase HCl, which subsequently interacts with NH_3 to make ammonium chloride or with dust to form chloride dust. Wang et al., (2016), confirmed that particulate-phase chlorides (such as sodium chloride and potassium chloride) react with sulfuric acid and/or nitric acid to generate gas-phase HCl, which then reacts with NH_3 to form ammonium chloride or with dust to form chloride dust. Wang et al., (2016), discovered that heterogeneous N_2O_5 reactions on chloride aerosols produce $ClNO_2$, which supplies Cl atoms. Various field experiments have demonstrated that a significant fraction of marine salts contains sulphates and nitrates (Lee et al., 2016; Wang et al., 2017). In addition, Jimenez et al., (2009), found that secondary particulate chlorides (produced from gas-phase HCl) were internally mixed with dust particles in long-range transport dust plumes over the Pacific.

1.3.2.5 Carbonaceous Aerosols

Carbonaceous aerosols are the main constituents of particulate matter ($PM_{2.5}$) and can pose a challenge to the urban environment due to their variable chemical and physical properties and their origin from a variety of pollution

sources (Oh et al., 2020). Carbonaceous aerosols have negative impacts on air quality and human health (Ouidir et al., 2021). Carbonaceous $PM_{2.5}$, which consists of organic carbon (OC), elemental carbon (EC) and water-soluble ions, poses a greater health risk compared to inorganic $PM_{2.5}$, such as nitrate, sulphate and ammonia (Cao et al., 2003; Ancelet et al., 2013; Zou et al., 2022). Carbonaceous aerosols, account for 20 – 70% of atmospheric aerosols, play a crucial role in the formation of haze, deterioration of visibility, adverse health effects and atmospheric warming. OC, which is divided into primary organic aerosol (POA) and secondary organic aerosol (SOA), is an important component released from both fossil and non-fossil sources such as coal combustion, automobile exhaust, biomass burning, vegetation emissions and cooking (Pachauri et al., 2013). The light-absorbing fractions of carbonaceous aerosols are usually elemental carbon (EC) (when measured by thermo-optical methods) and black carbon (BC) (when quantified by light absorption methods) (Safai et al., 2014). OC is the major contributor to carbonaceous aerosols, accounting for about 90 %, while EC accounts for a relatively small fraction of about ≤10 % (Bist et al., 2015). Due to its graphite-like structure, EC mainly contributes to light absorption, while OC is a mixture of thousands of particulate organic compounds, including polycyclic aromatic hydrocarbons (PAHs), polychlorinated dibenzo-p-dioxins, dibenzofurans (PCDD/Fs) and other hazardous components that can harm human health and increase morbidity and mortality (Pani et al., 2020; Lin et al., 2019). Recently, there has been a growing emphasis on BrC, an intriguing organic component that absorbs light and accounts for 20 – 40% of the total light absorption in aerosols. Research results indicates that +0.1 to +0.6 W/m^2 is the range of radiative forcing for BrC (Jo et al., 2016; Bali et al., 2024). Moreover, Zhang et al., (2020) found that BrC may be a more significant heating source in the free troposphere than BC. Furthermore, Lee et al., (2017) found that BC might be internally mixed with up to 20% of OA and some secondary inorganic aerosols. The "lensing effect" is a type of internal mixing that increases light absorption by 0.29–0.39 W/m^2 (Saleh et al., 2015). BrC, a subset of organic aerosols, contributes to atmospheric warming by absorbing UV–Visible radiation (Wang et al., 2019). Brown carbon deposition on snow and glaciers after long-range air transport lowers albedo, speeds up snowmelt, and affects water resources (Wu et al., 2020). Furthermore, the interaction of BrC with plants can influence photosynthesis and respiration processes, potentially releasing CO_2 back into the atmosphere. This can contribute to global warming and have significant impacts on the yield and quality of agricultural crops (Yan et al.,2020). In addition to its impacts on climate, brown carbon has been found to encapsulate heavy metals and persistent organic pollutants (POPs),

reducing their exposure to photocatalytic and ageing processes. While this encapsulation reduces the degradation of these pollutants, it paradoxically increases their persistence and potentially amplifies their harmful effects on human health (Yan et al.,2020). Therefore, it's critical to increase our knowledge of BrC sources, atmospheric processes, and potential. Although previous studies have extensively examined organic and inorganic aerosols, there is still limited understanding of how they transform under different environmental conditions. For example, while organic nitrates and secondary organic aerosols (SOAs) have been identified as major contributors to PM, their formation mechanisms in rural, urban, and coastal regions remain insufficiently understood. This research aims to bridge this gap by analysing chemical transformations using multi-site data, offering insights into the regional specificity of aerosol processes.

1.4 Main aerosol sources in rural environment

Rural environments contribute significantly to atmospheric aerosol concentrations through both anthropogenic and natural sources. These emissions influence air quality, climate change, and human health, making their characterization essential for developing effective mitigation strategies. Among the major aerosol sources in rural settings, biomass burning and biogenic emissions play dominant roles.

1.4.1 Biomass burning

Biomass burning stands out as a significant source of aerosols in rural environments, exerting substantial impacts on air quality, human health, and the broader climate system. In rural areas, where traditional cooking practices and agricultural activities often prevail, biomass burning releases a complex mixture of pollutants into the atmosphere, including particulate matter (PM), carbon monoxide (CO), volatile organic compounds (VOCs), and nitrogen oxides (NOx) (Zárate et al., 2005). Biomass burning has a significant influence not only in its immediate vicinity but also stretches to places located thousands of kilometers from its source (e.g. 220 – 13,500 Tg CO_2 yr^{-1}, 120 – 680 Tg CO yr^{-1}, ~38 Tg $PM_{2.5}$ yr^{-1}) (Alves et al., 2011b). Biomass burning, a prevalent ecological phenomenon, occurs under varying environmental conditions. Factors such as humidity levels, wind patterns, and fuel moisture content play a vital role in shaping the intensity and extent of these fires (Alves et al., 2011a). These conditions can lead to the release of a diverse range of pollutants, including greenhouse gases and particulate matter, impacting both local air quality and global climate (Alves et al., 2011b). The intricate

interplay between these conditions underscores the need for comprehensive understanding and effective management strategies to mitigate the far-reaching consequences of biomass burning (Janhäll et al., 2010). Biomass burning aerosols are primarily composed of carbonaceous compounds, including organic carbon (OC) and elemental carbon (EC), alongside various inorganic constituents such as potassium, ammonium, sulphate, and nitrate (Reid et al., 2005b). The inorganic fraction, largely composed of insoluble dust and ashes, contributes to the overall aerosol composition (Janhäll et al., 2010). Moreover, a substantial segment of the organic fraction, encompassing approximately 40 – 80%, exhibits water solubility and contains acidic components. Particularly, levoglucosan serves as a distinctive marker originating from the decomposition of cellulose (Alves et al., 2011a). However, the atmospheric aging sequence could potentially trigger the degradation of levoglucosan, potentially resulting in the underestimation of primary smoke origins attributable to biomass burning (Holden et al. 2011). From biomass burning emitted particles predominantly belong to the accumulation mode, exhibiting a count median diameter of 100 – 150 nm (Badarinath et al., 2009). A smaller coarse mode (2.5μm to 10μm), contains constituents like dust, carbon aggregates, ash, and unburnt fuel residues (Hungershoefer et al., 2008). Occasionally, a nucleation mode is also observed, introducing further complexity to particle sizes (Janhäll et al., 2010). Understanding these size variations is crucial for determining particle transport lifetimes, deposition processes, and climate effects (Janhäll et al., 2010). In Lithuania, research has elucidated the significant impacts of biomass burning on air quality and climate. The study of Svazas et al., (2021), have established specific emission factors for pollutants such as carbon monoxide, nitrogen oxides, and particulate matter from residential and agricultural biomass combustion. Furthermore, the inclusion of biomass burning aerosols in climate models has revealed their negative direct radiative forcing effects, altering regional radiative balances and, consequently, climate patterns (Byčenkienė et al., 2019, 2023). Studies also indicate that biomass usage for energy, particularly from forests, raises concerns regarding soil degradation and biodiversity loss (Kabašinskienė et al., 2019), with urban areas experiencing higher concentrations of black carbon due to biomass combustion for heating (Pauraitė et al., 2015). Wildfires, encompassing grass fires, forest fires, or bushfires, are uncontrollable and destructive, rapidly spreading through vegetation. These events are primarily fuelled by a combination of dry conditions, high temperatures, and flammable vegetation. The variability in wildfire behaviour due to factors like fuel type, humidity, and wind poses challenges for predicting fire behaviour and managing their

impacts (Reid et al., 2005b). Wildfire measurements utilize aircraft, satellite imagery, weather stations, drones, and ground-based sensors for accurate monitoring and prediction (Knobelspiesse et al., 2011; Urbanski et al., 2011). According to Ulevičius et al., (2010), the influence of regional wildfires, particularly in the Kaliningrad area, has been shown to dramatically increase black carbon concentrations in Lithuania, and deteriorating air quality (Ulevičius et al., 2010). In rural areas, domestic biomass burning for cooking, heating, and other household activities involves the combustion of wood, agricultural residues, and dung. This traditional source of energy is especially prevalent in regions with limited access to modern energy sources and has significant environmental and health implications (Liu et al., 2011). The combustion conditions, such as moisture, temperature, fuel type, and stove efficiency, affect emissions, which differ notably between traditional fireplaces and more advanced equipment (Chen et al., 2009). In Lithuania, a shift towards renewable energy, notably forest biomass, aims to significantly increase its share in energy consumption to 80% by 2050 (Valančius et al., 2022). Research by Kabašinskienė et al., (2019) in Lithuania underscores the importance of using high-quality biomass and optimizing combustion processes to reduce emissions and enhance energy efficiency. Agricultural burning involves the ignition of crop residues and vegetation for clearing fields and pest management. This practice releases a complex mixture of pollutants, including $PM_{2.5}$, CO, VOCs, and greenhouse gases like CH_4 and N_2O, impacting both local and global environments (Calvo et al., 2011; Werf et al., 2010). Different studies in Lithuania have further elucidated the multifaceted environmental repercussions of this practice. Nwokeh et al., (2016) study indicates that agricultural burning affects soil properties by altering pH levels, reducing organic matter content, and diminishing microbial biomass, which can harm beneficial soil microbes and compromise soil fertility. Despite stakeholders acknowledging a rapid post-fire recovery of vegetation, the practice raises concerns over its long-term effects on ecosystem health and soil productivity (Pereira et al., 2014).

1.4.2 Biogenic emissions

Biogenic emissions, originating from natural processes within rural environments, play a significant role in shaping air quality, atmospheric chemistry, and the Earth's climate system. These emissions arise from various sources such as vegetation, soils, and microbial activities, contributing to the formation of primary and secondary aerosols (Pöschl et., 2005). Primary biogenic aerosols (PBA), emitted directly from natural sources and

significantly impact atmospheric composition such as pollen, spores, and plant fragments, and other large particles with diameters of up to 100 μm. Particles below 10 μm originate from minute plant fragments, animal excretions, bacteria, viruses, carbohydrates, proteins, waxes, ions, etc. (Winiwarter et al., 2009). These aerosols undergo long-range transport and can ascend to considerable altitudes, reaching heights of up to 80 kilometers (Wainwright et al., 2003; Prospero et al., 2005). Biogenic volatile organic compounds (BVOCs) released by natural ecosystems can serve as potential precursors for the formation of secondary organic aerosol (SOA). Notably, isoprene is a dominant contributor with a global annual emission estimated at 440 – 660 Tg C yr^{-1} (Guenther et al., 2006). Additionally, minor quantities of alcohols, ketones, monoterpenes, and sesquiterpenes are also emitted as BVOCs (Warneke et al., 2010). Numerous investigations conducted in both laboratory and field conditions have provided evidence of the existence of oxidation products derived from terpenes and isoprene (Kroll et al., 2006; Kleindienst et al., 2007). Global biogenic volatile organic compound (BVOC) emissions are estimated to exceed anthropogenic VOC emissions by approximately a factor of 10 (Hallquist et al., 2009). These emissions are a significant precursor to secondary organic aerosol (SOA) formation, with BVOC oxidation considered the primary global source, ranging between 12 and 70 Tg yr^{-1} (Finessi et al., 2012). While biogenic emissions are a global phenomenon, regional studies, such as those conducted in Lithuania, provide specific insights into local sources and impacts. Research by Ulevičius et al., (2008) and Vebra et al., (2007) identified that coniferous forests in South-Southeast Lithuania are major sources of these emissions, emphasizing the role of forest management in regional air quality strategies. Lithuania has also been proactive in addressing these emissions by promoting biogas production from biodegradable waste. This approach not only helps manage biogenic emissions but also supports EU sustainability objectives. Further, incorporating environmental taxes and other policy measures aids in reducing reliance on traditional fuels and addresses the broader impacts of local agricultural practices on the environment (Byčenkienė et al., (2019); Katinas et al., (2019)). Incorporation of BVOCs occurs within diverse modelling frameworks, encompassing air quality forecasting, global chemistry climate, and regional regulatory models. This incorporation is driven by the notable impact of BVOCs on global and regional atmospheric chemistry, resulting in the production of secondary organic aerosol and ozone (Warneke et al., 2010). Biomass burning and biogenic emissions play a crucial role in atmospheric chemistry, yet they are still not well understood in many regions, especially when it comes to seasonal variations, long-range transport, and their impact

on climate. This study aims to address these gaps by analysing the chemical composition, sources, and climate effects of carbonaceous aerosols from biomass burning and biogenic sources in Lithuania. The findings will contribute to a better understanding of aerosol-climate interactions and inform mitigation strategies for reducing their environmental and health impacts.

1.5 Main aerosols sources in urban environment

Urban environments are characterized by high aerosol concentrations resulting from a variety of anthropogenic activities. These sources include traffic, industrial emissions, coal burning, food cooking, garbage burning, and fireworks, each contributing differently to atmospheric pollution. These aerosols play a crucial role in air quality deterioration, climate change, and public health risks. While extensive research has been conducted in developed countries, there remain significant knowledge gaps in developing regions such as the Philippines and Eastern Europe. This section reviews the major sources of urban aerosols and discusses the challenges in their characterization, emphasizing the need for further research.

1.5.1 Traffic

Urban environments are characterized by high levels of traffic-related aerosols, stemming from the complex interactions of various emission sources. Studies by Fang et al., (2006) and Martuzevicius et al., (2008) have extensively investigated the composition and sources of traffic-generated aerosols in urban environments, offering insights into their complexity and health implications. In the Philippines, a study by Madueño et al., (2019) focused on the emission factors of particle number and black carbon from public utility jeepneys in Manila, highlighting significant emissions from old diesel engines used in public transportation. Meanwhile, in Lithuania, Pauraitė et al., (2023) assessed the carbonaceous aerosol properties across an urban environment during the cold season, noting the substantial influence of residential heating systems on air quality, particularly through emissions from biomass burning. Urban road traffic is a predominant contributor to primary and secondary anthropogenic aerosols. The size and chemical composition of these particles exhibit significant variation, depending upon their formation mechanisms (Li et al., 2023). Exhaust emissions from road traffic are primarily composed of a mixture of gases and ultrafine primary carbon particles released through vehicle exhaust systems. These emissions arise from the combustion of fossil fuels in internal combustion engines, contributing to the atmospheric particle load (Jiang et al., 2005). Non-exhaust

emissions, on the other hand, encompass a diverse range of sources beyond exhaust emissions. These include particles released from brake wear, tire wear, road surface abrasion, and the resuspension of particles in the wake of passing traffic (Byčenkienė et al., 2022; Madueño et al., 2019). The abrasion of brakes and tires emits particles into the air, carrying trace elements like strontium, copper, molybdenum, barium, cadmium, chromium, manganese, and iron (Vera et al., 2021). Tire wear contributes significantly to PM_{10} emissions, with substantial rubber depletion annually in Europe (Thorpe et al., 2008). Research on brake emissions includes evaluations of commonly used brakes in the US and brake linings in Sweden and Japan (Li et al., 2023; Presto et al., 2021). Resuspension of particles from pavements also impacts air quality (Bukowiecki et al., 2010). Notably, elevated particle levels are observed in northern Europe during winter, attributed to the application of sand and salt on roads to prevent snow from freezing into ice (Rahman et al., 2017). Utilizing data from various European urban centers, Querol et al., (2004) demonstrated that both exhaust and non-exhaust origins contribute nearly equal proportions to the collective emissions arising from traffic-related activities. Nitrogen oxides, mainly originating from traffic, act as precursors to various nitrogen compounds, contributing to air pollution (Singh et al., 2006). The research by Duong et al., (2010) elucidated that variable like traffic volume, atmospheric dispersion from traffic rotaries, frequency of brake utilization, instances of vehicles halting completely, and vehicle speed exert an impact on the levels of heavy metal contamination. Recent research, exemplified by Li et al., (2023), continues to underscore the concerning levels of particulate matter (PM) emissions from diesel-powered vehicles, which are commonly 10 to 100 times more abundant compared to emissions from gasoline-powered vehicles. Particulate matter originates from diesel engines produce toxic elements like PAHs, substances well-known as genotoxic and carcinogenic agents. This underscores their capacity to damage genetic material and act as initiators of cancer (Chirico et al., 2010). Over the past few years, there has been a growing emphasis on exploring biofuels (such as soybean oil, rapeseed oil, and palm biodiesel) due to their potential to mitigate emissions of air pollutants (including CO, particle hydrocarbons, PAHs, and PM) originating from diesel engines (Rivas et al., 2021). These alternative fuel sources hold promise in contributing to improved air quality and reduced environmental impacts comes from diesel engine emissions (Papa et al., 2021). Broadly, a decline in PM levels was recorded alongside a decrease in the average particle diameter (Chirico et al., 2010). Research by Chien et al. (2009) highlights that with increasing proportions of biodiesel blending, emitted particles exhibit a transition towards ultrafine and nanoscale

dimensions. This shift is paralleled in the emission trends of polycyclic aromatic hydrocarbons (PAHs), found to closely correlate with PM concentrations, reinforcing the connection between particle size distribution and PAH emissions. Beyond automobiles, research has extensively investigated emissions from various vehicle types, including buses, trucks, tractors, and motorcycles (Liu et al., 2011). According to Alas et al., (2018) and Kecorius et al., 2019, in urban areas such as Manila (Philippines), jeepneys have been identified as the main contributors to particulate matter. Railway emissions have also gained significant scrutiny. For instance, recent findings by Rivas et al., (2021) reveal that iron particles constitute the predominant fraction in railway emissions, accounting for 67% or 2.9 $\mu g/m^3$ of the PM_{10} attributed to railways. Aluminium and calcium particles contribute 23% and 10% correspondingly (Vera et al., 2021). Moreover, aviation emissions contribute substantial amounts of NOx, SOx, black carbon, and organic carbon, impacting both ground-level and upper-atmospheric air quality (Barrett et al., 2010).

1.5.2 Industrial activities

Urban environments are significantly influenced by industrial activities, emitting both particulate matter and gases into the atmosphere, many of which act as precursors to aerosol formation. Aerosols, comprising small liquid droplets or solid particles suspended in air, are a consequence of diverse industrial operations like combustion, manufacturing, and construction (Sofia et al., 2020). Byčenkienė et al., (2014) revealed that elevated particle number concentrations in Vilnius are primarily attributed to the long-range transport of pollutants from industrial areas in Central Europe. Similarly, Braun et al., (2020) identified industrial activities as major emission sources in Metro Manila, Philippines. These studies highlight the significant role of industrial emissions in shaping urban aerosol landscapes. Industrial pollution stands out due to the large amounts of harmful substances released at different stages of industrial processes. The kind of pollutant is primarily influenced by the method of production, the technology applied, and the raw materials used (Shetty et al., 2023). Several industrial activities, including the production of ceramics, bricks, cement, foundries, mining, and quarrying, stand out as prominent sources of particle emissions. In a study conducted by Sánchez et al., (2021), an examination was carried out on emissions originating from mining activities, focusing on the presence of toxic metals and metalloids, including As, Cd, and Pb. The findings revealed a dual-peaked distribution with average sizes of approximately 0.3 μm and 7 μm. These sizes were linked

to distinct sources: a) smelting operations, and b) wind-driven dispersion of mine tailings and unintentional emissions, respectively. Foundries are frequent sources of emissions of metals such as nickel, vanadium, manganese, and copper (Manisalidis et al., 2020). According to the investigation by Ahn et al., (2006), the primary components of particles emitted from a steel plant were Fe_2O_3 (39.6 to 74.5%), while particles from a cement plant mainly consisted of CaO (41.8 to 65.5%). Conversely, in the case of particles from a coal power plant and a foundry, the predominant constituent was SiO_2 (53.3 to 80.6%), in the coal fly ash and foundry particles, respectively (Kumar et al., 2022). In a study examining an incident of industrial pollution plume, Choël et al. (2010) determined that steelworks play a significant role in emitting metallic pollutants (such as Fe, Mn, and Zn). The researchers emphasized the importance of coagulation interactions between particles from industrial origins and particles from different sources. They noted instances where metal-enriched particles were internally mixed with compounds from marine or continental sources (Manisalidis et al., 2020). Fossil fuel-based energy generation constitutes a significant origin of gases that serve as precursors for secondary aerosol formation. The combustion of coal within power plants gives rise to primary particles derived from residual coal components, including clay, sulphurs, carbonates, chlorides, and metals, prominently mercury. These particles also arise from the incomplete combustion of coal (Shindell et al., 2010). In a significant study Tohka et al., (2006) conducted an investigation into the emissions of fine particles and the potential for reducing emissions in industrial processes within Finland. Byčenkienė et al., (2014) in Lithuania and Braun et al., (2020) in the Philippines also report significant contributions of coal combustion to regional aerosol formation. These findings underscore the global relevance of industrial combustion processes as major sources of urban aerosols, highlighting similar trends across diverse geographical locations.

1.5.3 Coal burning

Coal burning serves as a prominent and consequential source of particulate matter and gaseous pollutants in rural environments, exerting significant impacts on both air quality and public health. When coal is burned for energy generation, a complex mixture of fine particles and gases is released into the atmosphere. These emissions can encompass a range of pollutants, including sulphur dioxide (SO_2), nitrogen oxides (NOx), CO, volatile organic compounds (VOCs), and heavy metals (Markovic et al., 2023). The emissions resulting from the combustion of coal, a significant fossil fuel, are influenced

by factors including coal maturity and combustion circumstances. Within these emissions, hazardous constituents like Polycyclic Aromatic Hydrocarbons (PAHs) and trace elements such as Arsenic (As), Selenium (Se), Mercury (Hg), Chromium (Cr), Cadmium (Cd), Lead (Pb), Antimony (Sb), and Zinc (Zn) have been identified. These elements are commonly found within the finer $PM_{2.5}$ particulate fraction of coal combustion emissions, due to which they become more dangerous for human health (Xu et al., 2011). In Lithuania, residential coal combustion significantly contributes to the air pollution, with biomass combustion for heating also being a notable source of black carbon (BC) and organic carbon (OC) mass concentrations (Pauraitė et al., 2015). This demonstrates the dual challenge of managing both coal and biomass burning to mitigate urban air pollution effectively. Similarly, in the Philippines, urban coal burning has been identified as a substantial contributor to air pollution. Gonzales et al., (2012) highlight the role of coal as a major source of particulate matter emissions across various cities, emphasizing the need for targeted pollution control measures in these urban settings. Residential coal combustion plays a vital role in China's air pollution landscape, accounting for a substantial 10.7% share of total emissions of PAHs in 2004. Interestingly, naphthalene emerged as the primary PAH in gaseous phases, while phenanthrene took precedence in particulate phases (Shen et al., 2010). Regarding BC and OC emissions, studies using household stoves for burning various coal types demonstrated significant differences in emission factors. Chen et al., (2009) conducted diverse combustion trials utilizing three typical household stoves for burning 13 distinct coal types, represented by honeycomb coal briquette and raw coal chunk formats. Notably, their investigation yielded average BC emission factors (EFs) of 4 mg kg^{-1} and 7 mg kg^{-1} for anthracite in briquette and chunk forms, respectively. For bituminous coal, EFs were much higher, especially in chunk form. Similarly, high EFs were recorded for organic carbon emissions from bituminous coal (Chen et al., 2009).

1.5.4 Food cooking

In urban environments, the food cooking releases a complex mixture of aerosols into the air, contributing to the intricate web of atmospheric pollutants. These aerosols comprise a variety of organic and inorganic particles, with their composition and emission levels influenced by factors such as cooking methods, oil types, and cooking ingredients. Recent studies have shed light on the significant role of food cooking emissions in urban air quality degradation, highlighting their contribution to both PM and VOC

levels (Li et al., 2019). Recent analyses utilizing source apportionment techniques and chemical mass balance (CMB) calculations have demonstrated that emissions originating from meat charbroiling and frying contribute to approximately 20% of the total organic matter present in fine particulate matter ($PM_{2.5}$) in the Los Angeles area. These culinary activities release a diverse array of organic compounds into the atmosphere, further exacerbating urban air quality concerns (Zhu et al., 2023). Further, Mažeikis et al., (2013) noted that cooking in urban areas like Vilnius significantly contributes to air pollution, which is exacerbated by urbanization affecting meteorological parameters that influence the dispersion of air pollutants. Studies have identified over 120 distinct compounds emitted from meat cooking, with palmitic, stearic, and oleic acids, along with cholesterol, noted for their high levels of abundance (Mohr et al., 2009). Additionally, the health effects of cooking fuels are crucial. The Capuno et al., (2016) study in the Philippines shows that using clean cooking fuels can lower respiratory illness risks in children, highlighting the health dangers of solid fuels in household air pollution. Buonanno et al., (2009) observed a significant rise in emission factors with increasing cooking temperatures, influencing aerosol characteristics. The investigation by Wu et al., (2023), put forward distinct markers for identifying emissions from meat cooking in both Western-style and Chinese cooking practices. See et al., (2008) explored the chemical attributes of $PM_{2.5}$ from different gas cooking techniques, finding that deep-frying discharged the most substantial $PM_{2.5}$ load. In a more recent study, Zhang et al., (2022) investigated the emissions of carcinogenic elements, specifically higher aldehydes and PAHs, resulting from various Norwegian beefsteak cooking methods involving pan frying. The research demonstrated the presence of these harmful compounds in the air within the cook's breathing space. Notably, the study found that cooking on a gas stove led to higher exposure to these hazardous constituents compared to electric stove cooking. Moreover, study highlighted the significant role of selecting appropriate kitchen ventilation systems and emphasized that different types and configurations of kitchen extraction hoods result in varying exposure scenarios.

1.5.5 Garbage burning

Garbage burning is a significant source of particulate matter in both urban and rural environments, posing severe health and environmental risks. Despite frequently being banned, this practice remains widespread. Recent research suggests that approximately 50% of the world's generated waste, equivalent to

around 1000 teragrams per year, is disposed of through open fires or incineration. This alarming estimate implies that a staggering 500 teragrams of carbon are released annually into the atmosphere from these activities (Christian et al., 2010). Garbage represents a diverse and mixed fuel source, containing not just significant amounts of biomass, but also a variety of materials like plastics, paper, textiles, rubber/leather, glass, and metal. Recent estimates indicate that a notable percentage, ranging from 12% to 40%, of households situated in rural regions across the United States engage in unregulated and spontaneous incineration of waste within their own premises. This behaviour is predominantly observed in rural areas, where individuals resort to the combustion of waste materials using 208-liter drums referred to as "burn barrels." Unfortunately, the potential health repercussions stemming from the discharge of hazardous compounds, such as dioxins, tend to be downplayed. (Christian et al., 2010). According to the findings of Akagi et al., (2011), emission factors (EFs) for pollutants released from garbage burning were assessed. Their study unveiled EFs of 9.8±5.7 g kg^{-1}, 0.65±0.27 g kg^{-1}, and 5.27±4.89 g kg^{-1} for $PM_{2.5}$, BC and OC, respectively. Furthermore, the researchers underscored a significant aspect-reliance on levoglucosan and potassium (K) as tracers for biomass burning might prove inadequate in certain regions. Significantly, garbage burning emissions exhibit notable concentrations of hydrogen chloride (HCl), a component uncommonly found in biomass burning emissions. Notably, Christian et al., (2010) discovered emission factors (EFs) for HCl spanning from 1.65 to 9.8 g kg^{-1}, accompanied by noteworthy additional chlorine content within the particles (EFs for soluble Cl^- alone ranging from 0.2 to 1.03 g kg^{-1}). These elevated EF values are intricately associated with substantial quantities of polyvinyl chloride (PVC), a compound commonly associated with discarded waste (Akagi et al., 2011). Furthermore, additional regional studies underscore the environmental and health impacts of waste incineration. The studies by Byčenkienė et al. (2022) and Denafas et al., (2007) reveal that in Lithuania solid waste incineration plants, particularly those near urban areas, release polychlorinated dibenzo-p-dioxins and dibenzofurans (PCDD/F), contributing to ecosystem degradation and human health risks, as well as acidification and eutrophication. Similarly, research conducted in the Philippines by Regmi et al., (2017) and Gonzales et al., (2012) identified the burning of agricultural waste, charcoal, and solid waste as major sources of fine particulate matter emissions in the cities of Cabanatuan, Pandacan, and Manila, highlighting a critical area of concern for air quality management in these urban settings.

1.5.6 Fireworks

Fireworks, well-known for their dazzling displays and celebratory charm, have a darker side often hidden by the brilliance they emit. These captivating pyrotechnics are not just a feast for the eyes; they also contribute significantly to PM pollution in urban areas, presenting both environmental and public health challenges. The captivating burst of colours and patterns belies the microscopic particles released into the air during and after fireworks events (Retama et al., 2019). Fireworks emerge as a notable source of concern, not only in various global locales during specific festivities but also as a consistent factor contributing to air quality degradation. Cities across Europe, North America, China, and India have been the focus of studies revealing consistent patterns of heightened particulate matter levels during fireworks events. These studies consistently highlight the presence of various pollutants, including metals, both inorganic and organic compounds, and toxic gases like O_3, SO_2, NO_2, and CO in the aftermath of firework displays (Yoo et al., 2024). The emissions from fireworks generate plumes of smoke laden with particles encompassing water-soluble ions and trace metals (Sr, K, Ba, Co, Pb, and Cu). Within this complex mixture, sulphate (SO_4^{2-}), nitrate (NO_3^-), ammonium (NH_4^+), potassium (K^+), and chloride (Cl^-) compounds can collectively constitute over 50% of the overall burden of $PM_{2.5}$. After the firework exhibitions, there is a gradual rise in the levels of secondary inorganic ions such as SO_4^{2-}, NO_3^-, and NH_4^+, which subsequently become predominant components on the subsequent day (Hao et al., 2023). The role of organic carbon within firework-generated particles is noteworthy, although its impact on black carbon is relatively moderate. Fireworks elevate the abundance of oxygenated organic aerosols, especially those characterized by moderate and low volatility levels. The detected components include aliphatic compounds, their derivatives, esters, alcohols, ketones, and various other species with potential health implications (Khaparde et al., 2012). Additionally, recent studies further illustrate regional impacts. Kalinauskaite et al., (2024) investigates the combined effects of fireworks and foggy weather conditions on air pollution during New Year's Eve from Vilnius (Lithuania), revealing significant increases in PM_1, $PM_{2.5}$, and PM_{10} concentrations. Similarly, research in the Philippines by Lorenzo et al., (2020), and Cruz et al., (2023), in Metro Manila and Quezon City indicates that fireworks significantly raise levels of SO_2, $PM_{2.5}$, and PM_{10}, along with notable spikes in metallic components such as Fe, Cr, Cu, Ni, V, Ti, and Ba. These events also alter particle composition, hygroscopicity, and aerosol backscatter, influencing aerosol properties and atmospheric dynamics. Despite extensive research, there are still significant gaps in understanding non-exhaust traffic emissions,

the impact of meteorological conditions on aerosols, and the effectiveness of biofuels, particularly in rapidly developing cities like Manila. Industrial emissions are difficult to distinguish from long-range pollution, and their interactions with natural particles in coastal areas remain unclear. Coal burning's impact in residential areas is understudied, particularly in North-Eastern Europe and Southeast Asia, requiring better assessment for effective mitigation strategies. This study aims to fill these research gaps by analysing the seasonal variability and source contributions of carbonaceous aerosols across urban environments in Lithuania and the Philippines. By differentiating between exhaust and non-exhaust traffic emissions, local and transported industrial pollutants, and coal versus biomass burning contributions, this research will provide scientifically robust data to support targeted air quality management and mitigation policies.

1.6 Main aerosols sources in coastal environment

1.6.1 Sea spray aerosols

Marine aerosols play a crucial role in the coastal environment, serving as dynamic carriers of oceanic and atmospheric interactions. These aerosol particles are generated by the ocean's breaking waves, where sea spray and other biological and chemical processes release them into the atmosphere. This aerosol-rich interface acts as a bridge connecting the oceans and the atmosphere, influencing various climatic, ecological, and biogeochemical processes (Meskhidze et al., 2006; Dowd et al., 2007; Brooks et al., 2017). The majority of marine aerosols are considered primary in nature. However, the oceanic surfaces host a range of sources, including phytoplankton that release diverse organic compounds such as dimethyl sulphide (DMS; CH_3SCH_3), as well as bacteria, viruses, and various trace elements. These aerosols possess the capability to be transported over long distances, consequently impacting atmospheric composition, cloud nucleation, and potentially even weather trends. This phenomenon is supplemented by their role in facilitating nutrient cycles, as they transport essential minerals and organic materials from the ocean to coastal ecosystems. The composition of marine salt primarily consists of sodium and chloride, accompanied by smaller amounts of other elements like sulphate, potassium, magnesium, and calcium (Brock et al., 2021). The primary origin of atmospheric sodium and chloride in coastal regions originates from the ocean. In the fine particles of sodium chloride (NaCl), a portion of the chloride undergoes a conversion into a gaseous form through atmospheric reactions involving sulfuric acid (in gaseous or aqueous phase) and nitric acid (in gaseous phase) (Claeys et al.,

2010). This transformation leads to the reduction in chloride content, thereby designating sodium as the principal tracer for particulate matter within marine salt aerosols (Kim et al., 2019; Bai et al., 2022).

$$NaCl_{(s)} + HNO_{3(g)} \longrightarrow HCl_{(g)} + NaNO_{3(s)} \quad (4)$$

$$2NaCl_{(s)} + H_2SO_{4(g+aq)} \longrightarrow 2HCl_{(g)} + Na_2SO_{4(s)} \quad (5)$$

Primary marine aerosols come into existence through the explosive emergence of rising bubbles via the sea-surface microlayer (SML). The abundance of marine particles within the ocean's threshold layer is directly linked to the speed of the wind. The bursting of a single air bubble in ocean has the potential to produce up to 10 marine aerosol particles, each with a diameter ranging from 2 to 4 μm (Ryu et al., 2007). These particles hold the capacity to ascend to heights of up to 15 cm above the water surface and are acknowledged as jet drops. The significance of primary marine aerosols has been inadequately recognized, despite their dual role as contributors to adverse biological effects and as a medium for the exchange of energy and material between the ocean and the atmosphere (Zhao et al., 2021). Although marine aerosol is typically associated with the coarse fraction, different studies has identified finer marine particles measuring as small as 0.05 μm. The submicron fraction gained specific attention because of its direct and indirect influence on radiative transfer processes. Furthermore, research by Ovadnevaite et al., (2018) on the Baltic Sea's east coast emphasizes the complexity of aerosol components, including sulphates, organics, nitrates, and ammonium, with varying size distributions between clean marine and polluted air masses, illustrating the necessity of distinguishing aerosol sources to effectively address their environmental and health impacts. Various investigations have approximated the worldwide emissions of organic matter in the sub-micron size range through sea spray processes at 8.2 Tg yr^{-1}, in comparison to 24 Tg fine yr^{-1} sea-salt emissions (Calvo et al., 2013). Notably, global models tend to underestimate OC, particularly during periods of plankton blooms, wherein the levels are often miscalculated by a factor of 5–20. OC displays a notable correlation with back-trajectory weighted chlorophyll, implying an oceanic OC source influenced by biological activity. The enrichment of micro floatable components in marine aerosol is attributed to the role of surfactants (Osto et al., 2017; Shank et al., 2012). Studies in Lithuanian coastal areas reveal that local emissions primarily stem from fossil

fuel combustion. During pollution peaks, air masses typically arrive from the south, southeast, or southwest, carrying pollutants from Eastern and Southern Europe to Lithuania. This long-range transport significantly impacts air quality and poses health risks due to increased $PM_{2.5}$ levels (Ovadnevaitė et al., 2007; Masalaite et al., 2017; Masalaite et al., 2020). The study underscores the importance of considering regional emission sources and their transport pathways when assessing the broader impacts of marine aerosols on coastal air quality and human health. Marine aerosols are not solely confined to coastal zones; they can also be detected at elevated inland heights, underscoring their ability to undergo long-distance (Wang et al., 2020).

1.6.2 Ships emissions

Ships emissions in coastal environments represent a significant concern due to their impact on air quality, human health, and the marine ecosystem. The maritime sector is a substantial contributor to air pollutants such as sulphur dioxide (SO_2), nitrogen oxides (NOx), PM, and greenhouse gases (GHGs) like carbon dioxide (CO_2) and methane (CH_4). Ships contribute to approximately 16% of the worldwide sulphur emissions and account for as much as 54% of the total sulphate aerosol column burden over the Mediterranean region during the summer months (Saliba et al., 2021; Ramacher et al., 2020; Corbett et al., 2007). Similarly, recent research conducted in Lithuania by Karl et al., (2019); Masalaite et al., 2020; Masalaite et al., 2022; Jonson et al., (2019); Rapalis et al., (2022), and Ducruet et al., (2024) has shown that ship emissions are major contributors to pollutants such as sulphur dioxide (SO_2), nitrogen dioxide (NO_2), ozone (O_3), fine particulate matter ($PM_{2.5}$), and non-methane volatile organic compounds (NMVOC). These emissions significantly impact air quality, contribute to climate change, and pose health risks, especially in urban port areas. Marine vessels emit a considerable amount of sulphur dioxide due to the high sulphur content in marine fuels. These emissions not only contribute to regional air pollution but also affect marine ecosystems, leading to ocean acidification and subsequent ecological consequences (Saliba et al., 2021). Nitrogen oxide emissions from ships contribute to the formation of ground-level ozone and particulate matter, both of which have adverse effects on human health and the environment. Additionally, ships emit PM that includes BC, OC, and other pollutants with significant health implications. In Manila, Philippines, studies by Cadondon et al., (2024), Pabroa et al., (2023), and Alas et al., (2018) have revealed that vehicle traffic significantly impacts air quality in the region. Many vehicles, including ships and boats, still utilize diesel engines that do not meet EURO emission standards, making them major contributors to particulate matter

($PM_{0.49}$ and $PM_{2.5}$) and black carbon emissions. This emphasizes the urgent need for adopting cleaner technologies and stricter emission regulations globally. The International Maritime Organization (IMO) has implemented regulations to address these emissions, including the global sulphur limit of 0.5% for marine fuels (IMO, 2018, 2020). However, compliance and enforcement remain challenges, leading to ongoing discussions about stricter regulations and the adoption of cleaner technologies. Alternative fuels like liquefied natural gas (LNG) and hydrogen have gained attention as potential solutions to reduce emissions, although challenges such as infrastructure and cost need to be addressed (Russo et al., 2023). According to Feng et al. (2019), the spatial distribution of ship emissions in coastal regions, showing higher concentrations near major ports and shipping routes. Coastal areas experience elevated pollution levels due to the combined effects of local emissions, ship traffic, and atmospheric dynamics. These emissions have health implications for coastal communities and tourists, emphasizing the need for effective monitoring and regulatory measures. Research has employed satellite remote sensing and atmospheric modelling to quantify and assess the impacts of ship emissions on air quality and climate. These methods provide valuable insights into emission patterns, pollutant concentrations, and their interactions with regional meteorology (Feng et al., 2019). Improving the accuracy of emission inventories and modelling techniques is crucial to understanding the full scope of ship-related pollution.

1.6.3 Fishing and aquaculture

Fishing and aquaculture activities are critical components of coastal economies, providing sustenance and livelihoods for communities around the world. However, beyond their economic significance, these activities also have the potential to impact the coastal environment through the generation of aerosols. Fishing operations can contribute to the production of aerosols through various mechanisms. One significant process is the shaking of water during activities like hunting, where fishing nets disturb the water column and entrain particles, including organic matter, minerals, and microorganisms. These entrained particles can become aerosols when they are ejected into the air due to the hydrodynamic forces generated by the moving vessel (Sühring et al., 2023). Recent studies have shown that fishing activities can result in the release of bioaerosols containing microorganisms such as bacteria and viruses. These microorganisms, originally suspended in the water, become airborne through the churning action of fishing vessels. Aquaculture, which involves the farming of aquatic organisms, can also contribute to aerosol generation. Intensive aquaculture practices, such as those in shrimp and fish farms, can

result in the release of particulate matter and organic compounds into the surrounding environment. A study by Uddin et al., (2018), investigated aerosols from shrimp farming operations and found that they contained elevated concentrations of organic carbon, likely originating from feed and waste materials. Additionally, the use of aerators in aquaculture ponds, designed to increase dissolved oxygen levels, can lead to the entrainment of water droplets into the air. These water droplets, carrying particulate matter and potentially harmful microorganisms, can become aerosolized and disperse over nearby areas (Yazdi et al., 2010).

Marine aerosols play a vital role in climate regulation and coastal air quality, yet there are still many unanswered questions about their composition, movement, and interactions with anthropogenic pollution. The impact of biological processes (e.g., plankton blooms) on organic aerosol formation is understudied, and sea spray interactions with industrial and ship emissions are poorly quantified, especially in Baltic and Southeast Asian regions. Ship emissions, a major but poorly regulated source of sulphur and nitrogen pollutants, require further study on long-range transport and secondary aerosol formation. Additionally, the impact of fishing and aquaculture aerosols on air quality and health risks remains largely overlooked. This study aims to address these knowledge gaps by quantifying seasonal variations and source contributions of marine, ship, and fishing-related aerosols in Lithuania and the Philippines. By distinguishing natural vs. anthropogenic aerosol contributions, this research will provide critical insights for air quality regulation and coastal climate impact assessments.

1.7 Actions to Mitigate Climate Change in rural, urban and coastal environment

Climate change mitigation requires a blend of global strategies and localized efforts. The goal to combat atmospheric change revolves around creating strategies to decrease greenhouse gas emissions globally. In 1994, the United Nations General Convention on Climate Change was established, gaining widespread approval and ratification from 197 countries (UNFCCC, 1994). However, there was less enthusiasm for certain legislative measures like the Kyoto Protocol, which only had 38 participating countries (UNFCCC, 1997). The momentum shifted with the introduction of the Paris Agreement in 2015, with 195 countries involved (UNFCCC, 2015). The subsequent provisions of the Katowice meeting in 2018 allowed the successful transfer of the main agreement on the fight against climate-related issues into real practice (UNFCCC, 2018). However, the effectiveness of these policies varies greatly across different regions, necessitating localized strategies to

complement these global efforts. The European Green Deal serves as a model for how regional strategies can support global climate objectives. With a goal of achieving carbon neutrality by 2050, this initiative integrates plans across sectors such as industry, construction and transportation. Investments are directed towards innovation and sustainable practices, with a target of mobilizing €1 trillion by 2030 to back these endeavours. The Green Deal highlights the importance of legislative support and financial investment in driving climate action (European Commission, 2020). Public awareness and advocacy play a crucial role in climate action. Both global and local movements, backed by environmental activists and organizations, play a key role in shaping policies and promoting sustainable practices. Through awareness campaigns, grassroots initiatives, and policy advocacy, these efforts influence public perception and push policymakers to take necessary actions. These initiatives highlight the importance of reducing emissions, adopting sustainable energy sources, and protecting natural ecosystems. In Asia, countries such as Philippines, Vietnam, China, Nepal, Bangladesh, and Pakistan face unique challenges due to their geographic and economic conditions. The Philippines' Climate Change Act, established in 1999 and revised in 2016, focuses on enhancing the country's capabilities to mitigate and adapt to climate impacts (Republic of Philippines, 1999, 2016). Strategies include community-based adaptation measures, integrated coastal management and the promotion of renewable energy sources, which represent a proactive approach to addressing the specific vulnerabilities of island nations. Rural regions are predominantly affected by changes in agricultural practices and land use. Strategies here focus on sustainable agriculture, afforestation, and bioenergy production. Sustainable practices such as crop rotation, organic farming, and the use of drought-resistant crop varieties help reduce the environmental footprint of agriculture. Afforestation not only helps sequester CO_2 but also aids in biodiversity restoration and soil quality enhancement. Bioenergy with carbon capture and storage is seen as a promising technology for producing energy while lowering overall atmospheric CO_2 levels. However, the successful implementation of such technologies hinges on carefully considering the impact on local ecosystems and socio-economic factors to prevent negative consequences such as land competition and water usage. In addition, minimizing the use of biomass and the burning of fossil fuels is crucial to reducing greenhouse gas emissions and improving the overall sustainability of these strategies. Urban areas, known for their dense population and industrial activities, play a significant role in global emissions. Efforts to mitigate urban climate issues involve improving energy efficiency in buildings, promoting public transportation and creating

green infrastructure. The shift towards renewable energy sources in cities is made easier by incorporating solar panels, wind turbines and sustainable public transportation systems. Initiatives like green buildings and smart cities utilize technology to optimize energy consumption and reduce emissions. Moreover, urban green spaces not only sequester carbon but also improve air quality and provide resilience against climate impacts like heatwaves. Coastal areas require special attention due to their vulnerability to sea-level rise and extreme weather events. Mitigation strategies in these areas include coastal reforestation, wetland rehabilitation and sustainable fisheries development. The restoration of mangroves not only shields coastlines but also acts as an efficient carbon absorber. Wetland restoration helps in carbon sequestration and provides buffer zones against storm surges. Maintaining the health of marine ecosystems is dependent on sustainable fishing and aquaculture practices that aim to prevent overfishing and habitat destruction. Furthermore, anthropogenic emissions from ships, boats, cranes, and cargo trucks must comply with Euro emission standards to significantly reduce particulate matter and black carbon emissions.

While global climate policies aim for net-zero emissions, implementation gaps persist, particularly in developing regions with financial and technological constraints. Rural mitigation strategies like bioenergy and sustainable agriculture lack long-term impact assessments, while urban policies on renewable energy and public transit need better evaluation of real-world emission reductions. Coastal mitigation efforts, including mangrove restoration and wetland rehabilitation, are not well quantified, and maritime emissions remain underregulated, with limited data on their climate interactions. This dissertation plays a critical role in bridging these research gaps by characterizing and performing source apportionment of organic, inorganic, and carbonaceous aerosol particles in rural, urban, and coastal regions across Europe and Asia. By identifying the primary emission sources, analysing seasonal variability, and evaluating the effectiveness of mitigation policies, this study will provide scientifically robust insights for developing targeted climate action strategies. The findings will be vital for policymakers in crafting region-specific climate policies that balance technological advancements with socio-economic realities, ultimately enhancing the effectiveness and fairness of climate mitigation efforts.

2 MATERIALS AND METHODS

2.1 Sampling sites description

The continuous measurements of the chemical composition and optical parameters of aerosol particles took place in three different environments: rural, urban, and coastal. These selected observation sites are strategically positioned in different geographical locations to assess the predominant sources of organic, inorganic and carbonaceous aerosol particles affecting the atmospheric heat balance not only in Europe (Lithuania) but also in Asia (Philippines) (Fig. 3).

The first measuring station characterized as a rural environment is the comprehensive measuring station in Aukštaitija integrated monitoring station (Fig. 3a). This remote location in the village of Rūgšteliškis (55°27'N, 26°00'E, 170 m a.s.l.) covers about 70% forested area, which is mainly characterized by pine stands (*Pinus sylvestris*) and vegetation varied from steppe to tundra species (Pauraitė et al., 2015). There are hardly any significant local sources of anthropogenic pollution in the immediate vicinity of the site. The nearest major town, Utena, is located 27 km south of Rūgšteliškis. The measurements were taken at a height of about 1.5 meters above the ground level, temperate climate zone characterized by a humid continental climate with moderately cool weather conditions, abundant rain and high humidity (European Environment Agency, 2023). Over a period of five years (2013, 2014, 2016, 2018, and 2019), the measurements were systematically carried out in three different seasons: spring, summer, and autumn.

The second measurement site was selected at the headquarters of the Center for Physical Sciences and Technology (FTMC) in Vilnius (54°38'N, 25°10'E, 197 m asl) (Fig. 3b). The inlet of the sampling system was placed on the top floor, about 20 m above ground level, 12 km southwest of the downtown area. Notably, the sampling site was strategically situated at a considerable distance from densely populated residential zones. The station found itself surrounded by forests to the north/northeast and villages to the south/east. The closest roadway was positioned 300 m to the southwest, while on the opposite side, a low-traffic road was 600 m away. Described as an urban background location, the site's geographical positioning under typical meteorological conditions limited the potential for the accumulation of vehicle emissions. During the winter of 2014 (January – February), an intensive 2-month field measurement campaign was conducted. The objective was to perform continuous real-time measurements to detect the composition of organic aerosols (OA) and mass concentrations of black carbon (BC) at this

urban site.

The third measurement campaign was conducted at two locations in Metro Manila, Philippines: Manila's North Port (14°61'N, 120°96'E) from December 20, 2019, to January 25, 2020 (Fig. 3c), and Quezon City's East Avenue roadside (14°67'N, 121°04'E) from January 29, 2020, to February 26, 2020 (Fig. 3d). The Port site was situated 12 km away from Quezon City's East Avenue. To ensure the quality of the collected data, measurement instrumentation was housed in a specialized, air-conditioned container. Aerosol instrumentation operated based on recommendations from the World Calibration Centre for Aerosol Physics (WCCAP) under the World Meteorological Organization's (WMO) Global Atmosphere Watch (GAW) Programme. The sampling was carried out following the guidelines presented in the GAW report 227 (WMO Report, 2016) to minimize particle loss due to diffusion, impaction, and settling. Classified as a coastal environment, the measurement site played host to an intensive field campaign specifically targeting the measurement of equivalent black carbon (eBC) mass concentration, aerosol particle number concentration, and particle light scattering coefficient.

Fig. 3. Location of four measurement sites. (a) Rūgšteliškis rural site (Lithuania), (b) Vilnius city site (Lithuania), (c) Quezon city site (Philippines) and (d) Manila port site (Philippines).

2.2 Methods of estimating physical and chemical parameters of the atmosphere

2.2.1 Measurement and source identification of organic aerosol particles

2.2.1.1 Mass spectrometry of aerosol particles

The Aerodyne Chemical Speciation Monitor (ACSM) (Aerodyne Research Inc., USA) is a sophisticated instrument for direct measurement of the chemical composition of airborne aerosol particles. This revolutionary device works on the basis of a comprehensive system of aerodynamic lenses and pumps that enable precise analysis of aerosol properties (Ng et al., 2011). The operating principle underlying the ACSM is illustrated in the schematic and detailed description by Ng et al., (2011). When aerosol particles are drawn into the device, they undergo a selective process within the aerodynamic lenses, which have a dual function. Firstly, these lenses efficiently exclude particles larger than 1 μm in diameter, ensuring that the focus is exclusively on the finer particles. Secondly, the lenses narrow down the particle stream, resulting in a focused and refined input for subsequent analysis. This pivotal step in the process is further explained by Liu et al., (2018), emphasizing the crucial role these lenses play in shaping the aerosol sample.

The journey of the aerosol particles continues into different chambers within the ACSM, each serving a specific purpose in the analysis process. In the first chambers, the aerosol particles are effectively separated from the surrounding air stream with the help of the pumps. This pre-processing step ensures that the subsequent analysis is targeted and accurate, focusing exclusively on the particles of interest. The third chamber is a critical phase in which the aerosol particles are deposited on a heating plate and subsequently vaporized. This process leads to the generation of vapours, which are then ionized with 70 eV electrons. The ionization of the aerosol particles leads to the formation of fragments of molecular ions, a key step in the analysis described by Ng et al., (2011). These fragments, which represent various chemical components of the aerosol particles, are fed into a quadrupole mass spectrometer. In this spectrometer, the mass-to-charge ratio (m/z) of each fragment is determined, providing valuable insight into the molecular composition of the aerosol particles. The ability to measure this spectrum over a range of m/z 12 to 149 enables a comprehensive analysis of the chemical composition of the aerosol.

The ACSM's temporal resolution is a notable feature of its operation. This sensor offers a time-dependent perspective on aerosol properties and operates at intervals of around 30-minutes. This temporal precision provides insights

into short-term fluctuations and trends and is essential for capturing dynamic changes in aerosol composition. The sophisticated design of the ACSM is highlighted by the complex interactions between its mass spectrometry, ionisation, pumps, chambers, heating plates, and aerodynamic lenses. By combining these elements, the ACSM becomes a state-of-the-art instrument for atmospheric research, guaranteeing a reliable and accurate measurement of aerosol particles.

2.2.1.2 Positive matrix factorization

To allocate organic aerosol (OA) to different sources, the positive matrix factorization (PMF) model (Paatero, 1997) was applied. PMF is a statistical method that converts mass spectra of OA into a linear combination of several factor profiles. Thus, it separates several time series together with the corresponding mass spectra profiles (Fig. 4). In short, PMF is based on organic mass spectra represented in a matrix system (x) together with source profiles and sub-matrices of time series (f and g):

$$x_{ij} = \sum_p g_{ip} . f_{pj} + e_{ij}, \quad (6)$$

where x_{ij} stands for various elements of the matrix x, p represents the number of investigated factors, f_{pj} and g_{ip} are elements of matrices f and g, respectively. The last element in the equation is a residual.

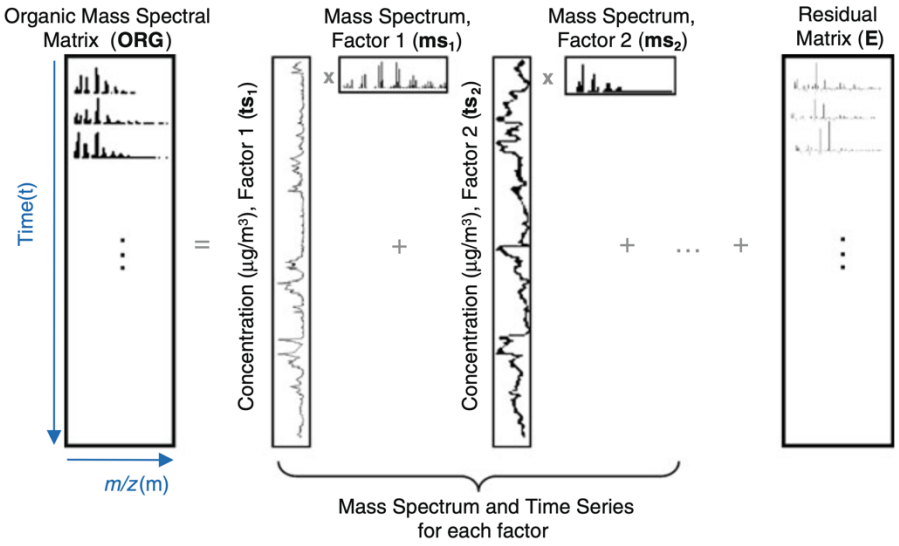

Fig. 4. Schematic diagram of the positive matrix factorization model (Zhang et

al., 2011).

2.2.1.3 Procedure for performing PMF analysis

All PMF analyses were carried out by following a standardized procedure. Matrixes were created using the Igor (IgorPro 6.37) tool to display *m/z* signal intensity and errors. After eliminating outliers, PMF is conducted to identify results with 2 to 8 factors, giving an initial insight into the potential number of factors and their consistency. This step also assesses the accuracy of the error matrix and determines if any adjustments need to be made to individual *m/z* signals.

The next phase involves constraining the first factor profile based on known traffic related hydrocarbons like OA (HOA). If this factor remains stable, exhibits recognizable rush hour peaks in diurnal patterns and correlates with external time series of BC, NO or NOx, then HOA can be considered a relevant source for the study. Subsequently, attention shifts to investigating biomass burning related OA (BBOA). If no distinctive BBOA spectra are detected at this stage, an external profile from previous research is required for reference. If the intensity of *m/z* 60 ($C_2H_4O^+$) accounts for at least 0.3% of the entire spectrum, according to specified criteria, biomass burning is identified as the source (Crippa et al., 2014; Paglione et al., 2020). Further indicators that support the designation of these signals as suggestive of BBOA include *m/z* 29 ($C_2H_5^+$) and 73 ($C_3H_5O_2^+$), which are particularly associated with the mass spectrum of levoglucosan, a byproduct of burning wood (Weimer et al., 2008a).

Understanding the levels of oxygenated organic aerosols (OOA) is crucial. Sometimes, it's feasible to distinguish between less oxidized OA (LOOA) and more oxidized OA (MOOA). LOOA is often linked to aerosols produced through the partitioning process of biogenic volatile organic compounds (BVOCs), while its anthropogenic origin is also well documented. A key marker for LOOA identification is *m/z* 43 ($C_3H_7^+$, $C_2H_3O^+$), and its intensity in relation to *m/z* 44 is important. Unfortunately, PMF doesn't allow for a detailed analysis of LOOA sources. On the other hand, MOOA is typically associated with long-range organic aerosols, identified by increased signals at *m/z* 18 (CH_6^+), 28 (CO^+), and 44 (CO_2^+). These are highly oxidized, internally mixed, and do not have a characteristic diurnal pattern

Following this investigation, additional organic aerosols may come into play. The presence of cooking related OA (COA) can be verified by introducing an additional factor with a constrained profile. Confirmation could be attained by observing if the diurnal trend of COA shows increased mass concentrations during lunch and dinner hours. The principal COA marker, *m/z*

41, is complemented by elevated signal intensities at *m/z* 43, 55, and 57, which correspond with the impact of biomass burning. Additionally, local organic aerosols (LOA) might be detected in certain instances, often tied to local fires, pollution events or nearby industrial emissions.

Once the suitable solution for atmospheric OA is identified, it's essential to carry out a statistical analysis. To achieve this, 1000 runs are conducted in the 'robust mode', where time series are randomly rearranged. If the data collection period spans over several months or includes multiple seasons, the 'moving window' mode should be opted for. In this mode, only two weeks of data per run are examined and then shifted by 1 or 2 days. This approach not only helps in assessing the uncertainty of each source but also provides insights into the changes occurring within them.

2.2.2 Light absorption by aerosol particles

2.2.2.1 Measurement of light absorption by Aethalometer

The Aethalometer (AE31 Magee Scientific), was used as an instrument to quantify the mass concentration of equivalent black carbon (eBC) in aerosol particles. The operating principle of the device, which is explained in Arnott et al., (2005), is based on measuring the attenuation of light intensity passing through a filter containing aerosol particles. Essentially, the aethalometer takes measurements at regular intervals, which are facilitated by the continuous accumulation of aerosol particles on the filter. The complicated operation of the device is that the light intensity is measured both in the presence (sample) and absence (control) of aerosol particles on the filter. The perceptible contrast in these intensities is directly proportional to the mass concentration of eBC. Sample concentration is significantly influenced by the filter's selected surface area; a smaller area yields a more concentrated sample, while a larger size disperses the sample across a greater area.

Notably, the surface area of the filter has a major impact on how quickly the filter fills. Reduced surface area increases the rate at which filters fill and so requires more frequent filter replacements, but also improves measurement accuracy. For the purposes of this investigation, filters with a 0.5 cm^2 sample area were carefully chosen for Aethalometer observations. This intentional decision is in line with the goal of achieving the highest level of precision possible when determining the eBC mass concentration. Because of the Aethalometer's versatility, measurements were made at seven different wavelengths in this study: 370, 470, 520, 590, 660, 880, and 970 nm. Most importantly, the measurement of the mass concentration of eBC precisely takes place at a wavelength of 880 nm.

The fact that the Aethalometer can measure at many wavelengths demonstrates its adaptability and ability to detect subtle variations in light intensity attenuation throughout the electromagnetic spectrum. This thorough technique helps improve the accuracy of eBC mass concentration estimates and enables a more sophisticated understanding of the aerosol composition. The careful examination of several wavelengths is consistent with the complexity of aerosol characteristics, since varied behaviours may be displayed by various particle sizes and compositions in response to different light wavelengths. As a result, employing a multi-wavelength technique strengthens the stability of the Aethalometer's readings and improves the accuracy of eBC mass concentration calculations.

2.2.2.2 Evaluation of parameters related to light absorption

The measurement of light intensity (I_0) is accomplished by assessing the light beam that traverses the control region of the filter. Simultaneously, I denote the intensity measured when the laser beam passes through the filter holding the deposited BC sample. The attenuation of light intensity (*Atn*) can be expressed through the following equation:

$$Atn = C \cdot \ln(I_o/I) \tag{7}$$

A spot on the filter that is hardly visible is represented by an attenuation value of *Atn* = 1, whereas a spot with a dark grey colour is represented by *Atn* = 100. In the visible spectrum, BC absorption of light decreases with increasing wavelength. The following equation provides a mathematical expression for the attenuation of light intensity at the wavelength λ under investigation:

$$Atn\ (\lambda) = \mathrm{MAC}\left(\frac{1}{\lambda}\right).\mathrm{BC} \tag{8}$$

In this context, BC represents the mass concentration of black carbon, while MAC (1/λ) denotes the mass absorption cross-section (λ), a parameter dependent on the wavelength and specific to the absorbing material. Another optical measure that is frequently used is the light absorption coefficient, or b_{abs}. The Beer-Lambert law introduces this parameter:

$$I = I_o e^{(-b_{abs}x)} \tag{9}$$

In the provided framework, I and I_0 denote the previously determined light intensities, b_{abs} is the light absorption coefficient, and x denotes the light transition layer thickness. The following is an analogous expression for the light absorption coefficient:

$$b_{abs}(\lambda) = \frac{MAC\ \left(\frac{1}{\lambda}\right)}{100}.BC \tag{10}$$

The light attenuation coefficient (b_{Atn}) is another useful measure that is used. The change in light attenuation during a normalized time interval Δt is reflected in this coefficient. The amount of b_{Atn} depends on the surface area A of the sample deposited on the filter as well as the airflow rate Q that enters the device.

$$b_{Atn} = \frac{A}{Q}\frac{\Delta Atn}{\Delta t} \tag{11}$$

Therefore, the three main factors that are being assessed while assessing the light absorption properties of aerosol particles are BC concentration, light intensity attenuation, and absorption coefficients.

Nevertheless, there are structural flaws in the methods that underlie the Aethalometer's functioning that need to be fixed. First of all, the presence of filter fibers attenuates light, which in turn causes an artificially higher BC mass concentration. A second challenge arises from light attenuation caused by scattering from deposited aerosol particles, where the scattering is erroneously interpreted as increased light absorption in the final calculations. The third problem, called the shadowing effect, arises when a significant quantity of BC is deposited on the filter. This causes some particles to block one another, which results in measures of light attenuation that are understated. It becomes vital to include extra parameters and modify current formulations in order to address these disparities and provide appropriate values in the computations. Weingartner et al., (2003) suggested adding further C and R(*Atn*) parameters to the calculation of the light absorption coefficient:

$$b_{abs} = b_{Atn}\frac{1}{C \cdot R(Atn)} \tag{12}$$

Here, C denotes the calibration factor, elucidating the multiple scattering of the filter beam utilized in measurements. The calibration factor, C, is mostly

determined by the type of filter used and the particular equipment used. However, the objective of the parameter R is to adjust for measurement errors caused by settling particles. The amount of deposited aerosol particles affects the function R(*Atn*). R is set to unity for any unutilized filters.

Numerous experiments have revealed that C values can range between 1.9 and 3.3, as documented in studies by Di Ianni et al. (2018) and Weingartner et al. (2003). It is noteworthy that the correction parameter C doesn't change when measured at various wavelengths. On the other hand, R could show wavelength dependency. Upon examining the R parameter, it was noted that its fluctuation is dependent upon *Atn*:

$$b_{Atn} = b_{10\%} R(Atn) \tag{13}$$

Here, the light attenuation coefficient b_{Atn}, for which 10% is the value of *Atn*, is approximated as $b_{10\%}$. The following equation, then, provides a mathematical expression for the parameter R:

$$R(Atn) = \left(\frac{1}{f} - 1\right) \frac{\ln(Atn) - \ln(10\%)}{\ln(50\%) - \ln(10\%)} + 1 \tag{14}$$

In this equation, the variable *f* represents a function that characterizes the slope of the curve, with its values varying for each wavelength and season (Sandradewi et al., 2008). After $R_{(Atn)}$ is calculated, it is possible to improve the formula for the mass concentration of BC:

$$BC = \frac{b_{abs}}{\sigma_{abs}} = \frac{b_{Atn}}{\sigma Atn \cdot \mathrm{R}(Atn)} + 1 \tag{15}$$

Nevertheless, upon further investigation, it was revealed that this correction in the calculations is valid at 880 nm but tends to underestimate multiple scattering at shorter wavelengths.

In addition to the main parameters, additional parameters are necessary for a more detailed analysis. If we graphically represent the dependence of the light absorption coefficient on the wavelength, we will observe a decreasing curve in the direction of increasing wavelength. Such a change can be written as a gradual dependence on the wavelength, and the resulting quantity is called the absorption Angstrom exponent (AAE). AAE indicates the negative coefficient of variation of the light absorption curve on a logarithmic scale.

AAE is proportional to the light absorption coefficient and can be expressed as an index of the power of the wavelength λ:

$$b_{abs} \propto \lambda^{-AAE} \tag{16}$$

The AAE value is computed by utilizing the ratio of light absorption coefficients at two specified wavelengths:

$$\mathrm{AAE} = -\frac{ln\left(\frac{b_{abs\lambda_1}}{b_{abs\lambda_2}}\right)}{ln\left(\frac{\lambda_1}{\lambda_2}\right)} \tag{17}$$

The research indicates that the principal combustion product may be identified with the use of AAE values (Zotter et al., 2017; Qin et al., 2018; Pauraitė et al., 2022; Minderytė et al., 2022; Byčenkienė et al., 2023). AAE values between 0.8 and 1.1 are representative of common aerosol particles that come from transportation sources. On the other hand, somewhat higher AAE values (1.2 to 2.9) are linked to BC from biomass burning and biofuels. The maximum AAE values (AAE > 3.6) are used to determine BrC. According to Qin et al. (2018), the wavelength dependency approach is used to estimate the light intensity factor for BrC.

$$\mathrm{b_{abs,BC}(370nm)} = \mathrm{b_{abs}(880nm)} - \left(\frac{880}{370}\right)^{\mathrm{AAE_{BC}}} \tag{18}$$

$$\mathrm{b_{abs,BrC}(370nm)} = \mathrm{b_{abs}(370nm)} - \mathrm{b_{abs,BC}(370nm)} \tag{19}$$

The specified AAE value for black carbon light absorption (AAE_{BC}) is set at 1 (Sandradewi et al., 2008). The light absorption coefficient ($b_{abs,BrC}$) for BrC is calculated at 370 nm since it is not significant at 880 nm. Sandradewi et al., (2008) introduced the Aethalometer model, which was used to evaluate transport-derived organic aerosols (OA). This particular model serves to enable the separation of black carbon mass concentration related to emissions from transportation (BC_{TR}) and biomass burning (BC_{BB}):

$$\mathrm{b_{abs,BC_{TR}}(880nm)} = \frac{\mathrm{b_{abs}\,(470nm)} - \left(\frac{470}{880}\right)^{\mathrm{AAE_{TR}}}}{\left(\frac{470}{880}\right)^{\mathrm{AAE_{BB}}} - \left(\frac{470}{880}\right)^{\mathrm{AAE_{TR}}}} \tag{20}$$

$$b_{abs,BC_{BB}}(880nm) = \frac{b_{abs}(470nm) - \left(\frac{470}{880}\right)^{AAE_{BB}}}{\left(\frac{470}{880}\right)^{AAE_{TR}} - \left(\frac{470}{880}\right)^{AAE_{BB}}} \quad (21)$$

According to Zotter et al. (2017), AAE_{TR} and AAE_{BB} stand for the AAE values in this context that relate to transport and different biomass burning sources, with values of 0.9 and 1.68, respectively.

2.2.2.3 MAC value assignment for different OA sources

Estimating the specific contribution of each source to light absorption is possible once the PMF model has determined the main sources of organic aerosols (OA). A multiparametric regression equation was presented by Qin et al., (2018) to calculate the contribution of each unique OA source to the light absorption coefficient of brown carbon (BrC):

$$b_{abs,BrC} = a \cdot [OA_1] + b \cdot [OA_2] + \cdots + r, \quad (22)$$

Here, the mass concentrations of different organic aerosols (OA) are denoted by $[OA_1]$ and $[OA_2]$, and their corresponding mass absorption cross-section (MAC) values are indicated by the multipliers a and b. The residue (r) is assigned a BrC light factor value that is not associated with any particular OA.

2.2.3 Particle number concentrations and size distribution method by Aerosol particle sizer (APS)

For particle number size distribution within a size range from 0.5 to 10.0 μm and number concentration assessment, an aerodynamic particle sizer (APS—model 3221, TSI Inc., USA, 2004) was used. It is worth noting that while the APS accurately determines the aerodynamic diameter for most aerosol particles (Bartley et al., 2000), its counting efficiency (CE) exhibits variability and is influenced by particle size, as demonstrated by Preifer et al. (2016). For $PM_{2.5}$ and PM_{10} calculation, we estimated the aerosol mass-weighted aerodynamic concentration by utilizing the APS data, which provided number-weighted particle size distributions (Peters et al., 2006; Pauraitė et al., 2021).

$$dM_{D_{ae}} = dN_{D_{ae}} \frac{\pi}{6} D_{ae}^{3} \left(\frac{\rho_o C_{ae} x}{C_{ve}}\right)^{3/2} \frac{1}{(\rho_p)^{1/2}} \quad (23)$$

Where, D_{ae} Where, D_{ae} is the aerodynamic diameter, dN_{Dae} differential number concentration for a given aerodynamic diameter, ρ_p is the density of the particle, D_{ve} is the volumetric equivalent diameter which can be calculated from the definition of terminal velocity (Hinds, 1998), ρ_0 is unit density (1 g cm^{-3}), *X* is the dynamic shape factor, C_{ae} – Cunningham correction factor associated with aerodynamic diameter, and C_{ve} – Cunningham correction factor associated with volume equivalent diameter (Zhou et al., 2017). The aerodynamic diameter is converted into the volumetric equivalent diameter for this purpose. According to (Salcedo, 2006), the aerosol particle density, ρ_p, was estimated to be 1.80 g cm^{-3}, and the shape factor *X* was also assumed to be 1.9 (Park et al., 2004).

2.2.4 Air Mass Backward Trajectories Techniques

The TrajStat software, presented by Wang et al., (2009), includes trajectory statistics and a geographic information system. This system uses a Potential Source Contribution Function (PSCF) model to determine the proportion of pollution pathways within a given study area. The weighted PSCF (WPSCF) is used to measure the impact on the concentration of a particular object, with higher values indicating a greater impact (Guo et al., 2021). However, a limitation of the WPSCF is that it is unable to represent trajectories associated with specific pollution levels, as noted by Ashbaugh et al., (1985). To overcome this limitation, the Concentration-Weighted Trajectory (CWT) method developed by Hsu et al., (2003) is used. This method calculates the weighted trajectory concentration and provides a more nuanced understanding of the pathways of air masses with elevated concentrations of organic aerosols (OA) and black carbon (BC) over a 72-hour period. The main objective of this study is to identify the trajectories of air masses with elevated OA and BC concentrations arriving at the measurement site and to determine the geographical source regions of OA and BC. To achieve this, three different methods are used to analyse the trajectories: cluster analysis, PSCF and CWT. The spatial domain of the study covers latitudes from 35° to 75° North and longitudes from -30° to 75° East, with a resolution of 0.3° × 0.3°. The meteorological data required for the Hybrid Single-Particle Lagrangian Integrated Trajectory (HYSPLIT) model are taken from the NCEP/NCAR Reanalysis Archive, which allows analysis on a global scale. This data enables the calculation of backward trajectories for air masses

arriving at the measurement site every hour between 00 and 23 UTC. The HYSPLIT model, which was developed by Draxler et al. (1998), uses the NCEP/NCAR Reanalysis Archive to determine the backward movements of the air masses. These trajectories are calculated at an hourly interval and originate at an arrival altitude of 20 meters above ground level (AGL), as defined by Guo et al. (2021). With this approach, the study aims to decipher the intricate pathways by which air masses with elevated concentrations of OA and BC traverse the studied geographic extent.

3 RESULTS AND DISCUSSION

3.1 Identification of NR-PM_1 and eBC sources in different environments

In order to investigate NR-PM_1 and eBC sources in different environments, the measurements were performed at different locations: Rūgšteliškis (rural), and Vilnius (urban) in Lithuania, and Quezon city east avenue (urban) and Manila port in Philippines. The NR-PM_1 measurement were carried by using ACSM and eBC measurement were performed by using AE in all measurement sites.

3.1.1 NR-PM_1 and eBC sources in Rūgšteliškis rural environment

The NR-PM_1 measurements were conducted over a 5-year period (2013, 2014, 2016, 2018, and 2019) (Fig. 5A and Table 4), while eBC measurements were carried out for 4 years (2013, 2014, 2018, and 2019) at the rural background site of Rūgšteliškis, Lithuania (Fig. 6A and Table 4).

Table 4. The average with standard deviation (Avg/SD), 25th and 75th percentiles (Q1 and Q3, respectively), minimum and maximum (Min and Max, respectively) of NR-PM_1 and eBC mass concentrations (μg/m^3) observed at four sites during measurement campaign.

	NR-PM_1				**eBC**			
	Rugšteliškis	Vilnius	Quezon	Manila	Rugšteliškis	Vilnius	Quezon	Manila
Avg	8.48	18.98		29.52	0.60	2.46	36.19	10.27
SD	5.25	11.82		19.62	0.41	1.99	16.02	5.99
Min	1.32	0.73		11.72	0.05	0.09	6.14	1.11
Q1	4.37	9.77		15.22	0.30	1.02	25.26	5.77
Q2	7.56	17.40		24.15	0.49	1.89	32.61	9.20
Q3	11.44	25.56		39.66	0.81	3.19	43.65	13.71
Max	33.01	64.96		108.38	2.71	14.59	104.54	35.82

The hourly average time series results indicated that higher concentrations of organic aerosol (OA) particles were observed, with a mean concentration of 29.20 μg/m³, contributing approximately 76.7% to the total NR-PM_1 mass. In contrast, lower concentrations and contributions were recorded for inorganic aerosol (IA) species: SO_4^{2-} (6.60 μg/m³; 15%), NO_3^- (4.40 μg/m³; 10%), NH_4^+ (2.80 μg/m³; 7%), and Cl^- (0.48 μg/m³; 1%) during the years 2013, 2014, 2016, 2018, and 2019 (Fig. 5A and Table 5). Similar results were reported in various long-term studies related to the chemical composition of aerosol particles in a forest environment by Heikkinen et al. (2020), Keskinen et al. (2020); and Kourtchev et al. (2013). Their results

showed a higher contribution of organic aerosols in summer (80 – 88%) than autumn (74 – 78%).

Table 5. The hourly average of NR-PM_1 and eBC mass concentrations ($\mu g/m^3$) observed during 2013, 2014, 2016, 2018 and 2019 at Rūgšteliškis (rural site).

Years	OA ($\mu g/m^3$)	SO_4^{2-} ($\mu g/m^3$)	NO_3^- ($\mu g/m^3$)	NH_4^+ ($\mu g/m^3$)	Cl^- ($\mu g/m^3$)	eBC ($\mu g/m^3$)
2013	21	7	4	4	1	0.54
2014	18	7	5	2	0.2	0.41
2016	32	4	3	1	0.8	---
2018	30	8	6	5	0.2	0.73
2019	45	7	4	2	0.2	0.71
Total average	29.20	6.60	4.40	2.80	0.48	0.60

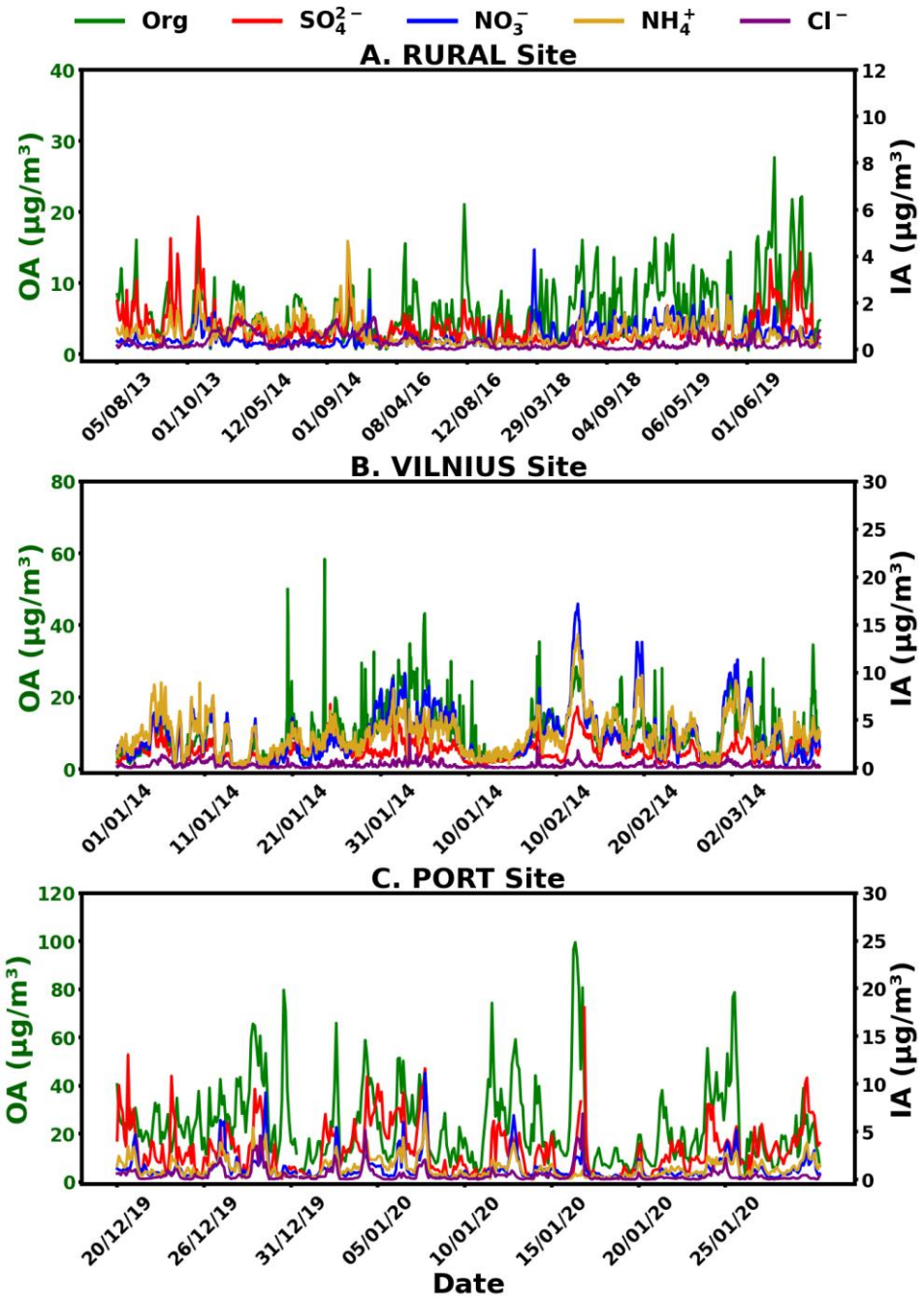

Fig. 5. The hourly average time series of OA, SO_4^{-2}, NO_3^-, NH_4^+, and Cl^- at Rūgšteliškis rural site (Lithuania) (A), Vilnius city site (Lithuania) (B), and Manila port site (Philippines) (C).

The hourly average time series analysis of equivalent black carbon (eBC) mass concentration indicated higher levels in 2018 (0.73 μg/m^3) and 2019 (0.71 μg/m^3) compared to the concentrations observed in 2013 (0.54 μg/m^3) and 2014 (0.41 μg/m^3) (Fig. 6A and Table 5). The findings of this research also resemble with the previous studies such as Masalaite et al. (2022); Cui et al. (2021), Yttri et al. (2019); Pauraitė et al. (2015); Yttri et al. (2011), Bycenkiene et al. (2011) and Carvalho et al. (2006). These earlier works similarly reported daily average seasonal trends that confirm the impact of local biomass burning and long-range transport on BC concentrations. Our comparison extends to other European rural sites, as outlined in Table 6, which indicated that local biomass burning and long-range transport enhance eBC concentration at rural background sites in Europe, especially during cold periods. These findings provide valuable insights into the temporal variations of both OA and IA, as well as eBC, at the specified rural background site.

Table 6. The daily average of eBC mass concentration values at the different European rural background sites carried out during different time periods.

Site	Measurement Period	Warm period (Spring, Summer), eBC (μg/m^3)	Cold Period (Autumn, Winter), eBC (μg/m^3)	Instrument	Reference
Rugšteliškis (Lithuania)	2013-2019	0.56	0.72	(AE31)	(This Study)
Rugšteliškis (Lithuania)	15 May- 27 Sep 2014	0.11		(AE33)	Masalaite et al. (2022)
Rugšteliškis (Lithuania)	May 2013 to October 2014	0.40	0.77	(AE33)	Pauraitė et al. (2015)
Hyltemossa (Sweden)	01 Jan - 31 Dec 2018	0.22		(AE33)	Ahlberg et al. (2023)
Złoty Potok (Poland)	01 January–31 March 2013 and 20 April–31 July 2019	0.79	2.17	(AE33)	Błaszczak et al. (2020)
Montelibretti (Italy)	2002-2003	1.03		(AE33)	Yttri et al. (2019)
Ispra (Italy)	2002-2003	1.50		(AE33)	
Payerne (Switzerland)	2002-2003	0.66		(AE33)	
K-puszta (Hungary)	2002-2003	0.77		(AE33)	
Košetice (Czech Republic)	2002-2003	0.32		(AE33)	
Melpitz (Germany)	2002-2003	0.40		(AE33)	
Mace Head (Ireland)	2002-2003	0.11		(AE33)	
Lille Valby (Denmark)	2002-2003	0.37		(AE33)	
Birkenes (Norway)	2002-2003	0.10		(AE33)	
Hyytiälä (Finland)	2007-2008	0.15	0.20	(AE33)	Aurela et al. (2011)
Hyytiälä (Finland)	Dec 2004 to Dec 2008	0.28	0.36	(AE33)	Hyvärinen et al. (2011)

Vavihill (Sweden)	0 Aug - 02 Sept 2009	0.30		(AE33)	Yttri et al. (2011)
Streithofen (Austria)	Jun. 1999 to May 2000		1.8	(AE31)	Carvalho et al., (2006)

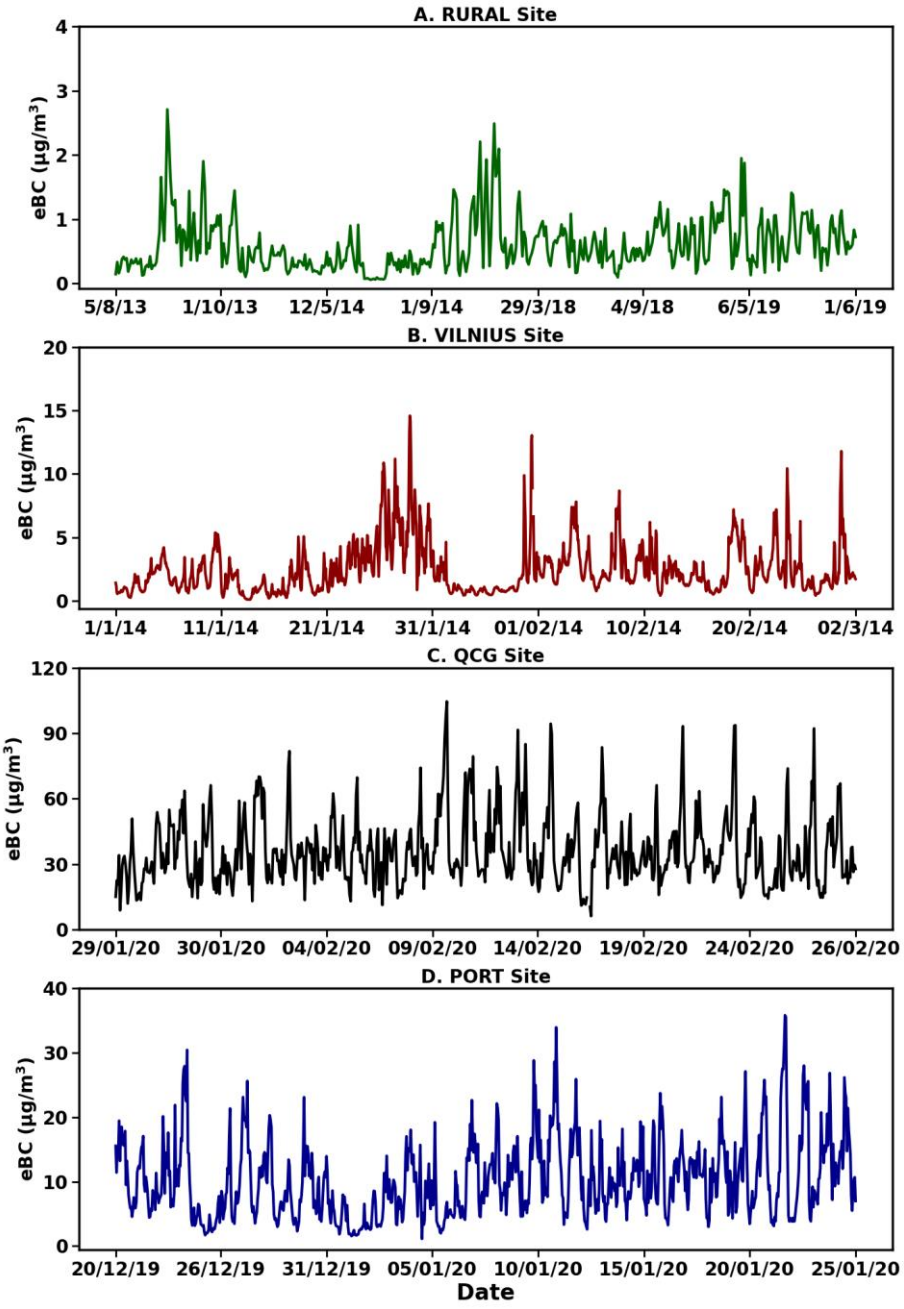

Fig. 6. The hourly average time series of eBC mass concentration at

Rūgšteliškis rural site (Lithuania) (A) (Green), Vilnius city site (Lithuania) (B) (Red), Quezon city site (Philippines) (C) (Black) and Manila port site (Philippines) (D) (Blue).

The calculated yearly averages of NR-PM_1 mass concentration were 8.37 μg/m^3, 6.67 μg/m^3, 4.91 μg/m^3, 9.86 μg/m^3 and 13.45 μg/m^3 for the years 2013, 2014, 2016, 2018, and 2019, respectively (Fig. 7A). These results revealed that the overall average NR-PM_1 concentrations were higher in the more recent years, with 9.86 μg/m^3 in 2018 and 13.45 μg/m^3 in 2019, compared to 8.37 μg/m^3 in 2013, 6.67 μg/m^3 in 2014, and 4.91 μg/m^3 in 2016. In five years, the total average of NR-PM_1 concentration was examined for spring (9.07 μg/m^3), summer (8.75 μg/m^3), and autumn (6.99 μg/m^3) (Fig. 7A). Notably, spring exhibited higher NR-PM_1 concentrations (9.07 μg/m^3) compared to summer (8.75 μg/m^3) and autumn (6.99 μg/m^3). However, the highest NR-PM_1 mass concentration was observed during the spring of 2018 (9.23 μg/m^3) and 2019 (14.20 μg/m^3). In contrast, the highest NR-PM_1 mass concentrations in 2013, 2016, and 2018 were observed during the summer seasons (8.53 μg/m^3, 6.21 μg/m^3, and 10.88 μg/m^3, respectively). Lower NR-PM_1 levels were noted during the autumn seasons of 2013 and 2016 compared to 2014 and 2018. These variations may be attributed to meteorological conditions, with higher NR-PM_1 levels associated with warmer temperatures, lower relative humidity, and stronger wind speeds during spring and summer (Heikkinen et al., 2020; Keskinen et al., 2020; and Kourtchev et al., 2013).

Over the course of four years, the total seasonal average eBC concentration was examined for spring (0.66 ± 0.56 μg/m^3), summer (0.46 ± 0.34 μg/m^3), and autumn (0.72 ± 0.58 μg/m^3) (Fig. 7E). Among these, autumn had a higher concentration than the other two seasons. Notably, the autumn presented the higher average concentration across the studied years such as 2013 (0.78 ± 0.62 μg/m^3), 2014 (0.56 ± 0.43 μg/m^3) and 2018 (0.82 ± 0.57 μg/m^3) (Fig. 7E). This increase in autumn is primarily attributed to the start of the heating season, during which there is a significant rise in the combustion of solid fuels like wood, coal, and biomass for domestic heating. The burning of these materials releases a substantial amount of black carbon into the atmosphere. Additionally, the stable atmospheric conditions typical of autumn, characterized by less wind and reduced vertical mixing in the air, also contribute to higher concentrations of black carbon as pollutants remain closer to the ground and disperse more slowly (Ahlberg et al., 2023). In the spring season, higher concentration of eBC was observed in 2018 and 2019, averaging 0.84 ± 0.65 μg/m^3 and 0.75 ± 0.40 μg/m^3, respectively. These values were approximately 27% and 14% higher than the overall spring seasonal average (0.66 ± 0.56 μg/m^3), and 83% and 63% higher than the summer seasonal average (0.46 ± 0.34 μg/m^3). Although autumn generally exhibited

the highest seasonal average eBC concentration (0.72 ± 0.58 μg/m³), spring values in 2018 and 2019 were comparable to, or even exceeded, autumn levels in some years such as 2014 (0.56 μg/m³) and 2018 (0.82 μg/m³). These elevated concentrations may be influenced by meteorological conditions that contribute to increased atmospheric stability and reduced dispersion of pollutants. For example, lower temperature and higher relative humidity can facilitate to trap pollutants near the surface and create an environment favourable to secondary organic aerosol formation, which may contain eBC and increase its atmospheric loading (Błaszczak et al., 2020; Aurela et al., 2011). In addition to that biomass burning and long-range transport, also contribute to the seasonal increase in eBC concentrations (Bycenkiene et al., 2011; Pauraitė et al., 2015). In contrast, the summers of 2013, 2014, 2018, and 2019 exhibited lower eBC concentrations (0.31 μg/m^3, 0.28 μg/m^3, 0.55 μg/m^3, and 0.68 μg/m^3 respectively than spring and autumn. This leads to increased vertical mixing in the atmosphere and, combined with enhanced precipitation, facilitate the washout of aerosol particles, thereby reducing atmospheric eBC levels Hyvärinen et al. (2011). Furthermore, reduced use of residential heating and lower agricultural burning during the summer contribute to decreased eBC emissions The growth of summer vegetation also assists in capturing airborne particles, further contributing to lower eBC concentrations (Cui et al., 2021). At the Rugšteliškis rural site, interannual contrasts between summer and other seasons suggest that cooler (average temperature around 14 °C) and more humid conditions (relative humidity averaging 74%) are strongly correlated with elevated eBC levels. These conditions, more prevalent in spring and autumn, limit atmospheric dispersion and promote pollutant accumulation near the surface.

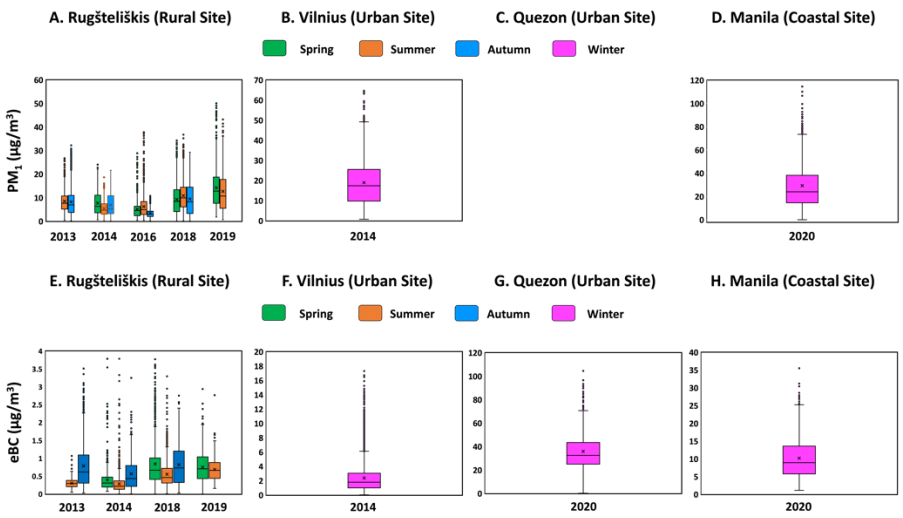

Fig. 7. NR-PM_1 (A, B, and D respectively) and eBC (E, F, G, and H respectively) mass concentrations during four seasons (spring, summer, autumn and winter) at Rūgšteliškis rural site (Lithuania), Vilnius city site (Lithuania), Quezon city site (Philippines) and Manila port coastal site (Philippines). In the box plots, the boundary of the box closest to zero indicates the 25th percentile, a black line within the box marks the median, a (×) sign within the box marks the mean, and the boundary of the box farthest from zero indicates the 75th percentile. Whiskers above and below the box indicate the 10th and 90th percentiles. Points above and below the whiskers indicate outliers outside the 10th and 90th percentiles.

The diurnal trend analysis of NR-PM_1 and eBC at Rūgšteliškis was conducted for spring, summer, and autumn, as winter data were not available during the measurement campaign. This provides a rural baseline for comparative seasonal evaluation. Results indicated that OA showed higher concentration (8.34 μg/m^3, 6.60 μg/m^3 and 5.62 μg/m^3, respectively) during morning hours (6 a.m. – 8 a.m.) and lower concentration (5.45 μg/m^3, 5.61 μg/m^3 and 4.69 μg/m^3, respectively) during the afternoon (12 p.m. – 3 p.m.) in all the three seasons spring, summer, and autumn respectively (Fig. 8A). Different studies conducted at rural environment revealed that OA higher concentration during the morning hours is due to lower boundary layer heights and remains elevated at night and early morning because of primary emissions and the presence of a relatively stable boundary layer. After sunrise, OA concentrations generally decrease during the daytime, reaching their lowest values between 12 p.m. and 3 p.m. This trend is likely influenced by the reduced formation of secondary organic aerosols (SOA) and a higher atmospheric boundary layer during these hours (Carbone et al., (2017); Li et al., (2019) and Yu et al., (2021); Heald et al., (2005)). Nitrates showed similar trend to organics and presented higher mass concentration (2.46 μg/m^3, 1.02 μg/m^3 and 1.53 μg/m^3, respectively) during morning hours (6 a.m. – 8 a.m.) and lower mass concentration (0.98 μg/m^3, 0.62 μg/m^3 and 0.88 μg/m^3, respectively) during the afternoon (12 p.m. – 3 p.m.) in all the three seasons spring, summer, and autumn respectively (Fig. 8A). A study conducted by Kiendler et al. (2016) and Sobanski et al. (2017) found consistently lower concentration of nitrates throughout the day in rural and suburban areas, attributed to higher planetary boundary layers (PBL). Both studies elucidated that higher morning concentrations due to photochemical processing, indicating a potential link between OA and NO_3^- in rural environments. Sulphates exhibited higher concentrations (0.96 μg/m^3, 1.03 μg/m^3, and 1.36 μg/m^3) during daytime (10 a.m. – 1 p.m.) and lower concentrations (0.67 μg/m^3, 0.82 μg/m^3, and 1.07 μg/m^3) during nighttime (1 a.m. – 4 a.m.) across all three seasons (spring, summer, and autumn) (Fig. 8A). A study carried out in a rural

area by Wang et al. (2016) in a rural area observed diurnal variations in sulphate concentrations, with higher concentration during the daytime as compared to nighttime. The researchers attributed this trend to the photochemical production of sulphate through the oxidation of sulphur dioxide (SO_2) in the presence of solar radiation. Additionally, findings by Kundu et al. (2014) highlighted those various factors such as solar radiation, temperature and PBL dynamics can affect the formation and transformation of sulphate in the atmosphere. These factors can lead to elevated sulphate levels during daylight hours. In addition to natural causes, human activities such as industrial emissions and traffic related pollution near rural regions can also contribute to the increased sulphate levels during the daytime when industrial and transportation activities are at their peak.

Ammonium (NH_4^+) mass concentration, however, did not show any clear diurnal pattern over all three seasons. Retama et al. (2019) stated that NH_3, which is associated with waste disposal, sewage and traffic exhaust, reacts with nitric acid (HNO_3) and sulphuric acid (H_2SO_4) to form SO_4^{2-}, NO_3^- and NH_4^+ particles. Gilardoni et al. (2016) proposed that agricultural operations, including manure management and soil emissions, are responsible for the majority of ammonia emissions worldwide. Ammonium acts as a counter ion that balances the concentrations of NO_3^- and SO_4^{2-}. Therefore, the diurnal trend of NH_4^+ is closely related of NO_3^- and SO_4^{2-} mass concentrations and respond to their variations. As the concentrations of NO_3^- and SO_4^{2-} change due to various factors such as emissions or long-range transport, NH_4^+ concentrations adjust accordingly to maintain equilibrium. For this reason, the diurnal pattern of NH_4^+ does not show significant diurnal pattern because it effectively stabilizes the fluctuations of NO_3^- and SO_4^{2-} concentrations. Previous studies by Mărmureanu et al. (2020), Drugé et al. (2019), and Bauer et al. (2007) suggest that ammonia is generated primarily by agricultural activities, which are less likely to exhibit diurnal trends. This is consistent with the observed behaviour of NH_4^+ in our study, where it does not show a clear diurnal pattern, which is consistent with the role of NH_4^+ as a counter ion to NO_3^- and SO_4^{2-}.

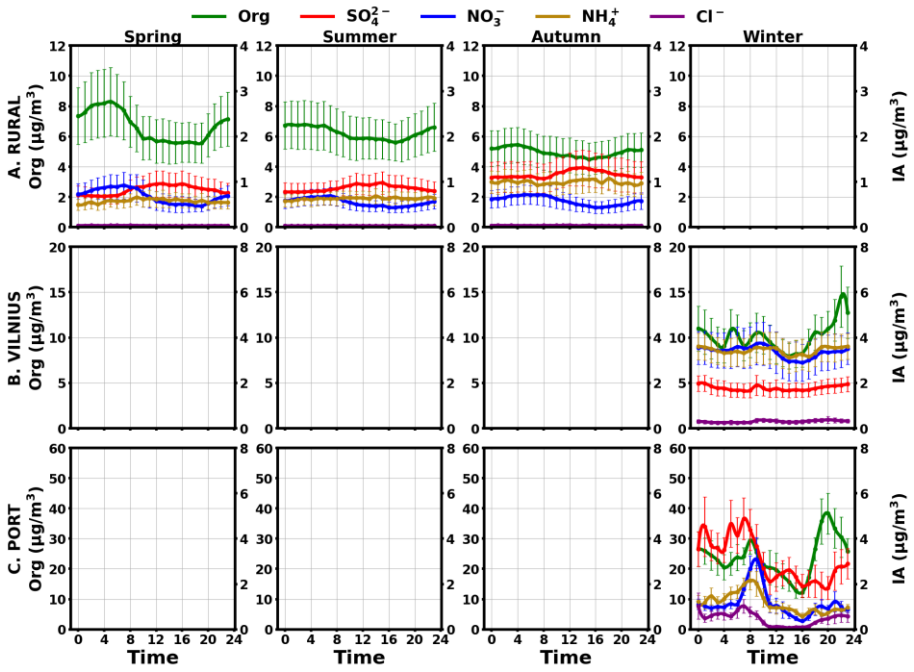

Fig. 8. Diurnal trend of OA and IA (NO_3^-, SO_4^{2-}, NH_4^+ and Cl^-) aerosol particles mass concentration during four seasons (spring, summer, autumn and winter) at Rūgšteliškis rural site (Lithuania) (A), Vilnius city urban site (Lithuania) (B), and Manila Port site (Philippines) (C). The square markers on each data point indicate the standard deviation, showing variability at measurement sites.

The diurnal variation pattern of eBC across the entire measurement period (four years) in spring, summer, and autumn is depicted in Fig. 9A. In each of these seasons, eBC exhibited higher mass concentrations (0.77 µg/m^3, 0.51 µg/m^3, and 0.76 µg/m^3, respectively) during the morning hours (8 a.m. – 12 p.m.) and lower concentrations (0.60 µg/m^3, 0.38 µg/m^3, and 0.60 µg/m^3, respectively) during the late night hours (12 a.m. – 2 a.m.) (Fig. 9A spring, summer, and autumn, respectively). Planetary Boundary Layer Height (PBLH) diurnal trend analysis was conducted for whole study period. The analysis of PBLH shows significant diurnal variation, with lower heights during the early morning and late evening hours. This compaction of the boundary layer could trap pollutants like eBC close to the ground, exacerbating morning peaks especially under stable atmospheric conditions when vertical mixing is minimal. During the day, increasing solar heating raises the PBLH, facilitating pollutant dispersion and contributing to lower eBC concentrations. Moreover, temperature inversions observed during early mornings and late evenings hours further inhibit vertical mixing, intensifying eBC concentrations near the surface. Additionally,

meteorological factor diurnal trend analysis for three different seasons (spring, summer, and autumn) were performed, which indicates that higher temperature, higher wind speed, and lower relative humidity were observed during the daytime. These conditions not only influence the dispersion and dilution of eBC but also correlate with the diurnal cycle of the PBLH, highlighting the meteorological control over pollutant behaviour across different seasons.

Similar findings were noted by Pauraitė et al. (2015), which demonstrated that eBC concentration levels are elevated in the morning, starting to rise from 5 a.m. and reaching a peak at 8 a.m., while the evening levels are reduced due to turbulent mixing and dispersion. Additionally, the concentrations of carbonaceous aerosol particles were found to be almost twice higher during colder periods (0.77 μg/m³) compared to warmer periods (0.40 μg/m³), attributed to seasonal influences and distinct emission sources such as residential biomass heating and the long-range transport of fossil fuel emissions. Furthermore, in the study conducted in Hyltemossa, Sweden, Ahlberg et al. (2023) recorded a climb in eBC concentrations to 0.11 μg/m³ during early morning hours (6 a.m. – 8 a.m.) and a decline to 0.08 μg/m³ after midday (12 p.m. – 3 p.m.). Similarly, Aurela et al. (2011) in Hyytiälä, Finland, observed higher eBC concentrations in the morning at 1.28 μg/m³ (6 a.m. – 9 a.m.) and lower eBC concentration levels in the evening at 0.95 μg/m³ (3 p.m. – 6 p.m.). Hyvärinen et al. (2011) also observed a morning eBC concentration peak of 1.34 μg/m³ (6 a.m. – 9 a.m.) at the Hyytiälä station, which decreased to 1.11 μg/m³ after midday (12 p.m. – 7 p.m.). These peaks were associated with residential wood burning, work-related traffic, and long-range transport, which correspond with observed lower boundary layer heights during these hours. Our study presents a detailed comparative analysis, contrasting the magnitude and timing of diurnal peaks in eBC concentrations within similar rural measurement sites across Europe. For example, the morning peak of eBC concentrations in Lithuania align closely with those observed in Hyytiälä, Finland, but are significantly higher than those in Hyltemossa, Sweden. This discrepancy may be linked to the more prevalent use of wood as a heating source in the Finnish and Lithuanian sites during colder seasons, compared to the Swedish site, where alternative heating methods may be more common. Additionally, the degree to which local versus long-range sources affect these patterns appears to vary among the regions. In Lithuania, the notable reduction in eBC concentrations during the evening hours in colder months suggests a strong influence of local sources like residential heating, which decreases overnight. In contrast, the Swedish data indicate a consistent influence of long-range transport throughout the day, due to its geographic position and prevailing wind directions. These observations underscore that eBC significantly impacts rural environments, influenced variably by local and long-distance sources such as biomass burning, work-related traffic, and long-range transport. This comprehensive comparison underscores the importance of considering local source

variations and atmospheric dynamics when analysing diurnal trends in eBC concentrations.

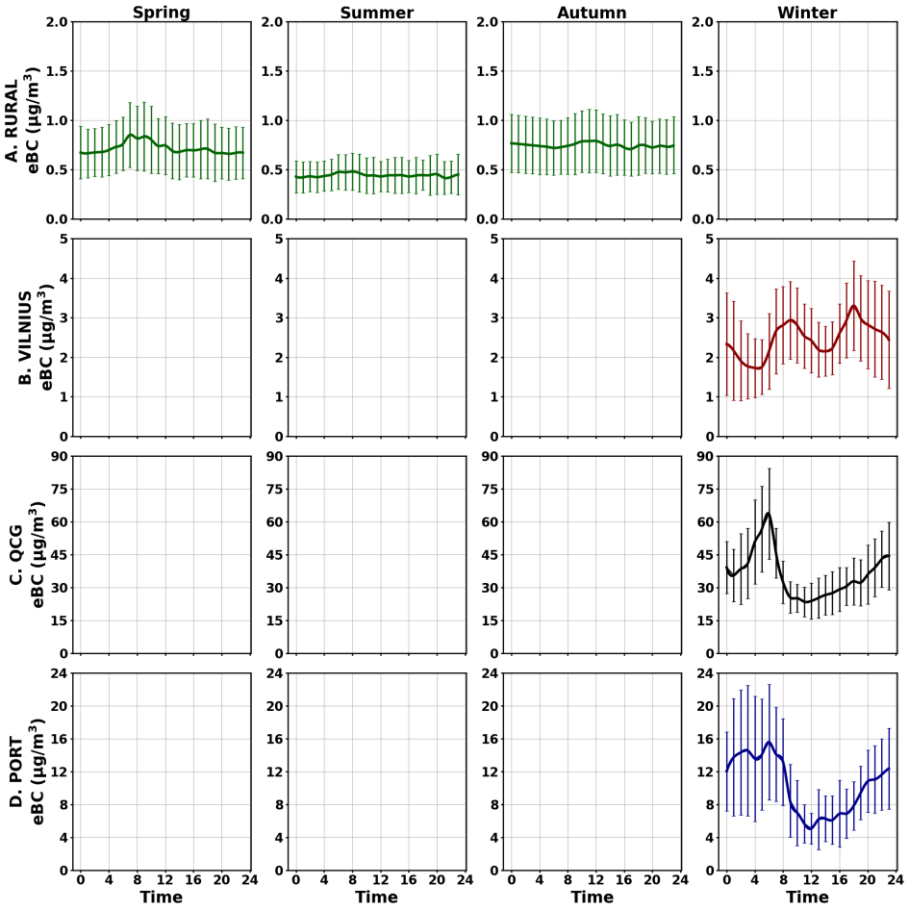

Fig. 9. Diurnal trend of eBC mass concentration during four seasons (spring, summer, autumn and winter) at Rūgšteliškis rural site (Lithuania) (A) (Green), Vilnius city urban site (Lithuania) (B) (Red), Quezon city site (Philippines) (C) (Black), and Manila port coastal site (Philippines) (D) (Blue). The square markers on each data point indicate the standard deviation, showing variability at measurement sites.

The source apportionment of equivalent black carbon (eBC) originating from traffic and biomass burning was rigorously examined by utilizing the Absorption Ångström Exponent for vehicle transport related fossil fuel combustion (AAE_{FF}) and Absorption Ångström Exponent for biomass burning (AAE_{BB}) values, as mentioned in Section 2.2.2.3.

In Figure 10A we present a comprehensive time series of eBC_{FF} and eBC_{BB}, coupled with their respective contributions to the overall eBC mass concentration during four years (2013, 2014, 2018, and 2019) measurement campaign at Lithuanian rural site. The percentage contribution reveals that during the 4-year measurement campaign eBC originating from fossil fuel (eBC_{FF}) accounted for 90% (average mass concentration – 0.52 μg/m³). Whereas eBC originating from biomass burning (eBC_{BB}) accounted for 10% (average mass concentration – 0.06 μg/m³) of the total eBC mass concentration (Fig. 10A). Our findings are in concordance with the results reported by Yttri et al. (2011) and Yttri et al. (2019). Their study, conducted at various European rural locations, indicated that the contribution of fossil-fuel-related black carbon was higher than wood-burning-related black carbon at all sites throughout the sampling period. Another study conducted by Hienola et al. (2013) at Hyytiälä, Finland, demonstrated that within the local and regional emissions, long range transport and domestic combustion (mainly wood burning) are the key sources of black carbon. In addition to that Kupiainen et al. (2006) reported that the main sources of carbonaceous aerosols in European rural areas are emissions from fossil fuel and residential biomass burning.

The persistent dominance of fossil fuel-derived equivalent black carbon (eBC_{FF}), as highlighted by our results, calls for a discussion on the regional efforts aimed at curbing these emissions. As reviewed in multiple studies, the past decade has witnessed numerous policy measures across Europe, including Eastern Europe, aimed at curtailing fossil fuel consumption. As reported by Drewnicki et al. (2024), the European Union's "2020 Climate and Energy Package", which establishes objectives for decreasing greenhouse gas emissions and enhancing energy efficiency, has played a crucial role in influencing fossil fuel consumption patterns. Despite these policy measures, our analysis reveals that substantial levels of eBC_{FF} remain, suggesting that such initiatives may not be fully effective or are implemented inconsistently across different regions. Studies on industrial and economic developments in Eastern Europe, such as those by Radovanović et al. (2022), indicate that the reliance on fossil fuels is still prevalent due to economic limitations, concerns over energy security, and the gradual nature of the shift to renewable resources. Additionally, fossil fuels continue to be a more affordable and readily available energy option, which further impedes the transition to renewable energy sources (Rabbi et al., 2022). These factors significantly contribute to the persistent levels of fossil fuel-derived related eBC. Moreover, Khabarova et al. (2019) discuss the ongoing dependence on outdated, coal-intensive technologies in industries and the slow progress in

modernizing energy sectors, which compounds this challenge. These elements underscore the complex relationship between policy intentions and tangible outcomes in various regional settings.

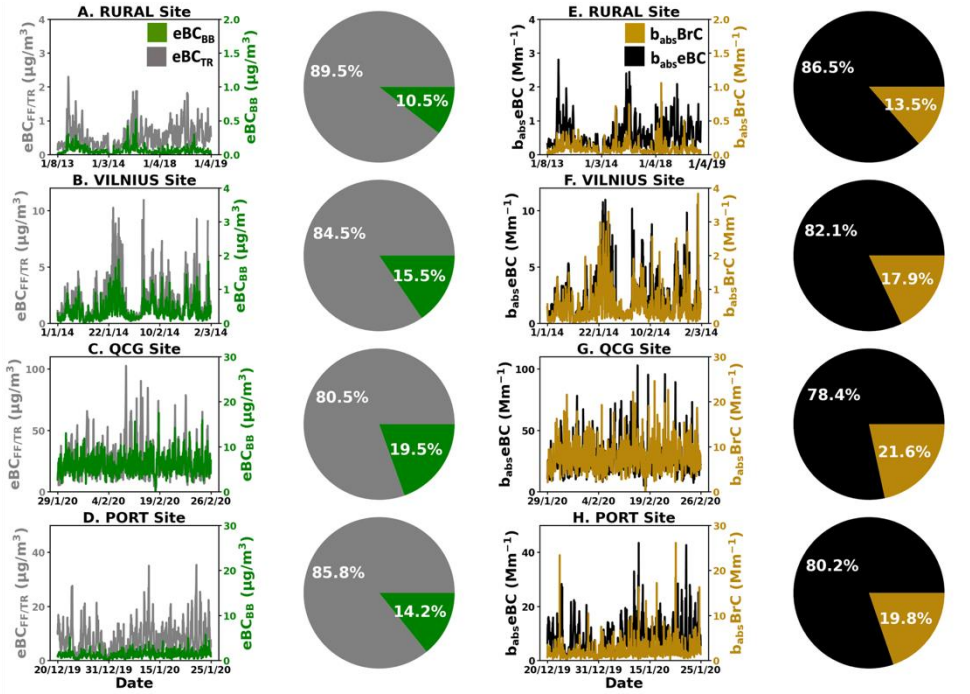

Fig. 10. Time series and contributions of the hourly average $eBC_{FF/TR}$ and eBC_{BB} to the total eBC, as well b_{abs} BrC and b_{abs} eBC to the total b_{abs} (Mm^{-1}) mass concentration at Rūgšteliškis rural site (Lithuania), Vilnius city urban site (Lithuania), Quezon city site (Philippines) and Manila port site (Philippines).

Equivalent black carbon (eBC) and brown carbon (BrC) have different spectral dependences, with brown carbon being expected to strongly absorb in UV range. Figure 10A depicts the time series of the light absorption coefficients of eBC and BrC during four years (2013, 2014, 2018, and 2019) measurement campaign at Lithuanian rural site. The light absorption coefficient of BrC at 370 nm ($b_{abs,\ BrC}$) varied spatially from 0.02 to 0.80 M m^{-1}. The $b_{abs,\ eBC}$ showed slightly higher contribution of 86% (average mass concentration – 0.57 μg/m³) to light absorption at a lower wavelength (370 nm) in 2013, 2014, 2018, and 2019 (Fig 10A). Whereas the contribution of BrC was only 14% (average mass concentration – 0.09 μg/m³) during the measurement campaign (Fig 10E). According to the studies by Liu et al., (2018) and Qin et al., (2018), it is obvious that the major source of BrC was a

biomass burning but there are several other known sources, e.g., biofuel combustion, photo-oxidation of anthropogenic and biogenic volatile organic compounds, or aqueous-phase chemical reactions (Wang et al., 2016; Pokhrel et al., 2017). Our findings are consistent with the results reported by Masalaite et al., (2022) which showed that BrC was affected far more by biomass burning than by biogenic origin sources.

The meteorological parameters along with NR-PM_1 and eBC were systematically recorded at 1-hour intervals throughout the measurement campaign at Rūgšteliškis (rural site), as illustrated in Fig. 11A, 11E, and 11I. Daily average T, RH, WS, WD observed at Rūgšteliškis station are presented in Table 7 (the number after "±" shows standard deviation).

Table 7. The daily average of meteorological factors (relative humidity (RH), wind speed (WS), temperature (T), and wind direction (WD) observed at four sites during measurement campaign.

	Rugšteliškis (Rural site)	Vilnius (Urban site)	Quezon (Urban site)	Manila Port (Coastal site)
RH (%)	74	81	66	69
WD (º)	185.73	156.57	211.90	123.91
WS (m/s)	1.34	1.23	0.33	1.42
T (ºC)	14	2	27	27

The wind rose analysis conducted for NR-PM_1 and eBC revealed predominant wind directions originating from the south (S), southwest (SW), south-southwest (SSW), southeast (SE), south-southeast (SSE), west (W), northwest (NW), and west-northwest (WNW) during the measurement period Fig. 11A. This depiction is derived from 1- or 2-minute wind speed and direction data, showcasing occasional wind speeds exceeding 5 m/s at the measurement site during measurement campaign. Within the wind rose diagram, each segment's length signifies the frequency of winds originating from a specific direction sector over time. Coloured sections within each segment offer insights into the frequency distribution of wind speed ranges. In order to determine the wind direction contributing to the highest NR-PM_1 and eBC concentration levels in Rūgšteliškis during measurement campaign, the NR-PM_1 and eBC concentrations were categorized by wind direction. The Fig. 11E and 11I presents the polar plot which indicated the measured NR-PM_1 and eBC concentrations Rūgšteliškis during measurement campaign. In these plots several additional and interesting features can be seen. The length of the slices represents the frequency of wind blows from a certain direction, and the colour diagram represents the NR-PM_1 and eBC average mass concentration. Wind direction range was described clockwise, for example, north, south- indicates wind range from north to south clockwise. During the whole campaign the prevailing wind direction was from the north, east and south (Fig. 11E and 11I). However, the diagram indicates that the higher NR-PM_1 and eBC concentrations could

be linked with dominant wind directions and higher wind speed from the northern, eastern and southern directions during whole measurement period (Fig. 11E and 11I). These directions may correspond to regional or local sources, for example, agricultural fields and residential areas are located to the south and east of the site, while the north may reflect long-range transport. Consequently, the study infers that organic species, including organic aerosols and organic nitrates, predominantly originate from local sources. In contrast, inorganic aerosol particles, such as inorganic nitrates, ammonium, sulphates, and black carbon, may have originated elsewhere and subsequently been transported to the sampling location. Since, Rūgšteliškis is located far away from the sea, major roads and power plants, there are no volcanoes in the area, and only small amounts of biomass are burned, therefore is very likely that not only inorganic aerosols but also its precursor species are brought by long-range transport to this rural site. Furthermore, source apportionment of eBC revealed that within the local and regional emissions, long range transport and domestic combustion (mainly wood burning) are the key sources of black carbon in rural areas.

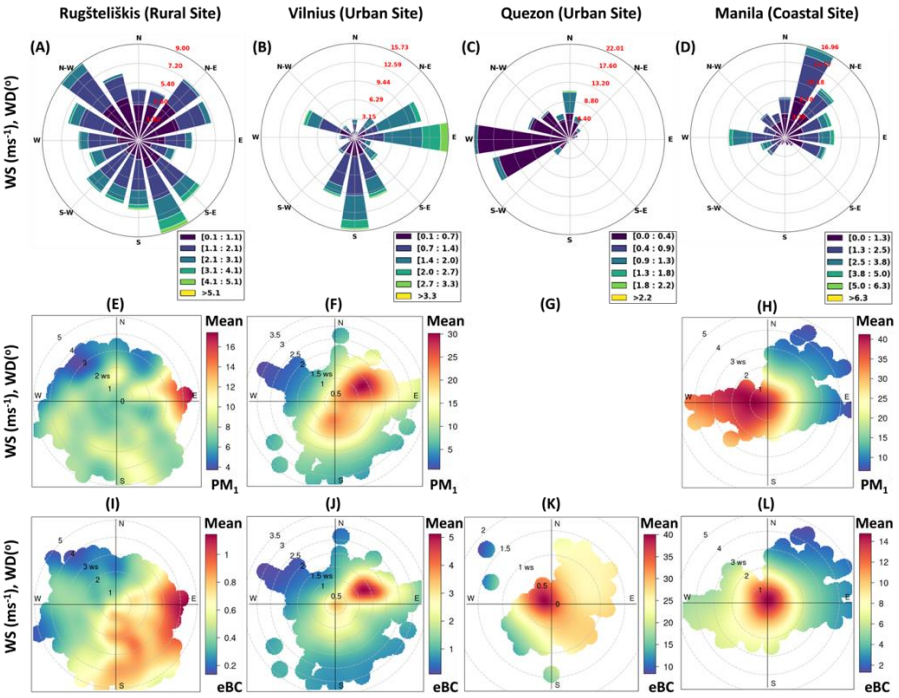

Fig. 11. Wind rose diagrams and open-air polar plots for NR-PM_1 and eBC showing wind speed (WS) and wind direction (WD) frequency at Rūgšteliškis rural site (Lithuania) (A, E, I), Vilnius city urban site (Lithuania) (B, F, J), Quezon urban site (C, K) and Manila port coastal site (Philippines) (D, H, L). The distance from the origin indicates wind speeds in m/s. The wind speed grid lines are presented with black

circles. The colour scales represent the PM_1 concentrations observed with each wind speed and direction combination.

3.1.2 NR-PM_1 and eBC sources in Vilnius urban environment

In the urban environment of Vilnius (Lithuania), measurements of NR-PM_1 and eBC were conducted during the winter of 2014 (January – February) as depicted in Fig. 5B, Fig. 6B, and Table 4. The time series results indicated that the maximum hourly average mass concentration of organics reached 58 μg/m³ throughout the measurement period. The maximum hourly average mass concentrations of NO_3^-, NH_4^+, SO_4^{2-}, and Cl^- were 17 μg/m³, 14 μg/m³, 8 μg/m³, and 4 μg/m³, respectively, of the total NR-PM mass (Fig. 5B). Additionally, eBC reached a maximum hourly average mass concentration of 14.59 μg/m³ (Fig. 6B). The high contribution of ammonia mainly came from the agriculture sector. Thus, it can be concluded that ammonia was long-range transported to the measurement site from more distant locations. The nitrate mainly came from oxidation processes of gaseous NO_X onto pre-existing particles or through new particle formation. It can be concluded that the nitrate content reflects the contribution of transport exhaust to the chemical makeup of aerosol particles, as there are no other significant sources of NO_X in Vilnius. The exceptional meteorological conditions also influenced the increase in pollutant emissions from combustion processes, contributed to the changes in the composition of the carbonaceous particles, and resulted in changes in their transport characteristics. Throughout the monitoring periods, a maximum temperature of 2°C and a minimum temperature of -25 °C were recorded, underscoring the role of weather conditions in shaping the aerosol dynamics in the urban environment of Vilnius during the winter season. Throughout the measurement period in Vilnius during the winter season, an analysis was conducted on the total average mass concentration of NR-PM_1 and eBC (Fig. 7). The findings indicate that the average concentration of NR-PM_1 was (18.98 ± 11.82 μg/m³), as depicted in Figure. 7B, while the average concentration of eBC stood at (2.46 ± 1.99 μg/m³), as illustrated in Figure. 7F.

The diurnal trend analysis was performed for organics, inorganics and eBC (Fig. 8B and Fig. 9B). The results revealed distinct patterns for each component. Organic aerosols exhibited two prominent peaks with higher concentrations (10.85 μg/m^3 and 14.50 μg/m^3) during the morning hours (5 a.m. – 8 a.m.) and late evening hours (10 p.m. – 11 p.m.), along with a lower mass concentration (7.93 μg/m^3) during the afternoon (12 p.m. – 4 p.m.) (Fig. 8B). Nitrates and ammonium demonstrated a similar trend, displaying elevated mass concentrations (3.72 μg/m^3 and 3.60 μg/m^3, respectively) during the morning hours (8 a.m. – 10 a.m.) and lower concentrations (2.87 μg/m^3 and 3.06 μg/m^3, respectively) in the afternoon (2 p.m. – 4 p.m.) (Fig. 8B). The study conducted by Minderytė et al. (2022) at the same site revealed that the diurnal pattern of nitrate concentration showed two peaks during the day

and evening, which are attributed to anthropogenic sources related to traffic emissions. Nitrate ions form via the oxidation of NO_2, which is a primary indicator of vehicle exhaust emissions. Sulphates and chloride showed quite similar trend to each other and presented higher mass concentration (2.01 μg/m^3 and 0.37 μg/m^3, respectively) during late evening hours (8 p.m. – 9 p.m.) and lower mass concentration (1.64 μg/m^3 and 0.24 μg/m^3, respectively) during the evening hours (4 p.m. – 6 p.m.) (Fig. 8B). In a study conducted by Minderytė et al. (2022), it was revealed that the highest sulphate concentration occurred at 4 p.m. This suggests that the concentration of this pollutant primarily depends on the condensation of SO_2 oxidation products, indicating a secondary origin. It is important to note that the main source of SO_2 emissions is energy production and distribution; therefore, higher SO_2 and sulphate concentrations are typically observed during the heating season (Teinilä et al., 2019).

Additionally, the diurnal trend of eBC displayed two peaks of high concentration (3.14 μg/m^3 and 2.83 μg/m^3) during the morning hours (8 a.m. – 10 a.m.) and evening hours (6 p.m. – 8 p.m.), along with a lower mass concentration (1.68 μg/m^3) in the early morning hours (4 a.m. – 6 a.m.) (Fig. 9B). Higher concentration peaks were directly related rush hours whereas the reduction in pollution was directly influenced by the low relative humidity of the air. Similarly, Minderytė et al. (2022) found that black carbon (BC) concentration varied significantly throughout the day. Higher concentration peaks were observed in the morning and evening, while lower concentrations were noted during the day. This pattern may be linked to the increased use of transportation during morning and evening rush hours, as well as higher domestic heating (cooking activities) during these times.

A comprehensive time series illustrating eBC_{FF} and eBC_{BB}, along with their respective contributions to the overall eBC mass concentration during the measurement campaign at the Lithuanian urban site is presented in Fig. 10B. The percentage contribution reveals that, throughout the measurement campaign, eBC originating from fossil fuels (eBC_{FF}) accounted for 85% (average mass concentration – 2.00 μg/m³), while eBC from biomass burning (eBC_{BB}) constituted 15% (average mass concentration – 0.36 μg/m³) of the total eBC mass concentration (Fig. 10B). Remarkably, the predominant contribution of eBC_{FF}, surpassing that of eBC_{BB}, persisted throughout the entire measurement campaign. This dominance is associated with fossil fuel related pollution from local sources and long-range transport. Furthermore, Fig. 10F illustrates the time series of the light absorption coefficients of eBC and BrC at the Lithuanian urban site. The $b_{abs,eBC}$ exhibited a higher contribution of 82% (average mass concentration – 2.34 μg/m³) to light absorption at a lower wavelength (370 nm) during the campaign (Fig. 10F), while the contribution of BrC amounted to 18% (average mass concentration – 0.51 μg/m³). The probable source of BrC at this site is attributed to biomass burning, particularly during the cold season

(Byčenkienė et al., 2023; Minderytė et al., 2022; Pauraitė et al., 2019).

The urban measurement site was subjected to a comprehensive analysis that included wind rose and polar plot assessments for NR-PM_1 and eBC, as shown in Figures 11B, 11F, and 11J. Daily average T, RH, WS, WD observed at Vilnius (urban site) during measurement campaign is presented in Table 7. The wind rose analysis revealed that the prevailing winds throughout the measurement campaign at the measurement site were predominantly from the west (W), northwest (NW), east (E), northeast (NE), south (S), southeast (SE), south (S) and southwest (SW) (Fig. 11B). The analysis of the polar diagrams also confirmed the predominant wind directions from the west, north, east and south (Fig. 11F and 11J). However, the diagrams showed a remarkable correlation between higher concentrations of NR-PM_1 and eBC with the prevailing wind directions and increased wind speeds, particularly from westerly directions, throughout the measurement period (Fig. 11F and 11J). These westerly directions likely reflect impact from industrial zones and traffic-intensive areas located to the west of the sampling site, while easterly WD may include contributions from suburban areas and potential regional transport. It can be deduced that the concentrations of NR-PM_1 and eBC in Vilnius originate from both local sources and long-distance transport to the sampling site.

3.1.3 NR-PM_1 and eBC sources in Quezon urban environment

The measurement of eBC in Asian urban environment were carried out between 29th January 2020 to 26th February 2020 at Quezon City's East Avenue (Philippines) (Fig. 6C and Table 4). The maximum hourly average eBC mass concentration reached up to 104.54 μg/m³ throughout the measurement campaign at the Quezon City site. Examining the entire measurement period, the average eBC concentration for the winter season was determined to be 35.97 ± 16.20 μg/m³ at the QCG site (Fig. 7G). In the Philippines, particularly in urban centers like Metro Manila, various studies using AE31 data have uncovered the concerning levels of elevated eBC concentrations. Research by Alas et al. (2018) and Madueño et al. (2022) demonstrated that high eBC mass concentrations were primarily caused by vehicle emissions and industrial activities within the area. According to Madueño et al. (2022), a five-month investigation in Manila disclosed that eBC mass concentrations are 2 to 17 times greater than those observed in urban and traffic-related areas of India, China, Europe, and the USA. However, the annual average eBC concentration in Manila has yet to be determined.

Expanding the scope to other Asian countries, the struggle with elevated eBC levels is a common issue, often linked with rapid urbanization and industrial growth. Noteworthy studies by Kumar et al. (2020), Dumka et al. (2019), and Bisht et al. (2019) in India; Bilal et al. (2022) in Pakistan; Quang et al. (2021) in Vietnam; Chen et al. (2019) in China; and Shakya et al. (2017) in Nepal all underscore the significant

impact of traffic and industrial sources on eBC concentrations. Comparing these findings with our results, it is evident that urban and industrial emissions are consistent drivers of higher eBC levels across various regions. Local regulatory frameworks and the intensity of industrial activities also significantly influence eBC concentrations. For example, the eBC levels at QCG site are significantly higher than those reported in densely populated urban areas of India and Nepal, predominantly due to the concentration of traffic and industrial emissions. Therefore, it is vital to develop tailored strategies that consider unique urban characteristics and regulatory contexts to effectively mitigate eBC pollution and enhance public health. Table 8 provides a comparative analysis of the daily average eBC mass concentrations observed at these sites against the backdrop of global research, emphasizing the pressing need for effective emission reduction measures.

Furthermore, diurnal trend analysis revealed two distinct peaks in eBC concentration, with values of 63.45 + 10.61 μg/m³ and 43.48 μg/m³ observed during the morning hours (6 a.m. – 8 a.m.) and late evening hours (10 p.m. – 11 p.m.), respectively. In contrast, lower mass concentrations (23.43 + 10.61 μg/m³) were recorded during the daytime (12 p.m. – 2 p.m.) (Fig. 9C). Similar studies conducted by Kecorius et al. (2017), Kecorius et al. (2019), Alas et al. (2018), Madueño et al. (2019), Madueño et al. (2022) and Tõnisson et al. (2020) at similar site revealed that in the morning rush hours eBC higher mass concentration may be ascribed to enhanced traffic emissions from cars and jeepneys, whereas late at night higher concentration may mostly be associated with emissions from diesel trucks. The heavy diesel trucks, which are major emission sources of eBC were allowed to enter the city from 10pm to 7 a.m. and banned during morning rush hours (Alas et al., 2018) therefore less emission observed than morning rush hours. Furthermore, different factors such as increased mixing layer and higher wind speed decreased the eBC_{TR} concentration during daytime at QCG site. Whereas, during late night hours lower wind speed and lower mixing layer enhanced eBC concentration.

Source apportionment analysis of eBC indicated that during the measurement campaign the transport sector (eBC_{TR}) contributed 80% (average mass concentration – 25.01 μg/m³) of the total eBC mass concentration, while biomass burning (eBC_{BB}) accounted for the remaining 20% (average mass concentration – 6.07 μg/m³) (Fig. 10C). At the QCG site, where eBC_{TR} also played a more substantial role, the primary source of eBC was likely linked to pollution stemming from on-road transport. The urban landscape of Quezon City typically features a dense network of roads, and the traffic-related emissions, especially from vehicles such as diesel-powered Jeepneys and light duty vehicles (Kecorius et al., 2017; Madueño et al., 2019; Alas et al., 2018). According to studies conducted at the Quezon City site by Tun et al. (2019), Salvador et al. (2022), and Pabroa et al. (2022), significant

sources of biomass burning-derived eBC include domestic and commercial cooking, particularly involving charcoal. Additionally, studies carried out by Liu et al. (2018) and Qin et al. (2018) have shown that biomass burning during cooking activities was the main source of BrC in Quezon City.

Fig. 10G illustrates the hourly average time series and contribution of light absorption coefficients for eBC and BrC during the measurement campaign at the QCG site. At a lower wavelength (370 nm), eBC contributed 78% (average mass concentration – 28.23 μg/m³) to light absorption, while BrC contributed 22% (average mass concentration – 7.79 μg/m³). These findings are comparable to those reported in other urban locations such as Manaus, Brazil; Singapore; Lyon, France; Kathmandu, Nepal; and Guangzhou, China, which reported BrC contributions of 15%, 15%, 20%, 25%, and 25%, respectively (De Sá et al., 2019; Kasthuriarachchi et al., 2020; Zhang et al., 2020a; Kim et al., 2021; Qin et al., 2018) (Table 9). Similar to our study sites, fossil fuel and traffic-related emissions were identified as the main contributors in these locations, with lower contributions from biomass burning sources. In contrast, lower BrC contributions were observed in other urban areas. For instance, Panyu, Xianlin, and Xianghe in China reported BrC contributions of 2%, 5%, and 10%, respectively, while Athens, Greece, and Gwangju, Korea, both recorded contributions of 10% (Li et al., 2019; Liakaou et al., 2019; Wang et al., 2018b; Yang et al., 2009; Park et al., 2019) (Table 9). Higher BrC contributions were observed in several European and Asian urban areas, such as Bordeaux, Nantes, Rouen, Poitiers, Marseille, Reims, and Grenoble in France, each reporting BrC contributions of 30%, and Chiang Mai, Thailand, and Beijing, China, reporting values of 45% and 46%, respectively (Zhang et al., 2020a; Pani et al., 2021; Xie et al., 2019) (Table 9). These elevated BrC levels are primarily attributed to residential wood burning and biomass burning, indicating that these areas are significantly influenced by these combustion sources.

Meteorological analysis for eBC mass concentration at the QCG site (Fig.11C, and 11K) indicated that winds primarily originated from various directions including west (W), southwest (SW), west-southwest (WSW), north (N), northwest (NW), north-northwest (NNW), and west-northwest (WNW). To determine the wind direction conditions contributing to the highest eBC concentration levels at the QCG site during the measurement campaign, eBC concentrations were categorized by wind direction. Daily average T, RH, WS, WD observed at Quezon urban environment during measurement campaign is presented in Table 7. The Fig. 11K presents a polar plot illustrating measured eBC concentrations at the measurement site. Although the prevailing wind direction during the campaign was from the north and east directions, the diagram suggests that higher eBC concentrations

could be linked to dominant wind directions and higher wind speeds from the eastern directions throughout the measurement period. These eastern WD likely represent emissions from densely populated areas with heavy vehicular traffic and residential activities located to the east of the sampling site. As a result, it can be concluded that eBC concentrations at the QCG site originate from both local sources and long-range transport to the sampled location.

Table 8. Comparative analysis of mean hourly and daily averages, maximum daily and hourly concentration values, and diurnal trends of various airborne pollutants at the Port site and QCG site, highlighting differences in pollutant levels between the different sites.

Sites	Instruments	Mean Hourly Avg (µg/m³)	SD Hourly	Max Hourly (µg/m³)	Mean Daily Avg (µg/m³)	SD Daily	Max Daily (µg/m³)	Max Diurnal (µg/m³)	Min Diurnal (µg/m³)	Reference
OA (Port)	ACSM	23.68	16.4	99.5	23.36	8.94	40.47	29.43	12.22	This Study
SO_4^{2-} (Port)	ACSM	3.09	2.6	18.0	3.14	1.55	6.84	4.89	1.91	This Study
NO_3^- (Port)	ACSM	1.18	1.32	11.2	1.18	0.52	2.01	3.08	0.37	This Study
NH_4^+ (Port)	ACSM	1.19	1.02	6.96	1.2	0.56	2.26	2.16	0.58	This Study
Cl^- (Port)	ACSM	0.47	0.78	6.9	0.47	0.28	1.15	1.03	0.07	This Study
eBC (Port)	AE31	10.27	5.99	35.82	10.32	3.01	15.25	15.57	5.05	This Study
eBC (QCG)	AE31	35.97	16.2	104.54	34.08	7.29	44.25	63.45	23.43	This Study
eBC (Port)	AE33				16.0	3.0	70.21			Cadondon et al. (2024)
eBC Manila (PHL)	AE33				25.7					Alas et al. (2018)
eBC (Quezon, PHL)	AE33				36.7					Madueño et al. (2022)
eBC (Delhi, India)	AE31				13.57					Kumar et al. (2020)
eBC (Delhi, India)	AE33				7.2					Dumka et al. (2019)
eBC (Delhi, India)	AE33				14.91					Dumka et al. (2019)
eBC (Delhi, India)	AE33				7.89					Bisht et al. (2019)
eBC (Lahore, PAK)	AE33				21.7					Bilal et al. (2022)
eBC (Hanoi,	AE33				32.5					Quang

Vietnam)										et al. (2021)
eBC (Guangzhou, China)	AE31				20.5					Chen et al. (2019)
eBC (Kathmandu, Nepal)	AE33				15.0					Shakya et al. (2017)
eBC_{BB} (Port)	AE31	1.28	0.72	5.73	1.28	0.61	5.73	1.86	0.77	This Study
eBC_{TR} (Port)	AE31	7.75	5.34	35.39	7.88	4.31	35.39	12.24	3.65	This Study
eBC (Port)	AE31	8.36	5.92	43.5	8.47	4.8	43.5			This Study
BrC (Port)	AE31	2.06	2.1	26.1	2.06	1.68	26.1			This Study
eBC_{BB} (QCG)	AE31	6.06	2.24	17.52	5.9	2.13	17.52	8.49	4.79	This Study
eBC_{TR} (QCG)	AE31	24.95	14.85	102.48	24.08	12.67	102.48	47.69	13.97	This Study
eBC (QCG)	AE31	28.16	14.59	102.9	27.31	12.92	102.9			This Study
BrC (QCG)	AE31	7.77	3.44	24.58	7.57	3.26	24.58			This Study
$PM_{2.5}$ (Port)	APS	32.24	14.25	92.98			92.98			This Study
PM_{10} (Port)	APS	47.45	19.2	117.95			117.95			This Study
$PM_{2.5}$ (QCG)	APS	85.38	36.52	236.37			236.37			This Study
PM_{10} (QCG)	APS	129.46	51.2	273.34			273.34			This Study

Table 9. Percentage contributions of $b_{abs,eBC}$ and $b_{abs,BrC}$ to b_{abs} at different worldwide urban locations.

Location	BrC (%)	eBC (%)	Reference
Panyu, China (Nov. 2014–Jan. 2015; 370 nm)	2	98	Li et al. (2019)
Athens, Greece (May 2015–Apr. 2019; 370 nm)	5	95	Liakaou et al. (2019)
Xianlin, China (Jun. 2013–May 2016; 365 nm)	10	90	Wang et al. (2018b)
Xianghe, China (Mar. 2005; 370 nm)	10	90	Yang et al. (2009)
Gwangju, Korea (Oct.–Nov. 2017; 370 nm)	10	90	Park and Yu, 2019
Manaus, Brazil (15 Aug.–15 Oct. 2014; 370 nm)	15	85	de Sá et al. (2019)
Singapore (May–Jun. 2017; 370 nm)	15	85	Kasthuriarachchi et al. (2020)
Lyon, France (Winter, 2014-2015; 370 nm)	20	80	Zhang et al. (2020a)
Manila Port, Philippines (Dec–Jan 2019-20; 370 nm)	20	80	Gill et al. (2025)
QCG, Philippines (Jan–Feb 2019-20; 370 nm)	22	78	Gill et al. (2025)
Kathmandu, Nepal (2013–2014; 370 nm)	25	75	Kim et al. (2021)
Guangzhou, China (Nov. 2014–Jan. 2015; 370 nm)	25	75	Qin et al. (2018)
Bordeaux, France (Winter, 2014-2015; 370 nm)	30	70	Zhang et al. (2020a)
Nantes, France (Winter, 2014-2015; 370 nm)	30	70	Zhang et al. (2020a)
Rouen, France (Winter, 2014-2015; 370 nm)	30	70	Zhang et al. (2020a)

Poitiers, France (Winter, 2014-2015; 370 nm)	30	70	Zhang et al. (2020a)
Marseille, France (Winter, 2014-2015; 370 nm)	30	70	Zhang et al. (2020a)
Reims, France (Winter, 2014-2015; 370 nm)	42	58	Zhang et al. (2020a)
Grenoble, France (Winter, 2014-2015; 370 nm)	42	58	Zhang et al. (2020a)
Chiang Mai, Thailand (Mar.–Apr. 2016; 370 nm)	45	55	Pani et al. (2021)
Beijing, China (Nov.–Dec. 2016; 370 nm)	46	54	Xie et al. (2019)

3.1.4 NR-PM_1 and eBC sources in Manila coastal environment

The measurements of NR-PM_1 and eBC in the coastal environment were conducted between 20th December 2019 to 25th January 2020, at Manila's (Philippines) North Port (Fig. 5C, Fig. 6D and Table 4). The total PM_1 mass concentration of the non-refractory species ranged from a few $\mu g/m^3$, with the maximum hourly average reaching up to 108.38 $\mu g/m^3$. Throughout the campaign, OA emerged as the predominant component of NR-PM_1, constituting a mean hourly average of 80% (23.68 ± 16.40 $\mu g/m^3$). While sulphate constituted the second-largest fraction of 10% (3.09 ± 2.60 $\mu g/m^3$) of the total NR-PM_1 mass (Fig. 5D). Notably, nitrates and ammonium exhibited an equivalent contribution of 4% each (1.18 ± 1.32 $\mu g/m^3$ and 1.19 ± 1.02 $\mu g/m^3$) to the total NR-PM_1 mass (Fig. 5D). In contrast, chloride represented a minor fraction, ~2% (0.47 ± 0.78 $\mu g/m^3$) (Fig. 5D). Comparable studies conducted at different locations provide additional insight into the composition of NR-PM_1. The study conducted by Stavroulas et al. (2021) at port city Piraeus, Greece, similarly highlights the higher concentration of OA (67%), than inorganics such as SO_4^{2-} (19%), NH_4^+ (7%), NO_3 (6%), and Cl^- (1%) in urban atmospheric composition. In a study conducted by Gani et al. (2019) in Delhi, India, OA similarly dominated and accounted for 50% of NR-PM_1 mass. Ammonium, chloride, and nitrate individually constituted approximately 10%, while sulphate contributed roughly 5% to the NR-PM_1 mass. Another study conducted in Delhi, India by Patel et al. (2021) showed a higher fraction of OA (78%) and lower fraction of sulphate (20%). Similarly, Warden et al. (2022) in the research in Kathmandu, Nepal, observed that average NR-PM_1 was composed by mass of OA (35%), SO_4^{2-} (21%), NH_4^+ (7%), NO_3 (3%), and Cl^- (2%). Nitrate aerosols are primarily formed through the oxidation of nitrogen oxides (NO_x), which are significant traffic-related pollutants (Draxler et al., 1998). NO_x gases, predominantly emitted from vehicle exhausts, react with other atmospheric components under sunlight to form secondary inorganic aerosols such as nitrates. The concentration of these pollutants is notably higher in urban areas with dense traffic, underscoring the direct impact of vehicle emissions on the chemical composition of urban aerosols (Sun et al., 2011). These emissions are particularly potent during peak traffic hours, leading to increased rates of nitrate formation in the atmosphere (Carslaw et al., 2005).

Additionally, the variation in vehicle types and fuel qualities across different regions can further affect the NO_x emissions profile and, consequently, nitrate aerosol levels. Besides traffic, industrial activities and agricultural operations also contribute to the ambient NO_x levels, further influencing nitrate aerosol concentrations (Fan et al., 2023).

Additionally, the mean hourly average eBC mass concentration at the Manila Port site was 10.27 ± 5.99 μg/m^3, as shown in Fig. 6D. The maximum hourly average eBC mass concentration reached up to 35.82 μg/m³ at the Manila Port site (Fig. 6D). Different studies conducted at Manila, Philippines, unveiled the alarming presence of elevated eBC concentrations. For example, studies conducted by Alas et al. (2018) revealed that higher eBC mass concentrations were attributed to emissions from vehicles and industrial activities in the region. Recent findings by Cadondon et al. (2024) at Manila Port reported that atmospheric particle pollution is predominantly from local anthropogenic sources, such as ship emissions and industrial activities. Moreover, the air mass backward trajectories analysis indicated that, although air masses originated from the Pacific in the Southeast region of the study area, high factor loadings were of local anthropogenic origins. Beyond the Philippines, other Asian countries have also struggled with elevated eBC levels, often associated with rapid urbanization and industrial expansion. Notably, research conducted by Talukdar et al. (2021) in India, Quang et al. (2021) in Vietnam, Chen et al. (2019) in China, and Shakya et al. (2017) in Nepal, highlighting the influence of traffic and industrial sources on eBC concentrations. On the other hand, our study showed the lower eBC levels at the Port site compared to the QCG site indicate stricter local regulations or lower industrial activity. Differences in measurement approaches used in various studies also contribute to discrepancies in reported levels. Table 8 provides a comparative analysis of the daily average eBC mass concentrations observed at various measurement sites against the backdrop of global research, emphasizing the pressing need for effective emission reduction measures. The total average mass concentrations of NR-PM_1 and eBC during the winter season at Manila Port were of 29.52 μg/m³ and 10.27 μg/m³, respectively (Fig. 7D and Fig. 7H).

The Fig. 8C and Fig. 9D present the diurnal trend analysis of NR-PM_1 and eBC during the measurement campaign. The results reveal distinct patterns for different aerosol components. Organic aerosols exhibit two prominent peaks, with higher concentrations at 29.43 μg/m^3 and 40.02 μg/m^3 during the morning hours (6 a.m. – 9 a.m.) and late evening hours (6 p.m. – 10 p.m.), while displaying a lower mass concentration of 7.93 μg/m^3 during the afternoon (2 p.m. – 4 p.m.) (Fig. 8C). The higher concentrations of organic aerosols (OA) occurred in the morning hours and late evening hours coinciding with typical peak traffic hours and mealtimes. In contrast, inorganic aerosols SO_4^{2-}, NO_3^-, NH_4^+ and Cl demonstrate higher mass concentrations (4.89 μg/m^3, 3.08 μg/m^3, 2.16 μg/m^3, and 1.03 μg/m^3, respectively) during the morning

hours (8 a.m. – 10 a.m.) and lower mass concentrations (1.92 μg/m^3, 0.37 μg/m^3, 0.59 μg/m^3, and 0.07 μg/m^3, respectively) in the evening hours (3 p.m. – 5 p.m.) (Fig. 8C). The increased concentration of SO_4 in the morning was attributed to traffic and industrial emissions, while lower concentrations were associated with an increase in wind speed.

Furthermore, eBC displays higher concentration peaks (15.57 ± 3.46 μg/m^3) during the morning hours (6 a.m. – 8 a.m.), with a lower mass concentration of 5.05 ± 3.46 μg/m^3 observed during the daytime (12 p.m. – 2 p.m.) (Fig. 9D). It can be assumed that at the Manila Port site, during the morning hours elevated concentrations of eBC may be attributed to the increased morning intensities of on-road traffic (such as private vehicles, heavy duty trucks, trollers, etc.) in addition to the maritime traffic. Additionally, cargo handling equipment, often diesel-powered, is active in the morning, and traffic congestion, along with road dust resuspension, collectively leading to higher concentrations of black carbon. In the afternoon at Manila Port site, traffic-related black carbon concentrations typically decrease due to reduced morning rush hour traffic, improved traffic flow and increased mixing layer (Kecorius et al., 2017, Kecorius et al., 2019, Alas, et al 2018, Madueño et al., 2019, Madueño et al., 2022 and Tõnisson et al., 2020).

During the measurement campaign at the Port site, a source apportionment analysis of eBC revealed a notable predominance of contributions from the transport sector. Specifically, eBC_{TR} accounted for a substantial 86% (average mass concentration – 7.75 μg/m³) of the total eBC mass concentration, overshadowing the contribution of eBC_{BB} at 14% (average mass concentration – 1.28 μg/m³) (Fig. 10D). According to previous study by Kecorius et al. (2017); Madueño et al. (2019); Alas et al. (2018) at the Port site, where eBC_{TR} constituted the majority, the predominant source of eBC was likely related to vehicle emissions from heavy duty trucks, trollers and diesel-powered cranes. Furthermore, the time series analysis of light absorption coefficients for eBC and BrC at the Port site (Fig. 10H) highlighted the dominance of eBC in light absorption, constituting 80% (average mass concentration – 8.36 μg/m³), whereas BrC accounted for a smaller yet notable contribution of 20% (average mass concentration – 2.06 μg/m³). According to the studies conducted by Tun et al., (2019), Salvador et al. (2022), and Pabroa et al. (2022), major sources of biomass burning at the port site include agricultural activities, residue burning (such as rice husk, straw, sugarcane waste, bagasse, coconut husk, and maize cobs), and forest fires. Additionally, research by Liu et al. (2018) and Qin et al. (2018) indicated that at the port site, BrC primarily originates from agricultural and residual burning operations. Distant agricultural activities and waste incineration are also major sources of biomass burning-derived eBC at the Port site, with long-range transport of these pollutants playing a significant

role (Ulevičius et al., 2010). Although vital, shipping and maritime operations at Port sites are not directly related to biomass burning emissions but primarily contribute through the combustion of fuels and the release of particulate matter (Geng et al., 2024). The primary source of BrC at the Port site is also linked to biomass burning, specifically from waste incineration and agricultural burning. The BC and BrC contributions presented in this study, along with those from various urban locations worldwide, were compared. At the Port site, BrC contributions accounted for 20% of the total light absorption, aligning with observations from other urban locations such as Manaus, Brazil; Singapore; Lyon, France; Kathmandu, Nepal; and Guangzhou, China, which reported BrC contributions of 15%, 15%, 20%, 25%, and 25%, respectively. Similar to our study site, fossil fuel and traffic-related emissions were identified as the main contributors in these locations, with lower contributions from biomass burning sources (De Sá et al., 2019; Kasthuriarachchi et al., 2020; Zhang et al., 2020a; Kim et al., 2021; Qin et al., 2018).

Meteorological data analysis of NR-PM_1 and eBC demonstrated in Fig. 11D, 11H, and 11L. Wind rose analysis at the port site revealed a prevailing pattern of winds originating from the west (W), north-west (NW), north (N), north-east (NE), east (E), and south-east (SE) (Fig. 11D). Daily average T, RH, WS, WD observed at Manila Coastal environment during measurement campaign is presented in Table 7. The analysis of the polar diagrams also confirmed the predominant wind from the west (W), north (N), and east (E) directions (Fig. 11H and 11L). However, noteworthy insights were drawn from the analysis indicating that elevated concentrations of NR-PM_1 and eBC were associated with prevailing winds from the western directions, coupled with higher wind speeds observed throughout the measurement period (Fig. 11H and 11L). These western WD are likely associated with emissions from nearby port operations, industrial facilities, and traffic corridors located to the west of the sampling site. For these reasons, it can be concluded that NR-PM_1 concentration at manila port originate from local sources as well as come from long range transport to the sample location.

4 INTER COMPARISON OF RURAL, URBAN, AND COASTAL ENVIRONMENTS

To compare different air quality dynamics across Rural (Rūgšteliškis), Urban (Vilnius), Urban (Quezon), and coastal (Manila North Port) environments, this section presents a detailed intercomparison. By analysing mass concentrations, diurnal trends, source apportionment, and air mass trajectories of NR-PM_1 and eBC, we aim to identify unique and shared pollution characteristics. These insights are essential for devising effective, location-specific air pollution management strategies.

The comparative analysis revealed significant spatial variations in NR-PM_1 and eBC concentrations, influenced by specific sources and atmospheric conditions, with Quezon City (urban site) showing the highest levels, followed by Manila North Port (Coastal site), Vilnius (urban site), and the lowest found in Rūgšteliškis (rural site) (Table 4). Seasonally, NR-PM_1 levels peaked in spring and summer, while eBC concentrations were highest in autumn at the Rūgšteliškis (rural site). In Vilnius (urban site), Quezon (urban site) and Manila (Port site) NR-PM_1 and eBC concentration were higher in winter season.

At the Rūgšteliškis (rural site), the increase in NR-PM_1 during spring and summer can be attributed to enhanced biological activities and rising temperatures. In contrast, the higher eBC levels in autumn are driven by increased combustion for heating and agricultural activities related to the harvesting season at this site. In Vilnius (urban site), elevated levels of NR-PM_1 and eBC are driven by household activities such as biomass and fossil fuel burning, traffic emissions, and long-range transport. These activities are also facilitated by winter meteorological conditions, which can substantially affect air quality in colder climates due to increased heating demands and stable atmospheric conditions that trap pollutants close to the ground level. The analysis in Quezon City (urban site) revealed the highest eBC concentrations during the study period, underscoring the impact of dense traffic and possibly industrial emissions. At Manila North Port (Coastal site), high concentrations of NR-PM_1 and eBC are influenced by port activities and vehicular emissions. Here, meteorological conditions such as clean breezes at the port site tend to lower pollutant levels compared to Quezon City. The results indicate specific actions that could improve air quality, like implementing stricter emission regulations in colder urban regions during winter and managing traffic and industrial emissions in densely populated cities such as Quezon City. It is crucial to have ongoing monitoring and customized policies in place for effective management of air pollution. This approach ensures that interventions are based on scientific evidence and tailored to the unique characteristics of different regions and seasons.

The diurnal trend analysis across rural, urban, and coastal sites revealed pronounced peaks of NR-PM_1 and eBC concentrations during morning and late evening hours driven by traffic emissions, industrial activities, and maritime operations. These peaks are further influenced by atmospheric conditions such as wind speed and boundary layer dynamics. Although the diurnal pattern of both NR-PM_1 and eBC was broadly consistent across the study sites, with morning and evening peaks, the magnitude of concentrations varied significantly. For eBC, the highest concentrations were observed in Quezon City (urban site), followed by Manila Port (coastal site) and Vilnius (urban site), with the lowest levels recorded in Rūgšteliškis (rural site). In the case of NR-PM_1, inter-site comparisons were conducted only for Vilnius, Manila Port, and Rūgšteliškis, as NR-PM_1 data were not available for Quezon City during the study period. Among these, Manila Port exhibited the highest NR-PM_1

concentrations, followed by Vilnius and Rūgšteliškis.

In rural settings like Rūgšteliškis, morning peaks of organic aerosols are mainly due to low boundary layer heights, which keep pollutants concentrated near the ground. As the sun rises, the boundary layer height increases due to warming, leading to a dilution of pollutants and lower concentrations during the afternoon. Similarly, higher eBC concentrations in the morning and evening are linked to wood burning, work-related traffic, and long-range transport, aligning with the lower boundary layer heights observed during these periods. These patterns underscore the significant impact of eBC on rural environments, driven by diverse sources such as biomass burning, traffic, and long-range transport. In urban environments like Vilnius, the winter months showed a significant peak of NR-PM_1 and eBC concentrations during the morning and late evening hours. The high levels of organics and ammonium were largely influenced by local and regional agricultural activities and traffic emissions. Whereas eBC higher concentration peaks may be linked to the increased use of transportation during morning and evening rush hours, as well as higher domestic heating (cooking activities) during these times whereas the reduction in pollution was directly influenced by the low relative humidity of the air. The diurnal trend analysis of eBC concentration at Quezon City, further examining urban effects on the diurnal variability of these pollutants. Diurnal trend analysis revealed two distinct peaks in eBC concentration observed during the morning hours and late evening hours. The morning rush hours eBC higher mass concentration may be ascribed to enhanced traffic emissions from cars and jeepneys, whereas late at night higher concentration may mostly be associated with emissions from diesel trucks. Diurnal trends of NR-PM_1 and eBC at Manila (Port site), showed higher concentrations peaks in the morning hours and late evening hours and lower concentration during daytime. The higher concentration peaks of organic aerosol particles are due to traffic hours and mealtimes. Whereas eBC peaks may be attributed to the increased morning intensities of on-road traffic (such as private vehicles, heavy duty trucks, and trollers) in addition to the maritime traffic. Additionally, cargo handling equipment, often diesel-powered, is active in the morning, and traffic congestion, along with road dust resuspension, collectively leading to higher concentrations of black carbon. In the afternoon at Manila Port site, traffic-related black carbon concentrations typically decrease due to reduced morning rush hour traffic, improved traffic flow and increased mixing layer. These findings underscore the importance of implementing customized pollution control plans that address the unique characteristics of rural, urban and coastal areas. Successful plans should take into account peak times and local weather conditions to reduce the adverse effects of air pollution on both health and the environment.

The comprehensive source apportionment analysis of eBC was performed at rural, urban, and coastal sites. Higher concentrations of eBC_{FF} and eBC_{BB} were observed at Quezon City (urban site), followed by Manila Port (coastal site), and

Vilnius (urban site), with the lowest concentrations recorded at Rūgšteliškis (rural site). Similarly, the concentration levels of Brown Carbon (BrC) were lower than those of BC_{FF} at all sites yet followed the same pattern such as highest at Quezon City, then Manila Port and Vilnius, and lowest at Rūgšteliškis.

Analysis revealed that the dominant source of equivalent black carbon (eBC) in Rūgšteliškis, Vilnius, Quezon City, and Manila North Port is primarily due to fossil fuel combustion, with transportation-related emissions from vehicles and industrial activities contributing significantly to the local air pollution profiles. Additionally, brown carbon (BrC), although a minor component compared to eBC, plays a crucial role in affecting the light absorption characteristics of aerosols. The presence of BrC, mainly from biomass burning, varies significantly with local practices. In rural areas like Rūgšteliškis, biomass burning related to residential heating and agricultural activities is a notable source of BrC. In urban settings like Vilnius and Quezon City, BrC arises not only from heating but also from domestic cooking and commercial activities, particularly where biofuels and charcoal are used extensively. In coastal areas like Manila North Port, BrC is primarily sourced from agricultural residue burning and port-related activities, impacting the local air quality distinctively. In order to tackle air pollution effectively, it is essential to focus on reducing fossil fuel combustion and addressing region specific biomass burning. Important steps involve enhancing traffic and vehicle emission regulations, encouraging the use of cleaner cooking and heating methods and implementing stricter oversight of agricultural and industrial emissions. It is vital to have enhanced monitoring systems and customized regulatory frameworks for targeted interventions that lead to better air quality.

The meteorological data analysis provides an in-depth understanding of how NR-PM_1 and eBC concentrations across rural, urban, and coastal environments are significantly influenced by both local sources and long-range transport. This relationship underscores the impact of regional meteorological conditions on air quality and highlights the need to incorporate these factors into air pollution control strategies.

At Rūgšteliškis, a rural site, wind rose and polar plot analyses show that winds primarily from the north, east, and south bring in higher concentrations of pollutants, indicating significant long-range transport effects alongside local emissions. This site, being remote from major industrial activities and not directly impacted by heavy traffic or maritime influences, suggests that the observed pollutants are largely due to atmospheric transport from distant sources (Fig. 11A, 11E, 11I, and Table 7). In contrast, the urban setting of Vilnius demonstrates a different dynamic. Here, prevailing winds from the west and northwest contribute to higher pollutant concentrations, likely carrying emissions from the city's dense traffic and industrial sectors. The polar plots distinctly highlight how local emissions are exacerbated by meteorological conditions that facilitate the accumulation of pollutants, particularly during periods of higher wind speeds from these directions (Fig. 11B, 11F, 11J, and

Table 7). At Quezon city site higher eBC concentrations could be linked to dominant wind directions and higher wind speeds from the eastern directions. Therefore, it can be concluded that at this site eBC concentration originate from both local sources and long-range transport to the sampled location (Fig. 11C, 11K, and Table 7). The coastal site of Manila North Port shows a similar pattern where prevailing western winds significantly influence pollutant levels. This site experiences complex interactions between local emissions from port activities, including shipping and heavy machinery, and pollutants carried by long-range transport (Fig. 11D, 11H, 11L, and Table 7). The analysis across these sites shows that managing air quality effectively requires a multifaceted approach. It is essential to tackle emissions from specific local sources like traffic, industrial activities and port operations while also taking into account the influence of wind patterns and speeds on pollutant dispersion. By incorporating meteorological information into air quality management practices, it becomes possible to forecast high pollution periods and develop proactive measures to minimize exposure and safeguard human health and the environment.

CONCLUSIONS

1. The mean hourly average mass concentrations of NR-PM_1 at Rugšteliškis, Vilnius, and Manila port were 8.48 μg/m³, 18.98 μg/m³, and 29.52 μg/m³, respectively. Mean hourly average mass concentrations of eBC at Rugšteliškis, Vilnius, Quezon, and Manila Port reported as 0.60 μg/m³, 2.46 μg/m³, 36.19 μg/m³, and 10.27 μg/m³, respectively. The comparative analysis revealed significant spatial variations in NR-PM_1 and eBC concentrations, with Quezon City showing the highest levels, followed by Manila North Port, Vilnius, and the lowest in Rūgšteliškis. Seasonal variations showed higher NR-PM_1 concentration (9.07 μg/m³) in spring and higher eBC concentration (0.72 μg/m³) in autumn at the Rūgšteliškis rural site, with particularly high eBC in Quezon urban (36 μg/m³) and Manila Port (10 μg/m³) during winter.
2. The diurnal trend analysis of NR-PM_1 and eBC across different environments reveals significant variations driven by the interplay of anthropogenic activities and natural atmospheric conditions. In rural areas, morning peaks of OA and eBC reflect emissions from biomass burning and vehicular traffic, along lower boundary layer height. Urban environments show more pronounced diurnal peaks due to high traffic and industrial activities, especially during morning and evening rush hours. In coastal areas, the diurnal patterns are similarly influenced by local traffic, port activities, and atmospheric conditions such as wind speed and boundary layer dynamics.
3. The comprehensive source apportionment analysis reveals that the dominant source of eBC at Rūgšteliškis, Vilnius, Quezon, and Manila North Port originated from fossil fuel and transport-related emissions, accounting for 90%, 85%, 81%, and 86% respectively. Although lesser, the contribution of biomass burning to eBC underscores the influence of local practices such as residential heating and agricultural burning. The contribution of BrC was 14%, 18%, 22%, and 20% at Rūgšteliškis, Vilnius, Quezon, and Manila North Port, respectively. The minor but notable presence of BrC, primarily from biomass burning, varies spatially with local practices such as domestic cooking, agricultural residue burning, and seasonal activities, impacting light absorption characteristics.
4. Both local sources and long-range transport significantly impacts the concentrations of NR-PM_1 and eBC at rural, urban, and coastal sites. Specifically, at the rural site of Rūgšteliškis, higher concentrations were associated with wind directions from south and west. In Vilnius,

elevated levels correlated with wind directions from the west and east. At the QCG site, higher eBC concentrations were linked to wind directions from the east, while at the Port site, elevated levels were tied to wind directions from west.

SANTRAUKA

ĮVADAS

Aerozolio dalelės, įskaitant organines, neorganines ir anglingas daleles, daro kompleksinę įtaką Žemės klimato sistemai. Padidėjusi šių aerozolio dalelių koncentracija daro ženklų poveikį vietinėms meteorologinėms sąlygoms ir atmosferos oro kokybei kaimo, miesto ir pakrančių vietovėse. Siekiant išspręsti atmosferos procesų neapibrėžtis labai svarbu visapusiškai suprasti aerozolio dalelių cheminę sudėtį, šaltinius, susidarymą, transformacijas ir dinaminę sąveiką Žemės klimato sistemoje. Naujausi tyrimai Vakarų ir Pietų Europoje išsamiai apibūdino aerozolio šaltinius, ypač miestuose ir kaimo vietovėse. Nepaisant to, Baltijos regione, ypač Šiaurės-Rytų Europoje, tyrimų aprėptis yra sąlyginai nedidelė, todėl jaučiamas išsamių duomenų trūkumas. Šiuo tyrimu siekiama užpildyti šią žinių spragą, pateikiant išsamią, ilgalaikę atmosferinių procesų analizę, daugiausiai dėmesio skiriant organinių, neorganinių ir anglingų aerozolio dalelių cheminei sudėčiai Lietuvos borealinių miškų kaimo aplinkoje (šiaurės-rytinė dalis) ir miesto aplinkoje. Tai apima vietinių tyrimo duomenų rinkinių panaudojimą, siekiant pateikti regioninę perspektyvą, kuri pagerintų mūsų supratimą apie aerozolio dalelių dinamiką šiame regione. Taip pat siekiama pagilinti žinias apie taršos sezoniškumą, šaltinių kintamumą ir jų reikšmę atmosferos oro kokybei. Atliekant mokslinius tyrimus Filipinuose pagrindinis dėmesys buvo sutelktas į kritinę juodosios anglies (BC) taršos problemą miesto ir pakrančių aplinkose. Nors anksčiau atlikti tyrimai ženkliai pagerino žinias apibūdinant aerozolio dalelių dydį, koncentraciją ir erdvinį kintamumą, vis dar jaučiamas žinių trūkumas, ypač siekiant suprasti ne tik kelių transporto poveikį, bet ir kitus BC šaltinius, taip pat Manilos uosto poveikį aerozolio dalelių koncentracijai. Šio tyrimo tikslas – suteikti naujų įžvalgų kaimo, miesto ir pakrančių vietovėse, pagilinant esamą supratimą apie sudėtingus atmosferos mechanizmus, reguliuojančius aerozolio dalelių sudėtį ir pasiskirstymą bei jų įtaką klimato kaitai.

PAGRINDINIS TIKSLAS IR UŽDAVINIAI

Šio tyrimo tikslas – nustatyti pagrindinius organinių, neorganinių ir anglingų aerozolio dalelių šaltinius ir palyginti jų savybes kaimo, miesto ir pakrantės aplinkose.

Šiam tikslui pasiekti buvo nustatytos šios užduotys:

- Organinių, neorganinių ir anglies aerozolio dalelių kaimo, miesto ir pakrantės aplinkoje apibūdinimas.

- Anglingų aerozolio dalelių kaimo, miesto ir pakrantės aplinkoje šaltinių pasiskirstymas.
- Meteorologinių sąlygų poveikio organinėms, neorganinėms ir anglies aerozolio dalelėms kaimo, miesto ir pakrantės aplinkoje vertinimas.

NAUJUMAS

Pagrindinis šio tyrimo naujumas yra Šiaurės Europos ir Pietų Azijos miestų aplinkose atlikta lyginamoji analizė, leidusi nustatyti, kad rudosios anglies santykinis indelis anglingoms aerozolio dalelėms išlieka panašus nepriklausomai nuo geografinės vietos ir metų laiko, nors abiejuose regionuose su skirtingais sezoniniais ir socialiniais ekonominiais veiksniais OA pagrindiniai biomasės deginimo šaltiniai yra skirtingi, t.y. gyvenamųjų namų šildymas Lietuvoje ir žemės ūkio atliekų deginimas Filipinuose.

GINAMIEJI TEIGINIAI

1. Kaimo, miesto ir pakrantės aplinkose dominuoja organinės aerozolio dalelės (53 – 80 %). Neorganinių aerozolio dalelių (SO_4^{2-}, NO_3^-, NH_4^+, ir Cl^-) koncentracija viso tyrimo metu buvo mažesnė už OA, o tai rodo nuolatinį organinių medžiagų vyravimą atmosferos aerozolio dalelių sudėtyje nepriklausomai nuo aplinkos skirtumų.

2. Pagrindinis eBC šaltinis kaimo, miesto ir pakrantės aplinkose buvo iškastinio kuro deginimas ir transporto sektorius (80 – 90%). Priešingai, biomasės deginimas sudarė ženkliai mažesnę dalį (10 – 20%), patvirtindamas didesnį transporto ir iškastinio kuro šaltinių poveikį BC kiekiui skirtingose aplinkose.

3. BrC kaimo, miesto ir pakrantės aplinkose sudarė tik 14 – 22 % visos anglies turinčio aerozolio sudėties. Biomasės deginimas yra pagrindinis BrC šaltinis ir santykinai daro mažesnį poveikį oro kokybei lyginant su kitais dominuojančiais eBC šaltiniais, tokiais kaip iškastinio kuro deginimas ir transporto išmetami teršalai.

4. eBC ir BrC koncentracijos Šiaurės Europos miesto aplinkoje yra 14 – 15 kartų mažesnės nei Pietų Azijos miesto aplinkoje, tačiau iškastinio kuro ir biomasės deginimo šaltinių santykinis indėlis išlieka panašus (4% skirtumas) nepriklausomai nuo geografinės vietos ir metų laiko.

AKTUALUMAS

Atmosferos submikroninių aerozolio dalelių cheminių komponentų kaimo, miesto ir pakrančių aplinkose charakterizavimas yra svarbus dėl jų neigiamo poveikio žmonių sveikatai ir reikšmingos įtakos Žemės klimato sistemai. Todėl labai svarbu gilinti supratimą apie aerozolio dalelių cheminę sudėtį ir jų susidarymo būdus. Šio tyrimo rezultatai galėtų pagerinti supratimą apie atmosferos cheminę sudėtį tiek vietiniu, tiek pasauliniu mastu. Be to, atkreipiamas dėmesys į nuolatinę padidintą eBC taršą besivystančiuose regionuose ir skatinama kurti moksliškai pagrįstas strategijas oro kokybės krizei sušvelninti.

AUTORIAUS INDĖLIS

Tyrimai, pateikti keturiose mokslinėse publikacijose (1 – 4) yra paties autoriaus idėjų ir diskusijų tarp autoriaus, vadovo ir bendraautorių rezultatas. Autorius atliko pagrindinį vaidmenį rengiant ir atliekant matavimo duomenų analizę. Organinių ir neorganinių nitratų atskyrimą, absorbcijos Ångströmo eksponentės nustatymą, pataisų taikymą ir Aethalometro matavimų duomenų interpretavimą daugiausia atliko autorius. Šioms užduotims atlikti buvo naudojama MATLAB programa dėl galingo priemonių rinkinio, tinkamo statistinei analizei ir didelių duomenų rinkinių tvarkymui, ypač naudingo matricų operacijoms ir vizualizacijai. “Python” programa buvo naudojama dėl jos gausių bibliotekų ir struktūrų, pritaikytų duomenų mokslui, įskaitant skaitinių duomenų apdorojimui skirtą “NumPy”, duomenų tvarkymui skirtą “Pandas”, ir pažangiam duomenų vizualizavimui skirtas “Matplotlib” bei “Seaborn” paprogrames. “R” buvo specialiai naudojama atviroms diagramoms kurti, panaudojant jos stiprias grafines galimybes, kad būtų galima veiksmingai perteikti sudėtingus aplinkos duomenų modelius. Šis priemonių derinys leido atlikti išsamią ir veiksmingą aerozolio duomenų analizę, siekiant atskleisti duomenų rinkinio dėsningumus ir sąsajas. Šaltinių kilmės nustatymą taikant PMF modelį (2) ir meteorologinių duomenų analizę taikant HYSPLIT modelį (1, 2 ir 4) atliko bendraautoriai. Mokslinėse konferencijose, publikacijose ir disertacijoje pateiktas išvadas autorius parašė bendradarbiaudamas su doktorantūros vadove ir kitais bendraautoriais.

METODAI

Matavimų vietovės

Nepertraukiami aerozolio dalelių cheminės sudėties ir optinių parametrų matavimai buvo atliekami trijose skirtingose aplinkose: kaimo, miesto ir pakrantės. Šios pasirinktos matavimų vietos strategiškai išdėstytos skirtingose geografinėse vietovėse, siekiant įvertinti vyraujančius organinių, neorganinių ir anglingų aerozolio dalelių šaltinius, darančius įtaką atmosferos šiluminiam balansui ne tik Europoje (Lietuvoje), bet ir Azijoje (Filipinuose) (1 pav.).

Pirmoji matavimo stotis, apibūdinama kaip kaimo aplinka, yra Aukštaitijos integruoto monitoringo kompleksinių matavimų stotis (1a pav.). Ši nuošali vieta Rūgšteliškio kaime (55°27'N, 26°00'E, 170 m virš jūros lygio) užima apie 70 % miškingo ploto, kuriam daugiausia būdingi pušų (*Pinus sylvestris*) medynai, o augalija įvairi – nuo stepių iki tundros rūšių (Pauraitė ir kt., 2015). Artimiausiose apylinkėse beveik nėra reikšmingų vietinių antropogeninės taršos šaltinių. Artimiausias didesnis miestas Utena yra už 27 km į pietus nuo Rūgšteliškio. Matavimai atlikti maždaug 1,5 m aukštyje virš žemės lygio, vidutinio klimato juostoje, kuriai būdingas drėgnas žemyninis klimatas su vidutiniškai vėsiais orais, gausiais lietumis ir didele oro drėgme (Europos aplinkos agentūra, 2023). Per penkerius metus (2013, 2014, 2016, 2018 ir 2019 m.) matavimai buvo sistemingai atliekami trimis skirtingais metų laikais: pavasarį, vasarą ir rudenį.

Antroji matavimo vieta buvo pasirinkta Fizinių ir technologijos mokslų centro teritorijoje Vilniuje (54°38'N, 25°10'E, 197 m virš jūros lygio) (1b pav.). Mėginių ėmimo sistemos įvadas buvo įrengtas viršutiniame aukšte, apie 20 m virš žemės paviršiaus, 12 km į pietvakarius nuo miesto centro. Pažymėtina, kad mėginių ėmimo vieta buvo strategiškai patogioje vietoje, gerokai nutolusi nuo tankiai apgyvendintų gyvenamųjų zonų. Iš šiaurės/šiaurės rytų stotis apsupta miškų, o iš pietų/rytų – nuosavų namų. Artimiausias kelias buvo už 300 m į pietvakarius, o priešingoje pusėje – už 600 m nuo stoties yra mažo eismo intensyvumo kelias. Apibūdinama kaip miesto foninė vietovė, geografinė vietos padėtis tipiškomis meteorologinėmis sąlygomis ribojo transporto priemonių išmetamųjų teršalų kaupimosi galimybes. 2014 m. žiemą (sausio-vasario mėn.) buvo vykdoma intensyvi 2 mėn. trukmės lauko matavimų kampanija. Tikslas buvo atlikti nuolatinius matavimus realiuoju laiku, siekiant nustatyti organinio aerozolio (OA) sudėtį ir BC masės koncentraciją šioje miesto vietovėje.

Trečioji matavimų kampanija buvo vykdoma dviejose vietose Manilos metropolitene (Filipinai): Manilos šiauriniame uoste (14°61'N, 120°96'E) nuo 2019 m. gruodžio 20 d. iki 2020 m. sausio 25 d. (1c pav.) ir Kesono miesto

Rytų prospekto pakelėje (14°67'N, 121°04'E) nuo 2020 m. sausio 29 d. iki 2020 m. vasario 26 d. (1d pav.). Uosto matavimų vieta buvo 12 km nutolusi nuo Kesono miesto Rytų prospekte. Siekiant užtikrinti surinktų duomenų kokybę, matavimo prietaisai buvo laikomi specializuotame, kondicionuojamame konteineryje. Aerozolio matavimo prietaisai buvo eksploatuojami pagal Pasaulinio aerozolio fizikos kalibravimo centro (WCCAP) rekomendacijas, parengtas pagal Pasaulinės meteorologijos organizacijos (WMO) Pasaulinės atmosferos stebėjimo (GAW) programą. Siekiant sumažinti dalelių nuostolius dėl difuzijos, koaguliacijos ir nusėdimo mėginiai buvo imami laikantis GAW 227 ataskaitoje (WMO ataskaita, 2016 m.) pateiktų rekomendacijų. Pakrantės aplinkoje buvo atliekami intensyvūs matavimai siekiant išmatuoti ekvivalentinės juodosios anglies (eBC) masės koncentraciją, aerozolio dalelių skaičiaus koncentraciją ir dalelių šviesos sklaidos koeficientą.

Matavimų įranga ir metodai

Organinių aerozolio dalelių koncentracijos matavimai ir šaltinio nustatymas

Dviejose tyrimų vietovėse, Lietuvoje ir Filipinuose, buvo naudojamas Aerodyne Chemical Speciation Monitor (ACSM), skirtas submikroninių aerozolio dalelių cheminei sudėčiai matuoti (Ng ir kt., 2011). ACSM leidžia atlikti tiesioginius matavimus, selektyviai sutelkiant dėmesį į ≤1 μm dydžio daleles per aerodinaminius lęšius, kurie neįtraukia didesnių dalelių ir patikslina aerozolio srautą, kad būtų galima atlikti tikslią analizę (Liu ir kt., 2018). Aerozolio dalelės atskiriamos nuo oro srauto, nukreipiamos į kaitinimo plokštelę ir išgarinamos. Susidarę garai jonizuojami naudojant 70 eV elektronus ir generuojami molekulinių jonų fragmentai. Šie jonų fragmentai analizuojami kvadrupoliniu masės spektrometru pagal masės ir krūvio santykį (*m/z* 12-149), kad būtų galima nustatyti aerozolių cheminę sudėtį. Tolesnė organinių aerozolių masės spektrų analizė buvo atlikta taikant pozityviosios masės faktorizavimą (PMF), leidžiantį nustatyti konkrečius organinių aerozolių šaltinius ir indėlį.

Siekiant įvertinti $PM_{2.5}$ ir PM_{10}, aerozolio masės svertinę aerodinaminę koncentraciją miesto ir pakrantės aplinkose (Filipinai) dalelių skaičiaus pasiskirstymui pagal dydį nuo 0,5 iki 10,0 μm ir skaičiaus koncentracijai įvertinti buvo naudojamas aerodinaminis dalelių spektrometras (APS modelis 3221, TSI Inc., JAV, 2004 m.).

Ekvivalentinės juodosios anglies matavimai

Aethalometras (AE31 Magee Scientific) buvo naudojamas kaip prietaisas, kuriuo buvo kiekybiškai įvertinta ekvivalentinės juodosios anglies (eBC) masinė koncentracija aerozolio dalelėse. Prietaiso veikimo principas pagrįstas šviesos intensyvumo silpnėjimo matavimu per filtrą, kuriame yra aerozolio dalelių Arnott ir kt., (2005). Matavimai buvo atliekami esant septyniems skirtingiems bangos ilgiams: 370, 470, 520, 590, 660, 880 ir 970 nm. eBC masės koncentracijos matavimai atliekamai esant 880 nm bangos ilgiui.

Šaltinio kilmės nustatymo metodas remiasi skirtingų sugerties spektrų stebėjimu įvairiais šviesos bangos ilgiais iš atskirų dalelių. Šiuo tikslu Rūgšteliškio kaimiškoje aplinkoje ir Vilniaus miesto foninėje aplinkoje surinktiems eBC duomenims buvo taikoma Weingartner ir kt. (2003) pasiūlyta pataisa, siekiant sumažinti „šešėlį“, daugialypę sklaidą ir kitus efektus, sukeliančius matavimo paklaidas. Filipinų miesto ir pakrantės aplinkose surinktiems eBC duomenims buvo taikoma Virkkula ir kt. (2007) pataisa.

Oro masės atgalinių trajektorijos

Tolimosios oro masių pernašos poveikio oro kokybei įvertinimui buvo naudojama programinė įranga TrajStat (Wang ir kt., 2009), sujungianti trajektorijų statistiką ir geografines informacines sistemas, kad būtų galima analizuoti taršos kelius taikant Potencialaus šaltinio indėlio funkcijos (PSCF) modelį. Su konkrečiais taršos lygiais susijusių trajektorijų svertinės koncentracijos buvo apskaičiuojamos naudojantis Koncentracijos svertinės trajektorijos (CWT) metodu (Hsu ir kt., 2003 m.), leidžiančiu detaliai įvertinti 72 valandų laikotarpio oro masių trajektorijas su padidėjusiomis OA ir eBC koncentracijomis. Šis tyrimas leidžia nustatyti oro masių trajektorijas, kurios į matavimo vietą perneša dideles OA ir BC koncentracijas, bei jų geografinių šaltinių regionus.

Papildomai buvo naudojamas HYSPLIT modelis skaičiuojant 72 valandų atgalines oro masių, atvykstančių į matavimo vietą, trajektorijas. Šis modelis leidžia išsamiai išanalizuoti atgalines oro masių trajektorijas ir padidėjusių OA ir BC koncentracijų geografinę kilmę bei išsiaiškinti jų judėjimą tiriamame regione.

TYRIMO REZULTATAI

NR-PM_1 ir eBC šaltinių nustatymas skirtingose aplinkose

Siekiant ištirti karščiui neatsparių aerozolio dalelių, kurių skersmuo mažesnis už 1 μm, (NR-PM_1) ir eBC šaltinius skirtingose aplinkose, matavimai buvo atliekami skirtingose vietose: Lietuvoje – Rūgšteliškis (kaimo aplinka) ir Vilnius (miesto foninė aplinka), Filipinuose – Kesono miesto rytinis prospektas (miesto aplinka) ir Manilos uostas (pakrantės aplinka). Visose matavimo vietose NR-PM_1 matavimai buvo atliekami naudojant ACSM, o eBC matavimai - naudojant AE.

NR-PM_1 ir eBC šaltiniai kaimo aplinkoje

NR-PM_1 matavimai buvo atliekami penkerius metus (2013, 2014, 2016, 2018 ir 2019 m.) (5A pav. ir 4 lentelė), o eBC matavimai buvo atliekami ketverius metus (2013, 2014, 2018 ir 2019 m.) Rūgšteliškio stotyje (kaimo aplinka), Lietuvoje (6A pav. ir 4 lentelė).

Nustatyta, kad viso matavimo laikotarpiu (2013, 2014, 2016, 2018 ir 2019 m.) buvo stebima didesnė organinio aerozolio (OA) dalelių koncentracija (vidurkis – 29,20 μg/m³), sudaranti apie 76,7 % visos NR-PM_1 masės. Neorganinio aerozolio (IA) komponentų koncentracijos ir įnašas atitinkamai buvo mažesnis: SO_4^{2-} (6,60 μg/m³; 15 %), NO_3^- (4,40 μg/m³; 10 %), NH_4^+ (2,80 μg/m³; 7 %) ir Cl^- (0,48 μg/m³; 1 %) (5A pav. ir 5 lentelė). Panašius rezultatus įvairiuose ilgalaikiuose tyrimuose, susijusiuose su aerozolio dalelių chemine sudėtimi miško aplinkoje, nustatė Heikkinen ir kt. (2020) ir Keskinen ir kt. (2020). Jų rezultatai parodė, kad vasarą organinių aerozolio dalelių dalis yra didesnė (80 – 88 %) nei rudenį (74 – 78 %)

Atlikus ekvivalentinės juodosios anglies (eBC) valandos vidurkio analizę nustatyta, kad eBC masės koncentracija buvo didesnė 2018 m. (0,73 μg/m^3) ir 2019 m. (0,71 μg/m^3), lyginant su 2013 m. (0,54 μg/m^3) ir 2014 m. (0,41 μg/m^3) stebėtomis koncentracijomis (6A pav. ir 5 lentelė). Šio tyrimo rezultatai taip pat sutampa su Mašalaitė ir kt. (2022), Cui ir kt. (2021), Yttri ir kt. (2019), Pauraitė ir kt. (2015), Yttri ir kt. (2011), Byčenkienė ir kt. (2011) anksčiau atliktais tyrimais. Šiuose darbuose pateikiamos panašios vidutinės paros sezoninės tendencijos, kurios patvirtina vietinio biomasės deginimo ir tolimosios pernašos poveikį eBC koncentracijai. Mūsų palyginimas apima ir kitas kaimo aplinkas Europoje (6 lentelė), kuris parodė, kad vietinis biomasės deginimas ir tolimoji pernaša didina eBC koncentraciją Europos kaimo foninėse aplinkose, ypač šaltuoju laikotarpiu. Šios išvados suteikia vertingų įžvalgų apie OA ir IA, taip pat eBC laikinius svyravimus kaimo foninėse aplinkose.

Apskaičiuoti metiniai NR-PM_1 masės koncentracijos vidurkiai 2013, 2014, 2016, 2018 ir 2019 m. atitinkamai buvo 8,37 μg/m^3, 6,67 μg/m^3, 4,91 μg/m^3, 9,86 μg/m^3 ir 13,45 μg/m^3 (7A pav.). Šie rezultatai atskleidė, kad

bendra vidutinė NR-PM_1 koncentracija 2018 m. (9,86 μg/m³) ir 2019 m. (13,45 μg/m³) buvo didesnė lyginant su 2013 m. (8,37 μg/m³), 2014 m. (6,67 μg/m³) ir 2016 m. (4,91 μg/m³). Apskaičiuotas penkerių tyrimo metų bendras vidutinis sezoninis NR-PM_1 koncentracijos vidurkis ir nustatyta, kad pavasarį NR-PM_1 koncentracija buvo didesnė (9,07 μg/m^3) lyginant su vasara (8,75 μg/m^3) ir rudeniu (6,99 μg/m^3) (7A pav.). Tačiau didžiausia NR-PM_1 masės koncentracija buvo stebima 2018 m. (9,23 μg/m^3) ir 2019 m. (14,20 μg/m^3) pavasariais. Ir priešingai, didžiausios NR-PM_1 masės koncentracijos 2013, 2016 ir 2018 m. buvo stebimos vasaros sezonais (atitinkamai 8,53 μg/m^3, 6,21 μg/m^3 ir 10,88 μg/m^3). Žemesnė NR-PM_1 koncentracija buvo stebėta 2013 ir 2016 m. rudens sezonais, lyginant su 2014 ir 2018 m. Šie svyravimai gali būti siejami su meteorologinėmis sąlygomis, kai pavasarį ir vasarą aukštesnė NR-PM1 koncentracija yra siejama su aukštesne oro temperatūra, mažesne santykine oro drėgme ir didesniu vėjo greičiu (Heikkinen ir kt., 2020; Keskinen ir kt., 2020; Kourtchev ir kt., 2013).

Įvertinta ketverių metų trukmės bendra vidutinė sezoninė eBC koncentracija ir nustatyta, kad rudenį bendra vidutinė sezoninė eBC koncentracija (0,72 ± 0,58 μg/m³) buvo didesnė nei pavasarį (0,66 ± 0,56 μg/m³) ir vasarą (0,46 ± 0,34 μg/m³) ir (7E pav.). Pažymėtina, kad vidutinė eBC koncentracija rudenį buvo didesnė visais tiriamaisiais metais, pavyzdžiui, 2013 m. (0,78 ± 0,62 μg/m^3), 2014 m. (0,56 ± 0,43 μg/m^3) ir 2018 m. (0,82 ± 0,57 μg/m^3) (7E pav.). Šis padidėjimas rudenį pirmiausia gali būti siejamas su šildymo sezono pradžia, kurio metu labai padaugėja kietojo kuro (pvz.: medienos, anglies ir biomasės) deginimas namų ūkių šildymui. Degant šioms medžiagoms į atmosferą išsiskiria didelės juodosios anglies koncentracijos. Be to, rudeniui būdingos stabilios atmosferos sąlygos, kurioms būdingas silpnesnis vėjas ir sumažėjęs vertikalusis oro maišymasis, taip pat prisideda prie didesnės juodosios anglies koncentracijos, nes teršalai lieka arčiau žemės ir lėčiau išsisklaido (Ahlberg ir kt., 2023). Pavasario sezono metu 2018 m. ir 2019 m. buvo stebimas eBC koncentracijos padidėjimas (vidurkis atitinkamai 0,84 ± 0,65 μg/m³ ir 0,75 ± 0,40 μg/m³). Šios reikšmės buvo apie 27% ir 14% didesnės nei bendra pavasario sezono vidutinė koncentracija (0,66 ± 0,56 μg/m³), ir atitinkamai 83% ir 63% didesnės nei vasaros sezono vidutinė koncentracija (0,46 ± 0,34 μg/m³). Nors rudenį paprastai buvo stebima didžiausia sezono vidutinė eBC koncentracija (0,72 ± 0,58 μg/m³), pavasario reikšmės 2018 ir 2019 m. buvo panašios arba net viršijo rudens reikšmes kai kuriais metais, pvz., 2014 m. (0,56 μg/m³) ir 2018 m. (0,82 μg/m³). Pavyzdžiui, žemesnė temperatūra ir didesnė santykinė oro drėgmė gali padidinti teršalų kaupimąsi pažemio sluoksnyje ir sukurti palankias sąlygas antrinių organinių aerozolio dalelių susidarymui, kurių

sudėtyje gali būti eBC ir padidinti jų koncentraciją atmosferoje (Błaszczak ir kt., 2020; Aurela ir kt., 2011). Biomasės deginimas ir tolimoji pernaša taip pat didina sezonines eBC koncentracijas (Byčenkienė ir kt., 2011; Pauraitė ir kt., 2015). Tuo tarpu 2013, 2014, 2018 ir 2019 m. vasaromis eBC koncentracija buvo mažesnė (0,31 $\mu g/m^3$, 0,28 $\mu g/m^3$, 0,55 $\mu g/m^3$ ir 0,68 $\mu g/m^3$ atitinkamai) nei pavasarį ir rudenį. Tam įtakos galėjo turėti padidėjęs atmosferos vertikalusis maišymasis ir gausesni krituliai, kurie padidina aerozolio dalelių išplovimą, todėl atmosferoje sumažėja eBC koncentracija (Hyvärinen ir kt., 2011). Šiltuoju laikotarpiu yra sumažėjęs gyvenamųjų patalpų šildymas arba jo iš viso nėra, taip pat mažiau deginami žemės ūkio naudmenys, todėl sumažėja ir eBC emisijos. Vasarą auganti augmenija taip pat padeda sulaikyti ore esančias daleles, o tai dar labiau prisideda prie mažesnės eBC koncentracijos (Cui ir kt., 2021). Rūgšteliškio kaimo aplinkos stotyje nustatyti kasmetiniai vasaros ir kitų sezonų skirtumai rodo, kad vėsesnės (vidutinė temperatūra apie 14 °C) ir drėgnesnės oro sąlygos (vidutinė santykinė drėgmė 74 %) yra glaudžiai susijusios su padidėjusia eBC koncentracija. Tokios sąlygos, dažniau pasitaikančios pavasarį ir rudenį, riboja teršalų sklaidą atmosferoje ir skatina jų kaupimąsi pažemio sluoksnyje.

NR-PM_1 ir eBC parinių koncentracijų kaitos analizė Rūgšteliškio stotyje buvo atlikta įvairiais metų laikais, todėl kaimo vietovėje buvo galima atlikti palyginamąjį vertinimą. Rezultatai parodė, kad visais trimis sezonais (atitinkamai pavasarį, vasarą ir rudenį) didesnė OA koncentracija (atitinkamai 8,34 $\mu g/m^3$, 6,60 $\mu g/m^3$ ir 5,62 $\mu g/m^3$) nustatyta rytinėmis valandomis (6 – 8 val.), o mažesnė – popietinėmis valandomis (12 – 15 val.), atitinkamai 5,45 $\mu g/m^3$, 5,61 $\mu g/m^3$ ir 4,69 $\mu g/m^3$ (8A pav.). Kaimo aplinkoje atlikti tyrimai atskleidė, kad didesnė OA koncentracija rytinėmis valandomis yra susijusi su mažesniu pažemio sluoksnio aukščiu, o naktį ir anksti ryte išlieka padidėjusi dėl susikaupusių pirmtakinių išmetamųjų teršalų palyginti stabiliame pažemio sluoksnyje. Patekėjus saulei OA koncentracija dienos metu paprastai mažėja ir mažiausias vertes pasiekia tarp 12 ir 15 val. Tikėtina, kad šiai tendencijai įtakos turi sumažėjęs antrinių organinių aerozolio dalelių (SOA) susidarymas ir padidėjęs atmosferos pažemio maišymosi sluoksnis šiomis valandomis (Carbone ir kt., (2017); Li ir kt., (2019) ir Yu ir kt., (2021); Heald ir kt., (2005)). Nitratai pasižymėjo panašiomis parinės eigos tendencijomis kaip ir organinės medžiagos, nes visais trimis sezonais (atitinkamai pavasarį, vasarą ir rudenį) rytinėmis valandomis (6 – 8 val.) pasižymėjo didesne masės koncentracija (atitinkamai 2,46 $\mu g/m^3$, 1,02 $\mu g/m^3$ ir 1,53 $\mu g/m^3$) ir mažesne masės koncentracija (atitinkamai 0,98 $\mu g/m^3$, 0,62 $\mu g/m^3$ ir 0,88 $\mu g/m^3$) popietinėmis valandomis (12 – 15 val.) (8A pav.). Kiendler ir kt. (2016) ir Sobanski ir kt. (2017) kaimo ir priemiesčio vietovėse

nustatė nuosekliai mažesnes nitratų koncentracijas dienos metu, o tai siejama su aukštesniu planetos f sluoksniu (PBL). Abiejuose šiuose tyrimuose teigiama, kad didesnė rytinė OA koncentracija susijusi su atmosferoje vykstančiomis fotocheminėmis reakcijomis, o tai rodo galimą ryšį tarp OA ir NO_3^- kaimo aplinkoje.

Visais trimis metų laikais (pavasarį, vasarą ir rudenį) sulfatų koncentracija buvo didesnė (0,96 $\mu g/m^3$, 1,03 $\mu g/m^3$ ir 1,36 $\mu g/m^3$) dienos metu (10 – 13 val.) ir mažesnė (0,67 $\mu g/m^3$, 0,82 $\mu g/m^3$ ir 1,07 $\mu g/m^3$) nakties metu (1 – 4 val.) (5A pav.). Wang ir kt. (2016) atliktame tyrime kaimo vietovėje nustatyta parinė sulfatų koncentracijos kaita: dienos metu koncentracija buvo didesnė lyginant su nakties metu. Tyrėjai šią tendenciją siejo su fotochemine sulfatų gamyba, kai veikiamas saulės spinduliuotės oksiduojasi sieros dioksidas (SO_2). Be to, Kundu ir kt. (2014) išvadose pabrėžiama, kad įvairūs veiksniai, tokie kaip saulės spinduliuotė, temperatūra ir PBL dinamika, gali daryti įtaką sulfatų susidarymui ir transformacijai atmosferoje. Šie veiksniai gali lemti padidėjusį sulfatų kiekį dienos metu. Be gamtinių priežasčių, prie padidėjusio atmosferinių sulfatų kiekio dienos metu taip pat gali prisidėti ir žmogaus veikla, pvz.: pramonės išmetami teršalai ir su eismu susijusi tarša netoli kaimo regionų, kai pramonės ir transporto veikla yra aktyviausia. NH_4^+ masės koncentracija Rūgšteliškyje visų trijų sezonų metu nerodė jokios aiškios paros eigos. Retama ir kt. (2019) teigė, kad NH_3, kuris yra susijęs su atliekų šalinimu, nuotekomis ir transporto išmetamosiomis dujomis, reaguoja su azoto rūgštimi (HNO_3) ir sieros rūgštimi (H_2SO_4), sudarydamas SO_4^{2-}, NO_3^- ir NH_4^+ daleles. Gilardoni ir kt. (2016) pasiūlė, kad žemės ūkio veikla, įskaitant mėšlo tvarkymą ir dirvožemio emisijas, yra atsakinga už didžiąją dalį pasaulyje išmetamo amoniako kiekio. Amonis veikia kaip priešingas jonas, kuris subalansuoja NO_3^- ir SO_4^{2-} koncentracijas. Todėl NH_4^+ koncentracijos paros eiga priklauso nuo nitratų ir sulfatų koncentracijų svyravimų. Kadangi NO_3^- ir SO_4^{2-} koncentracijos keičiasi dėl įvairių veiksnių, pvz.: teršalų emisijų ar tolimosios jų pernašos, NH_4^+ koncentracija atitinkamai koreguojasi, kad būtų išlaikyta pusiausvyra. Dėl šios priežasties nėra ryškios NH_4^+ koncentracijos paros eigos kaitos, nes jis veiksmingai stabilizuoja NO_3^- ir SO_4^{2-} koncentracijos svyravimus. Anksčiau publikuotuose Mărmureanu ir kt. (2020), Drugé ir kt. (2019) ir Bauer ir kt. (2007) tyrimuose teigiama, kad amoniakas daugiausia susidaro dėl žemės ūkio veiklos, kuriai mažiau tikėtina, kad pasireikš parinės eigos tendencijos. Tai atitinka mūsų tyrimo laikotarpiu stebėtą NH_4^+ koncentracijos eigą, kuri neturi aiškios parinės kaitos tendencijos, o tai patvirtina NH_4^+ kaip NO_3^- ir SO_4^2 priešingo jono vaidmenį.

Rūgšteliškio stotyje sezoninė (pavasario, vasaros ir rudens) eBC paros

eiga visų ketverių metų matavimų laikotarpiu pateikta 9A pav. Visais metų laikais eBC koncentracija buvo didesnė rytinėmis valandomis (8 – 12 val.), atitinkamai 0,77 μg/m³, 0,51 μg/m³ ir 0,76 μg/m³, ir mažesnė vėlyvomis nakties valandomis (0 – 2 val.), atitinkamai 0,60 μg/m³, 0,38 μg/m³ ir 0,60 μg/m³. Analizuojant planetos pažemio sluoksnio aukštį (PBLH) nustatyta, kad jis labai kinta paros metu, nes ankstyvą rytą ir vėlai vakare būna žemesnis, todėl teršalai, pvz.: eBC, sulaikomi prie paviršiniame Žemės sluoksnyje. Rytinius pikus sustiprina temperatūros inversijos ir minimalus vertikalus maišymosi aukštis, o dieną kylantis PBLH sudaro sąlygas teršalų skaidai, todėl jų koncentracija yra mažesnė. Meteorologinių parametrų tendencijos dienos metu rodo aukštesnę oro temperatūrą, didesnį vėjo greitį ir mažesnę santykinę drėgmę, o tai turi įtakos eBC sklaidai ir koreliuoja su PBLH svyravimais.

Panašius rezultatus pateikė Pauraitė ir kt. (2015), kur eBC koncentracija didėjo nuo 5 val. ryto, aukščiausią tašką pasiekė 8 val. ryto, o vakare dėl turbulentinio maišymosi koncentracija sumažėjo. Anglies sudėtyje turinčių aerozolio dalelių koncentracija buvo beveik dvigubai didesnė šaltuoju laikotarpiu (0,77 μg/m³) lyginant su šiltuoju (0,40 μg/m³) ir to priežastis yra sezoniniai emisijos šaltiniai, pvz.: biomasės deginimas namų šildymui ir iškastinio kuro degimo produktų tolimoji pernaša. Ahlberg ir kt. (2023) Hyltemosos stotyje (Švedija) registravo rytinį (6 – 8 val. ryto) eBC koncentracijos padidėjimą iki 0,11 μg/m³, kuris iki vidurdienio (12 – 15 val.) sumažėjo iki 0,08 μg/m³. Panašiai Aurela ir kt. (2011) Hyytiälä stotyje (Suomija) registravo padidėjusius rytinius eBC koncentracijos lygius (1,28 μg/m³, 6 – 9 val.) ir mažesnius vakarinius lygius (0,95 μg/m³, 15 – 18 val.). Hyvärinen et al. (2011) Hyytiälä stotyje nustatė, kad rytinis maksimalus 1,34 μg/m³ eBC koncentracijos lygis (6 – 9 val.) po vidurdienio (12 – 19 val.) sumažėjo iki 1,11 μg/m³ ir yra susijęs su malkų deginimu gyvenamosiose patalpose, transporto eismu ir tolimąja pernaša. Mūsų tyrime buvo atlikta išsami lyginamoji analizė, kurioje palygintas parinių eBC koncentracijų eiga panašiose kaimo matavimo vietose visoje Europoje. Rytiniai eBC koncentracijų maksimumai Lietuvoje sutampa su užregistruotais Hyytiälä stotyje (Suomija), tačiau jie yra didesni nei Hyltemossa stotyje (Švedija). Šį skirtumą galėjo lemti tai, kad Suomijoje ir Lietuvoje yra labiau paplitęs namų šildymas malkomis šaltuoju metų laiku, o Švedijoje gali būti populiaresni alternatyvūs šildymo būdai. Be to, panašu, kad šiuose regionuose skiriasi vietinių ir nutolusių šaltinių įtakos proporcija. Sumažėjusios vakarinės eBC koncentracijos Lietuvoje gali rodyti stiprią vietinių šaltinių, pavyzdžiui, gyvenamųjų namų šildymo šaltuoju metų laiku arba galimai malkų deginimo maisto ruošimui, įtaką, kuri naktį sumažėja. Tačiau reikėtų pažymėti, kad vasaros metu, kai šildymas nevyksta, eBC koncentracijos paprastai yra žemesnės. Tuo tarpu Švedijos stoties duomenys rodo nuolatinę tolimosios pernašos įtaką dėl šalies geografinės padėties ir vyraujančių vėjo krypčių. Šie tyrimai išryškina skirtingą vietinių ir nutolusių šaltinių įtaką eBC koncentracijai kaimo aplinkoje.

Transporto eismo ir biomasės deginimo metu išmetamų eBC šaltinių

kilmės nustatymas buvo atliekamas naudojant iškastinio kuro deginimo (AAE_{FF}) ir biomasės deginimo (AAE_{BB}) absorbcijos Ångströmo eksponentes. eBC_{FF} ir eBC_{BB} laikinė eiga kartu su jų indėliu į bendrą eBC masės koncentraciją per ketverių metų matavimo kampaniją (2013, 2014, 2018, 2019 m.) Lietuvos kaimo vietovėje pateiktos 10A pav. Iškastinio kuro deginimo metu susidaręs eBC_{FF} sudarė 90% (vidutinė masės koncentracija – 0,52 μg/m³) bendros eBC koncentracijos, o biomasės deginimo metu gaunama eBC_{BB} sudarė 10% (vidutinė masės koncentracija – 0,06 μg/m³) viso eBC (10A pav.). Šie rezultatai sutampa su Yttri ir kt. (2011 ir 2019) tyrimų rezultatais, kurie parodė didesnį su iškastiniu kuru susijusį juodosios anglies indėlį Europos kaimo vietovėse. Panašiai Hienola ir kt. (2013) ir Kupiainen ir kt. (2006) tyrimuose nustatyta, kad Hyytiälä stotyje Suomijoje iškastinis kuras ir biomasės deginimas gyvenamosiose vietovėse yra pagrindiniai eBC šaltiniai Europos kaimo aplinkoje. Nepaisant tokių politikos priemonių kaip „2020 klimato ir energetikos paketas“, kuriuo siekiama sumažinti iškastinio kuro naudojimą Europos Sąjungoje (ES), mūsų išvados rodo, kad eBC_{FF} lygis išlieka aukštas. Tai rodo nenuoseklų ES priemonių įgyvendinimą arba ekonomines ir energetinio saugumo problemas, ypač Rytų Europoje (Radovanović ir kt., 2022; Rabbi ir kt., 2022). Priklausomybė nuo pasenusių, daug anglies dioksido išskiriančių technologijų ir lėtas perėjimas prie atsinaujinančiųjų energijos šaltinių (Khabarova ir kt., 2019 m.) dar labiau aštrina problemą, pabrėžiant veiksmingesnių regioninių strategijų poreikį.

eBC ir rudosios anglies (BrC) spektrinės priklausomybės skiriasi, nes BrC turėtų stipriai absorbuoti ultravioletinių spindulių srityje. 10A pav. pateiktos eBC ir BrC šviesos sugerties koeficientų laikinės eigos ketverių metų (2013, 2014, 2018 ir 2019) matavimo Lietuvos kaimo vietovėje laikotarpiu. BrC šviesos sugerties koeficientas 370 nm bangos ilgio ruože ($b_{abs,BrC}$) erdviškai kito nuo 0,02 iki 0,80 M m^{-1}. $b_{abs,eBC}$ indėlis šviesos sugerčiai trumpesnio bangos ilgio (370 nm) ruože 2013, 2014, 2018 ir 2019 metais sudarė 86% (vidutinė masės koncentracija – 0,57 μg/m³), o BrC indėlis buvo tik 14% (vidutinė masės koncentracija – 0,09 μg/m³) (10E pav.). Remiantis Liu ir kt. (2018) ir Qin ir kt. (2018) publikuotais tyrimais yra akivaizdu, kad pagrindinis BrC šaltinis buvo biomasės deginimas, tačiau žinomi ir keli kiti galimi šaltiniai, pvz.: biokuro deginimas, antropogeninių ir biogeninių lakiųjų organinių junginių fotooksidacija arba vandens fazės cheminės reakcijos (Wang ir kt., 2016; Pokhrel ir kt., 2017). Mūsų gauti rezultatai sutampa su Masalaitės ir kt. (2022), kad BrC pagrindinis šaltinis yra biomasės deginimas, o ne kiti biogeninės kilmės šaltiniai.

Viso matavimo laikotarpiu Rūgšteliškyje (kaimo vietovė) kartu su NR-PM_1 ir eBC sistemingai 1 valandos intervalais buvo registruojami

meteorologiniai parametrai (11A, 11E ir 11I pav.). Rūgšteliškio stotyje registruotų paros vidutinių T, RH, WS, WD reikšmių duomenys pateikti 7 lentelėje (skaičius po "±" yra standartinis nuokrypis).

Atliktus NR-PM_1 ir eBC vėjo rožių analizę nustatyta, kad matavimo laikotarpiu vyravo pietų (S), pietvakarių (SW), pietų-pietvakarių (S-SW), pietryčių (SE), pietų-pietryčių (S-SE), vakarų (W), šiaurės vakarų (NW) ir vakarų-šiaurės vakarų (W-NW) krypčių vėjai (11A pav.). Šis vėjo greičio ir krypties grafinis vaizdinimas, gautas iš 1 arba 2 minučių duomenų, rodo, kad matavimo laikotarpiu vėjo greitis šioje kaimo vietovėje retkarčiais viršijo 5 m/s. Vėjo rožių diagramoje kiekvieno segmento ilgis reiškia vėjų, kylančių iš tam tikros krypties sektoriaus, dažnį laikui bėgant. Siekiant nustatyti su didžiausiomis NR-PM_1 ir eBC koncentracijomis susijusias vėjo kryptis Rūgšteliškio stotyje, šios koncentracijos buvo suskirstytos į kategorijas pagal vėjo kryptis. Atlikta analizė atskleidė, kad tyrimų laikotarpiu vyravo vėjai iš šiaurės, rytų ir pietų krypčių (11E ir 11I pav.). Nustatyta, kad didesnės NR-PM_1 ir eBC koncentracijos buvo susijusios su vyraujančiomis vėjo kryptimis ir didesniais šių krypčių vėjo greičiais iš šiaurės, rytų ir pietų krypčių. Tikėtina, kad vėjas iš pietinių ir rytinių krypčių pernešė teršalus iš aplinkinių gyvenviečių ir žemės ūkio teritorijų, o šiauriniai – iš nutolusių regioninių šaltinių. Atlikus tyrimą padaryta išvada, kad organinės medžiagos, įskaitant organines aerozolio daleles ir organinius nitratus, yra iš vietinių šaltinių, o neorganinės aerozolio dalelės (tokios kaip neorganiniai nitratai, amonis, sulfatai ir juodoji anglis) yra iš nutolusių taršos šaltinių, į matavimų stotį patekusios tolimosios pernašos būdu. Kadangi Rūgšteliškis yra dideliu atstumu nutolęs nuo jūros, pagrindinių kelių, elektrinių ir ugnikalnių, o vietinėje aplinkoje biomasė deginama minimaliai, labai tikėtina, kad į šią kaimo vietovę tolimoji pernaša atneša ne tik neorganines aerozolio daleles, bet ir jų pirmtakus. Be to, eBC šaltinių. Be to, eBC šaltinių kilmės nustatymo analizė atskleidė, kad pagrindiniai juodosios anglies šaltiniai kaimo vietovėse yra tolimoji pernaša ir deginimas buityje (daugiausia medienos deginimas).

NR-PM_1 ir eBC šaltiniai Vilniaus miesto aplinkoje

Vilniuje NR-PM_1 ir eBC matavimai atlikti 2014 m. žiemą (sausio – vasario mėn.) (5B pav., 6B pav., 4 lentelė) ir nustatyta, kad didžiausia vidutinė valandinė organinių medžiagų masės koncentracija siekė 58 μg/m³, o NO_3^-, NH_4^+, SO_4^{2-} ir Cl^- didžiausios vidutinės valandinės masės koncentracijos buvo atitinkamai 17 μg/m³, 14 μg/m³, 8 μg/m³ ir 4 μg/m³ (5B pav.). eBC didžiausia vidutinė valandinė koncentracija siekė 14,59 μg/m³ (6B pav.).-Tikėtina, kad amonio (NH_4^+) kilmės šaltinis yra žemės ūkis ir į matavimo vietą jis buvo perneštas dėl tolimosios pernašos, o nitratai (NO_3^-) atspindėjo išmetamąsias dujas iš vietinio transporto. Išskirtinės meteorologinės sąlygos, kai

temperatūra svyravo nuo -25 °C iki 2 °C, turėjo įtakos teršalų emisijai ir dinamikai žiemos sezono metu. Vidutinė NR-PM_1 ir eBC koncentracija tyrimų metu buvo atitinkamai 18,98 ± 5,25 μg/m³ ir 2,46 ± 1,99 μg/m³ (7B pav., 7F pav.). Atlikus paros eigos analizę nustatyta, kad organinių aerozolio dalelių koncentracija pasižymėjo dviem ryškiais pikais: ryte (5 – 8 val.) ir vėlai vakare (22 – 23 val.) ji buvo aukštesnė (atitinkamai 10,85 μg/m³ ir 14,50 μg/m³), o po pietų (12 – 16 val.) – žemesnė (7.93 μg/m³) (8B pav.). NO_3^-, NH_4^+, SO_4^{2-} ir Cl^- koncentracijos taip pat buvo aukščiausios ryte (atitinkamai 3,72 μg/m³, 3,60 μg/m³, 2,01 μg/m³ ir 0,37 μg/m³) ir žemiausios po pietų (atitinkamai 2,87 μg/m³, 3,06 μg/m³, 1,64 μg/m³ ir 0,24 μg/m³) (8B pav.). Šie dėsningumai rodo, kad nitratų ir sulfatų susidarymas priklauso nuo transporto išmetamų teršalų ir SO_2 oksidacijos šildymo sezono metu (Teinilä ir kt., 2019). eBC paros eigos tendencijos parodė, kad aukščiausia koncentracija buvo ryte (3,14 μg/m³, 8 – 10 val.) ir vakare (2,83 μg/m³, 18 – 20 val.), o anksti ryte (4 – 6 val.) ji buvo žemiausia (1,68 μg/m³, 9B pav.). Didesnės koncentracijos koreliavo su piko valandomis ir namų ūkio šildymu, o tai atitinka Minderytė ir kt. (2022) tyrimo rezultatus. Iš eBC_{FF} ir eBC_{BB} laikinės eigos nustatyta, kad iškastinio kuro nulemtas eBC_{FF} sudarė 85% (vidutinė masės koncentracija – 2,00 μg/m³) viso eBC, o su biomasės deginimu susijęs eBC_{BB} – 15% (vidutinė masės koncentracija – 0,36 μg/m³) (10B pav.). Pagal šviesos sugerties koeficientus nustatyta, kad ties 370 nm bangos ilgiu eBC sudarė 82% (vidutinė masės koncentracija – 2,34 μg/m³), o BrC – 18% (vidutinė masės koncentracija – 0,51 μg/m³) (10F pav.). Atlikus vėjo rožių ir plotinių pasiskirstymų analizę (11B pav., 11F pav., 11J pav.) nustatyta, kad vyravo vakarų, šiaurės vakarų, rytų, pietų ir pietryčių krypčių vėjai. Aukštesnės NR-PM_1 ir eBC koncentracijos buvo susijusios su vakarų vėjais ir padidėjusiu vėjo greičiu, o tai rodo, kad koncentracijų padidėjimui įtakos turėjo tiek vietiniai taršos šaltiniai, tiek tolimoji pernaša iš nutolusių šaltinių. Vakarų kryptis atitinka pramoninius ar intensyvaus eismo rajonus į vakarus nuo matavimo vietos, o rytinės kryptys gali būti susijusios su priemiesčių ar regioniniais šaltiniais.

NR-PM_1 ir eBC šaltiniai Kesono miesto aplinkoje

eBC matavimai Kesono Sičio Rytų (QCG) prospekte (Filipinai) buvo atliekami 2020 m. sausio 29 d. – vasario 26 d. (6C pav., 4 lentelė). Didžiausia vidutinė valandinė eBC masės koncentracija siekė 104,54 μg/m³, o žiemos vidurkis buvo 36,19 ± 16,02 μg/m³ (7G pav.). Didelės eBC koncentracijos pirmiausia buvo siejamos su transporto priemonių išmetamais teršalais ir pramonine veikla, o tai atitinka Alas ir kt. (2018) bei Madueño ir kt., (2022) tyrimų rezultatus. Šie tyrimai atskleidė, kad eBC koncentracija Manilos metropolitene yra 2 – 17 kartų didesnė nei Indijos, Kinijos, Europos ir JAV miestų teritorijose, o tai rodo didelį sparčios urbanizacijos ir pramonės augimo neigiamą poveikį oro kokybei. Vidutinė metinė eBC koncentracija Maniloje

dar nenustatyta, tačiau gauti rezultatai pabrėžia, kad būtina skubiai imtis klimato kaitos mažinimo strategijų. Paros eigos analizė atskleidė du ryškius eBC koncentracijos padidėjimus: 63,45 ± 10,61 μg/m³ rytinio piko metu (6 – 8 val. ryto) ir 43,48 μg/m³ vėlyvo vakaro metu (22 – 23 val. vakaro), o dienos metu (12 – 21 val.) koncentracija buvo mažesnė (23,43 ± 10,61 μg/m³) (9C pav.). Rytiniai eBC koncentracijos maksimumai buvo susiję su transporto išmetamais teršalais, įskaitant lengvųjų automobilių ir džipnių eismą, o vakariniai maksimumai – su sunkiasvoriais dyzeliniais sunkvežimiais, kuriems miesto gatvėmis leidžiama važiuoti nuo 22 iki 7 val. ryto (Alas ir kt., 2018). Mažesnei paros eBC koncentracijai įtakos taip pat turėjo didesnis vėjo greitis ir aukštesnis maišymosi sluoksnio aukštis, kuris palengvino teršalų sklaidą, o naktinė koncentracija atitinkamai buvo padidėjusi dėl mažesnio vėjo greičio ir sumažėjusio maišymosi sluoksnio aukščio. Šaltinių kilmės nustatymo analizė atskleidė, kad transporto išmetamų teršalų kiekis (eBC_{TR}) sudarė 80% (vidutinė masės koncentracija – 25,01 μg/m³) viso eBC, o biomasės deginimas (eBC_{BB}) – 20% (vidutinė masės koncentracija – 6,07 μg/m³) (10C pav.). Daugiausia teršalų išmetė iškastiniu kuru varomas transportas, ypač dyzelinu varomi džipniai ir lengvosios transporto priemonės (Kecorius ir kt., 2017; Madueño ir kt., 2019). Dėl biomasės deginimo susidaranti eBC_{BB} buvo priskiriama maisto ruošimui namuose ir komerciniais tikslais, ypač medžio anglies naudojimas, o tai atitinka Liu ir kt., (2018) ir Qin ir kt., (2018) tyrimo rezultatus. Šviesos sugerties koeficientų laikinė eiga (10C pav.) atskleidė, kad 370 nm bangos ilgio ruože eBC sudarė 78% (vidutinė masės koncentracija – 28,23 μg/m³) bendros šviesos sugerties, o BrC – 22% (vidutinė masės koncentracija – 7,79 μg/m³). Panašus BrC indėlis buvo stebėtas tokiuose miestuose kaip Manausas (Brazilija), Singapūras, Lionas (Prancūzija), Katmandu (Nepalas) ir Guangdžou (Kinija), kur BrC indėlis svyravo nuo 15 iki 25% (De Sá ir kt., 2019; Kasthuriarachchi ir kt., 2020; Zhang ir kt., 2020a; Kim ir kt., 2021; Liu ir kt., 2018; Qin ir kt., 2018) (9 lentelė). Tačiau gerokai didesnis BrC kiekis užfiksuotas Čiangmajuje (Tailandas, 45%) ir Pekine (Kinija, 46%), visų pirma dėl medienos ir biomasės deginimo gyvenamuosiuose namuose. Priešingai, mažesnė BrC indėlio dalis (2 – 10%) nustatyta kituose Kinijos ir Korėjos miestų teritorijose, kur biomasės deginimas yra mažiau paplitęs (Zhang ir kt., 2020a; Pani ir kt., 2021; Xie ir kt., 2019) (9 lentelė). Meteorologinė analizė (11C, 11K pav.) parodė, kad QCG vyrauja vakarų (W), pietvakarių (SW), vakarų-pietvakarių (WSW), šiaurės (N) ir rytų (E) vėjai. Plotinių pasiskirstymų analizė parodė, kad aukštesnė eBC koncentracija buvo susijusi su rytinėmis vėjo kryptimis ir didesniu vėjo greičiu, o tai nurodo, kad eBC koncentracijai įtakos turi tiek vietiniai šaltiniai, tiek tolimoji pernaša. Tikėtina, kad rytinių krypčių vėjai pernešė teršalus iš

tankiai apgyvendintų miesto rajonų su intensyviu transporto srautu į rytus nuo matavimo vietos. Atgalinių oro masių trajektorijų analizė patvirtino, kad didžiausia eBC koncentracija buvo esant oro masėms iš pietvakarių, pietų, pietryčių, rytų ir šiaurės rytų krypčių. Šie dėsningumai rodo dvejopą vietinių miesto išmetamųjų teršalų ir pernešamų teršalų įtaką oro kokybei QCG vietovėje.

NR-PM_1 ir eBC šaltiniai Manilos pakrantės aplinkoje

NR-PM_1 ir eBC tyrimai Manilos šiauriniame uoste buvo atliekami nuo 2019 m. gruodžio 20 d. iki 2020 m. sausio 25 d. (5C pav., 6D pav. ir 4 lentelė). Bendra NR-PM_1 masės koncentracija siekė iki 108,38 μg/m³, o organinių aerozolio dalelių (OA) masės koncentracija dominavo ir sudarė 80% (23,68 ± 16,40 μg/m³) NR-PM1 masės. Antras pagal dydį indelis buvo sulfatų (10%, 3,09 ± 2,60 μg/m³), tuomet nitratų (4%, 1,18 ± 1,32 μg/m³), amonio (4%, 1,19 ± 1,02 μg/m³) ir chlorido (2%, 0,47 ± 0,78 μg/m³) (5D pav.). Mūsų gauti rezultatai sutampa su kituose miestuose atliktais tyrimais, pvz.: Stavroulas ir kt. (2021) Pirėjuje (Graikija) nustatė panašiai didelę OA frakciją (67%), o sulfatų (19%) ir nitratų (6%) indėlis buvo mažesnis. Tyrimai Delyje, Indijoje (Gani ir kt., 2019; Patel ir kt., 2021), ir Katmandu, Nepale (Warden ir kt., 2022), taip pat rodo OA dominavimą, nors ir su tam tikrais regioniniais neorganinių komponentų skirtumais dėl vietinio transporto eismo ypatumų ir pramonės išmetamų teršalų. Vidutinė valandinė eBC koncentracija Manilos uoste buvo 10,27 ± 5,99 μg/m³, o didžiausia – 35,82 μg/m³ (6D pav.). Kaip pažymima Alas ir kt. (2018) ir Cadondon ir kt. (2024), padidėjusi eBC koncentracija visų pirma buvo susijusi su transporto priemonių, pramoninės veiklos ir laivų veiklos išmetamais teršalais. Atgalinių oro masių trajektorijų analizė patvirtino, kad oro masės daugiausia buvo užsistovėjusios prie tiriamos teritorijos, o iš Ramiojo vandenyno jų indėlis buvo nedidelis. Palyginti su Kvezono miestu, eBC koncentracija uoste buvo mažesnė, o tai galbūt atspindi geresnes sąlygas taršos sklaidai, mažesnį transporto eismo ir pramoninės veiklos intensyvumą. Vidutinė NR-PM_1 ir eBC koncentracija tyrimų laikotarpiu buvo atitinkamai 29,52 μg/m³ ir 10,27 μg/m³ (7D pav., 7H pav.). Paros eiga parodė ryškius OA koncentracijos padidėjimus: 29,43 μg/m³ rytinio piko metu (6 – 8 val. ryto) ir 40,02 μg/m³ vakare (18 – 22 val.), kurie sutapo su didžiausio eismo intensyvumo ir maisto gamybos laiku (8C pav.). Priešingai, neorganinių aerozolio dalelių koncentracija ryte buvo didesnė (SO_4^{2-} – 4,89 μg/m³, NO_3^- – 3,08 μg/m³, NH_4^+ – 2,16 μg/m³ ir Cl^- – 1,03 μg/m³), o vakare – mažesnės (atitinkamai 1,92 μg/m^3, 0.37 μg/m^3, 0,59 μg/m^3 ir 0,07 μg/m^3).

eBC koncentracijos taip pat buvo didžiausios ryte (15,57 ± 3,46 μg/m³) dėl intensyvesnio kelių transporto eismo, didesnio dyzelinu varomų transporto priemonių kiekio ir jūrų transporto išmetamų teršalų. Po pietų eBC koncentracija sumažėjo iki

5,05 ± 3,46 μg/m³ dėl sumažėjusio transporto eismo srauto ir aukštesnio maišymosi sluoksnio (9D pav.). Panašūs dėsningumai buvo stebėti ir kituose tyrimuose (Kecorius ir kt., 2017; Madueño ir kt., 2019), pabrėžiant transporto eismo ir pramoninės veiklos įtaką aerozolio dalelių koncentracijai šiame regione. Šaltinių pasiskirstymo analizė parodė, kad transporto išmetami teršalai (eBC_{TR}) sudarė 86% (vidutinė masės koncentracija – 7,75 μg/m³) visos eBC, o biomasės deginimas (eBC_{BB}) – 14% (vidutinė masės koncentracija – 1,28 μg/m³) (10D pav.). Transporto išmetami teršalai buvo susiję su lengvaisiais automobiliais, sunkiasvoriais sunkvežimiais, dyzelinu varomais mažais žvejybiniais laiveliais ir kranais, o biomasės deginimo šaltiniai buvo medienos ir žemės ūkio atliekų deginimas (Liu ir kt., 2018; Qin ir kt., 2018). Analizuojant šviesos sugerties koeficientus nustatyta, kad prie 370 nm bangos ilgio dominuoja eBC – 80% (vidutinė masės koncentracija – 8,36 μg/m³), o BrC indėlis sudarė 20% (vidutinė masės koncentracija – 2,06 μg/m³) (10H pav.). Panašus BrC indėlis buvo registruotas tokiuose miestuose kaip Manausas, Singapūras ir Lionas (15 – 25%), o vietovėse, kuriose deginama daug biomasės, pvz. Čiangmajuje ir Pekine, užfiksuotas didesnis BrC indėlis (45 – 46%) (De Sá ir kt., 2019; Zhang ir kt., 2020a). Meteorologiniai duomenys (8D, 8H, 8L pav.) parodė, kad vyravo vakarų (W), šiaurės vakarų (NW), šiaurės (N), šiaurės rytų (NE), rytų (E) ir pietryčių (SE) vėjai. Plotinių pasiskirstymų analizė parodė, kad padidėjusi $NR\text{-}PM_1$ ir eBC koncentracija buvo susijusi su vakarų vėjais ir padidėjusiu vėjo greičiu. Tikėtina, kad vakarų krypties vėjai pernešė teršalus iš uosto veiklos zonų, pramoninių rajonų ir eismo intensyvių teritorijų į vakarus nuo matavimo vietos. Šie duomenys rodo, kad Manilos uoste užregistruoti teršalai yra tiek iš vietinių šaltinių, pvz. jūrinė ir pramoninė veikla, tiek dėl tolimųjų pernašų atnešti iš nutolusių šaltinių.

KAIMO, MIESTO IR PAKRANTĖS APLINKŲ PALYGINIMAS

Siekiant palyginti oro kokybės dinamiką kaimo (Rūgšteliškis), miesto (Vilnius ir Kesonas) ir pakrantės (Manilos šiaurinis uostas) aplinkose, šiame skyriuje pateikiamas išsamus $NR\text{-}PM_1$ ir eBC masių koncentracijų, paros eigų, šaltinių pasiskirstymo ir oro masių trajektorijų palyginimas siekiant nustatyti kiekvienai vietovei būdingas unikalias ir bendras taršos charakteristikas. Šios įžvalgos yra labai svarbios kuriant veiksmingas, konkrečiai vietovei pritaikytas oro taršos valdymo strategijas.

Lyginamoji analizė atskleidė didelius erdvinius $NR\text{-}PM_1$ ir eBC koncentracijos skirtumus, kuriuos lemia vietiniai taršos šaltiniai ir atmosferos sąlygos: didžiausios koncentracijos nustatytos Kesono mieste (miesto vietovė), mažesnės – Manilos Šiaurės uoste (pakrantės vietovė), Vilniuje (miesto vietovė), o mažiausi – Rūgšteliškyje (kaimo vietovė) (4 lentelė). Atlikus sezoninę analizę nustatyta, kad Rūgšteliškyje (kaimo vietovėje) didžiausios $NR\text{-}PM_1$ koncentracijos buvo pavasarį ir vasarą, o didžiausios eBC koncentracijos buvo rudenį. Vilniuje ir Kesone (miesto vietovė) bei

Manilos uosto vietovėje NR-PM_1 ir eBC koncentracija buvo didesnė žiemos sezonu.

Rūgšteliškyje (kaimo vietovėje) NR-PM_1 padidėjimą pavasarį ir vasarą galima sieti su padidėjusia biologine veikla ir aukštesne vidutine paros temperatūra. Tuo tarpu didesnę eBC koncentraciją rudenį lemia padidėjęs deginimas namų šildymui ir žemės ūkio veikla, susijusi su derliaus nuėmimo sezonu šioje vietovėje. Vilniaus mieste aukštesnę NR-PM_1 ir eBC koncentraciją žiemos metu lemia buitinė veikla, pvz. biomasės ir iškastinio kuro deginimas, transporto išmetami teršalai ir tolimojo susisiekimo transportas. Prie šio koncentracijos padidėjimo taip pat prisideda meteorologinės žiemos sąlygos, kai šaltesniame klimate dėl padidėjusio šildymo poreikio ir stabilesnių atmosferos sąlygų, sulaikančių teršalus pažemio sluoksnyje, gali daryti didelę neigiamą įtaką oro kokybei. Kesono Sityje (miesto vietovė) buvo registruojamos didžiausios eBC koncentracijos lyginant su kitomis vietovėmis tiriamuoju laikotarpiu, o tai rodo intensyvaus transporto eismo ir vietinės pramonės išmetamų teršalų poveikį. Manilos šiauriniame uoste (pakrantės vietovė) didelei NR-PM_1 ir eBC koncentracijai įtakos turėjo uosto veikla ir transporto priemonių išmetami teršalai. Čia meteorologinės sąlygos, pvz. didesnis vėjo greitis uosto teritorijoje, paprastai sumažina teršalų koncentraciją, lyginti su Kesonu ir kitomis tirtomis vietovėmis. Rezultatai rodo, kad oro kokybę galima pagerinti konkrečiais veiksmais, pvz. įgyvendinant griežtesnes išmetamųjų teršalų taisykles šaltesniuose regionuose esančiuose miestuose žiemą ir valdant transporto eismo bei pramonės išmetamųjų teršalų kiekį tankiai apgyvendintose teritorijose, pvz. Kesono mieste. Siekiant veiksmingai valdyti oro taršą, labai svarbu vykdyti nuolatinę stebėseną ir taikyti vietovei pritaikytą oro kokybės valdymo politiką. Toks požiūris užtikrintų, kad intervencinės priemonės būtų pagrįstos moksliniais įrodymais ir pritaikytos prie unikalių skirtingų regionų ir metų laikų ypatybių.

Atlikus paros eigos analizę kaimo, miesto ir pakrantės vietovėse nustatyta, kad tiek NR-PM_1, tiek eBC koncentracijos ryte ir vėlai vakare pasiekia ryškius maksimumus, kuriuos lemia transporto išmetami teršalai, pramoninė veikla ir jūrinės operacijos. Šioms tendencijoms papildomai įtakos turėjo atmosferos sąlygos, tokios kaip vėjo greitis ir pažemio sluoksnio dinamika. Nors tiek NR-PM_1, tiek eBC koncentracijų paros eigos raštas visose tyrimų vietose išliko panašus, su ryto ir vakaro piko valandomis, koncentracijų dydis reikšmingai skyrėsi. Didžiausios eBC koncentracijos užfiksuotos Kesono mieste (miesto vietovė), mažesnės – Manilos uoste (pakrantės vietovė) ir Vilniuje (miesto vietovė), o mažiausios – Rūgšteliškio kaime (kaimo vietovė). Tuo tarpu NR-PM_1 koncentracijų palyginimas atliktas tik tarp Vilniaus, Manilos uosto ir Rūgšteliškio, nes Kesono mieste NR-PM_1 duomenys nebuvo prieinami. Iš šių vietovių didžiausia NR-PM_1 koncentracija nustatyta Manilos uoste, šiek tiek mažesnė – Vilniuje, o mažiausia – Rūgšteliškyje. Rūgšteliškio stotyje rytiniai OA maksimumai buvo susiję su žemu pažemio sluoksnio maišymosi aukščiu, dėl kurio teršalai kaupėsi prie žemės paviršiaus.

Šiltėjant oro temperatūrai didėjo pažemio sluoksnio aukštis, todėl po pietų NR-PM_1 ir eBC koncentracijos sumažėjo. Didesnės eBC koncentracijos ryte ir vakare buvo susiję su medienos deginimu, vietinio transporto eismu ir tolimąja pernaša. Žiemos sezonu Vilniuje paros eigos analizė parodė, kad NR-PM_1 ir eBC koncentracijų maksimumus ryte ir vėlai vakare, kuriuos lėmė vietinio transporto išmetami teršalai, buitinis šildymas ir regioninė žemės ūkio veikla. eBC koncentracijos maksimumas taip pat buvo susijęs su transporto eismo intensyvumo piko valandomis ir maisto ruošimu namuose, o taršos sumažėjimas atitiko mažą santykinę oro drėgmę. Kesono mieste ryte ir vėlai vakare eBC koncentracijos maksimumas buvo susijęs su transporto eismo išmetamais teršalais, įskaitant lengvuosius automobilius ir džipnius piko valandomis, o vėlai vakare – su padidėjusiu dyzelinu varomo sunkiasvorio transporto eismo intensyvumu.

Manilos uoste rytinis ir vakarinis NR-PM_1 ir eBC pikas taip pat buvo susijęs su transporto eismu, jūrų operacijomis ir dyzelinu varomais krovos įrenginiais. Popietinė NR-PM_1 ir eBC koncentracija buvo mažesnė sumažėjus transporto eismo srautams, sumažėjus spūstims ir padidėjus pažemio maišymosi sluoksnio aukščiui. Šios išvados rodo, kad norint veiksmingai sumažinti oro taršos poveikį sveikatai ir aplinkai, reikia taikyti specialiai vietovei pritaikytas taršos kontrolės strategijas, kuriose būtų atsižvelgta į konkrečiai vietovei būdingus taršos šaltinius, didžiausios taršos laiką ir vietines oro sąlygas.

Atlikus išsamią eBC šaltinių kilmės nustatymo analizę nustatyta, kad didesnė eBC_{FF} ir eBC_{BB} koncentracija yra Kesono Sityje (miesto vietovėje), po to Manilos uoste (pakrantės vietovėje) ir Vilniuje (miesto vietovėje), o mažiausia Rūgšteliškio stotyje (kaimo vietovėje). BrC koncentracijos, nors ir mažesnės nei BC_{FF}, kito taip pat: didžiausios buvo Kvezono mieste, o mažiausios - Rūgšteliškio miestelyje. Nustatyta, kad visose vietovėse pagrindiniu eBC šaltiniu yra iškastinio kuro deginimas, ypač transporto priemonių ir pramoninės veiklos metu. BrC, daugiausia susidarantis deginant biomasę, buvo svarbus šviesos absorbcijos šaltinis.

Tokiose kaimo vietovėse kaip Rūgšteliškis BrC susidarė dėl gyvenamųjų namų šildymo ir žemės ūkio veiklos. Miesto vietovėse, pavyzdžiui, Vilniuje ir Kesono mieste, jis buvo susijęs su maisto gaminimu ir biokuro naudojimu, o Vilniuje – taip pat su pastatų šildymu. Manilos uoste BrC šaltiniai buvo su uostu susijusi veikla ir žemės ūkio atliekų deginimas nutolusiuose regionuose. Sprendžiant oro taršos problemą reikia mažinti iškastinio kuro deginimą ir konkrečiam regionui būdingą biomasės deginimą griežtinant eismo ir išmetamųjų teršalų reguliavimo priemones, skatinant švaresnius maisto gaminimo būdus bei griežčiau prižiūrint žemės ūkio ir pramonės išmetamųjų teršalų kiekį.

Meteorologinių duomenų analizė rodo, kad kaimo, miesto ir pakrantės vietovėse NR-PM_1 ir eBC koncentracijoms įtaką darė vietiniai šaltiniai ir tolimosios pernašos. Rūgšteliškyje (kaimo vietovė) šiaurės, rytų ir pietų vėjai lėmė didesnes NR-PM_1 ir eBC

koncentracijas, o tai nurodo didelį tolimosios pernašos poveikį kartu su mažu vietinių taršos šaltinių indėliu, nes vietovė yra nutolusi nuo didelių pramonės ir eismo šaltinių (11A, 11E, 11I pav., 7 lentelė). Vilniuje (miesto vietovė) vakarų ir šiaurės vakarų vėjai lėmė didesnes NR-PM_1 ir eBC koncentracijas, kurios siejamos su miesto transporto ir pramonės sektorių tarša. Atlikus plotinių pasiskirstymų analizę nustatyta, kad vietines emisijas dar labiau sustiprino meteorologinės sąlygos, pvz.: mažesnis vėjo greitis, todėl teršalai kaupėsi pažemio sluoksnyje (11B, 11F, 11J pav., 7 lentelė). Kesono mieste didesnė eBC koncentracija buvo susijusi su vyraujančiomis vėjų kryptimis ir didesniu vėjo greičiu iš rytų, o tai rodo, kad registruotai koncentracijai įtakos turėjo ir vietiniai šaltiniai, ir tolimoji pernaša (11C, 11 pav., 7 lentelė). Manilos šiauriniame uoste (pakrantės vietovė) vyraujantys vakarų vėjai turėjo įtakos padidėjusiai NR-PM_1 ir eBC koncentracijai. Šioje vietovėje susidarė sudėtinga sąveika tarp vietinių uosto išmetamų teršalų, įskaitant laivybą ir sunkiąją techniką, ir iš nutolusių šaltinių pernešamų teršalų (11D, 11H, 11L pav., 7 lentelė). Ištirtų skirtingų vietovių analizė rodo, kad veiksmingam oro kokybės valdyti reikia taikyti įvairiapusį požiūrį. Būtina spręsti konkrečių vietinių šaltinių, tokių kaip transporto eismas, pramoninė veikla ir uosto veikla, išmetamų teršalų problemą, kartu atsižvelgiant į vyraujančio vėjo krypties ir greičio įtaką teršalų sklaidai. Į oro kokybės valdymo modelius įtraukus meteorologinę informaciją būtų galima prognozuoti ilgesnius taršos laikotarpius ir parengti veiksmingas priemones taršos poveikio mažinimui ir žmonių sveikatos bei aplinkos apsaugai.

IŠVADOS

1. Vidutinės valandinės NR-PM_1 masės koncentracijos Rūgšteliškyje, Vilniuje ir Manilos uoste buvo atitinkamai 8.48 μg/m³, 18.98 μg/m³ ir 29.52 μg/m³. Vidutinės valandinė eBC masės koncentracija Rūgšteliškyje, Vilniuje, Kesone ir Manilos uoste buvo atitinkamai 0.60 μg/m³, 2.46 μg/m³, 36.19 μg/m³ ir 10.27 μg/m³. Palyginamoji analizė atskleidė didelius erdvinius NR-PM_1 ir eBC koncentracijos skirtumus (mažėjimo tvarka): didžiausios koncentracijos nustatytos Kesono mieste, Manilos Šiaurės uoste, Vilniuje, o mažiausi – Rūgšteliškio stotyje. Sezoninės kaitos tyrimai nurodė, kad Rūgšteliškio kaimo vietovėje didžiausia NR-PM_1 koncentracija (9.07 μg/m³) buvo pavasarį, o didžiausia eBC koncentracija (0.72 μg/m³) – rudenį. Žiemos sezono metu ypač didelės eBC koncentracijos buvo Kesono mieste (36 μg/m³) ir Manilos uoste (10 μg/m³).
2. NR-PM_1 ir eBC parinės eigos analizė skirtingose aplinkose atskleidė reikšmingą kaitą, kurią lemia antropogeninės veiklos ir natūralių atmosferos sąlygų sąveika. Kaimo vietovėse rytiniai OA ir eBC

koncentracijų maksimumai atspindi biomasės deginimo ir transporto priemonių eismo metu išmetamų teršalų kaupimąsi pažemio sluoksnyje dėl žemo maišymosi aukščio. Miestų teritorijose dėl intensyvaus eismo ir pramoninės veiklos, ypač rytinio ir vakarinio piko valandomis, pastebimi ryškesni parinių koncentracijų maksimumai. Pajūrio teritorijose paros eigai panašią įtaką daro vietinio transporto eismas, uosto veikla ir atmosferinės sąlygos, t.y. vėjo greitis ir atmosferos pažemio sluoksnio dinamika.

3. Išsami šaltinių kilmės nustatymo analizė nurodo, kad Rūgšteliškio, Vilniaus ir Kesono vietovėse bei Manilos šiauriniame uoste dominuojantis eBC šaltinis yra iškastinio kuro deginimas ir su transporto priemonių išmetamieji teršalai, atitinkamai 90%, 85%, 81% ir 86%. Nors ir mažesnis, biomasės deginimo indėlis eBC pabrėžia vietinės taršos įtaką, pvz.: gyvenamųjų namų šildymas ir žemės ūkio atliekų deginimas. Rūgšteliškio, Vilniaus, Kesono ir Manilos Šiaurės uosto matavimo vietovėse BrC dalis sudarė atitinkamai 14%, 18%, 22% ir 20%. Sąlyginai nedidelės BrC koncentracijos pagrindinis šaltinis yra biomasės deginimas, o jos koncentracija erdvėje kinta priklausomai nuo vietos žmonių įpročių, t.y. maisto gaminimo, žemės ūkio atliekų deginimo ir sezoninės veiklos, turinčios įtakos šviesos sugerties savybėms.
4. Nustatyta, kad tiek vietiniai taršos šaltiniai ir tolimoji pernaša daro didelę įtaką NR-PM_1 ir eBC koncentracijai kaimo, miesto ir pakrantės vietovėse. Rūgšteliškio kaimo vietovėje didesnės koncentracijos buvo susijusios su vėjo kryptimis iš pietų ir vakarų. Vilniuje didesnės koncentracijos koreliavo su vėjo kryptimis iš vakarų ir rytų. Kesono vietovėje didesnės eBC koncentracijos buvo susijusios su vėjo kryptimi iš rytų, o uosto vietovėje padidėjusi koncentracija buvo susijusi su vėjo kryptimi iš vakarų.

REFERENCES

Abbott, B.W., Brown, M., Carey, J.C., Ernakovich, J., Frederick, J.M., Guo, L., Hugelius, G., Lee, R.M., Loranty, M.M., Macdonald, R., Mann, P.J., Natali, S.M., Olefeldt, D., Pearson, P., Rec, A., Robards, M., Salmon, V.G., Sayedi, S.S., Schädel, C., Schuur, E.A.G., Shakil, S., Shogren, A.J., Strauss, J., Tank, S.E., Thornton, B.F., Treharne, R., Turetsky, M., Voigt, C., Wright, N., Yang, Y., Zarnetske, J.P., Zhang, Q., Zolkos, S., 2022. We Must Stop Fossil Fuel Emissions to Protect Permafrost Ecosystems. Front. Environ. Sci. 10, 1–13. https://doi.org/10.3389/fenvs.2022.889428

Ahn, Y.C., Lee, J.K., 2006. Physical, chemical, and electrical analysis of aerosol particles generated from industrial plants. J. Aerosol Sci. 37, 187–202. https://doi.org/10.1016/j.jaerosci.2005.04.008

Akagi, S.K., Yokelson, R.J., Wiedinmyer, C., Alvarado, M.J., Reid, J.S., Karl, T., Crounse, J.D., Wennberg, P.O., 2011. Emission factors for open and domestic biomass burning for use in atmospheric models. Atmos. Chem. Phys. 11, 4039–4072. https://doi.org/10.5194/acp-11-4039-2011

Alas, H.D., Müller, T., Birmili, W., Kecorius, S., Cambaliza, M.O., Simpas, J.B.B., Cayetano, M., Weinhold, K., Vallar, E., Galvez, M.C., Wiedensohler, A., 2018. Spatial characterization of black carbon mass concentration in the atmosphere of a southeast Asian megacity: An air quality case study for metro Manila, Philippines. Aerosol Air Qual. Res. 18, 2301–2317. https://doi.org/10.4209/aaqr.2017.08.0281

Allen, S.A.A., Ree, A.G., Ayodeji, S.A.M., Deborah, S.A.E., Ejike, O.M., 2019. Secondary inorganic aerosols: impacts on the global climate system and human health. Biodivers. Int. J. 3, 249–259. https://doi.org/10.15406/bij.2019.03.00152

Alves, C., Vicente, A., Nunes, T., Gonçalves, C., Fernandes, A.P., Mirante, F., Tarelho, L., Sánchez de la Campa, A.M., Querol, X., Caseiro, A., Monteiro, C., Evtyugina, M., Pio, C., 2011. Summer 2009 wildfires in Portugal: Emission of trace gases and aerosol composition. Atmos. Environ. 45, 641–649. https://doi.org/10.1016/j.atmosenv.2010.10.031

Alves, C.A., Vicente, A., Monteiro, C., Gonçalves, C., Evtyugina, M., Pio, C., 2011. Emission of trace gases and organic components in smoke particles from a wildfire in a mixed-evergreen forest in Portugal. Sci. Total Environ. 409, 1466–1475. https://doi.org/10.1016/j.scitotenv.2010.12.025

Ancelet, T., Davy, P.K., Trompetter, W.J., Markwitz, A., Weatherburn, D.C., 2013. Carbonaceous aerosols in a wood burning community in rural New Zealand. Atmos. Pollut. Res. 4, 245–249. https://doi.org/10.5094/APR.2013.026

Arnott, W.P., Hamasha, K., Moosmüller, H., Sheridan, P.J., Ogren, J.A., 2005. Towards aerosol light-absorption measurements with a 7-wavelength

aethalometer: Evaluation with a photoacoustic instrument and 3-wavelength nephelometer. Aerosol Sci. Technol. 39, 17–29. https://doi.org/10.1080/027868290901972

Ashbaugh, L.L., Malm, W.C., Sadeh, W.Z., 1985. A residence time probability analysis of sulfur concentrations at grand Canyon National Park. Atmos. Environ. 19, 1263–1270. https://doi.org/10.1016/0004-6981(85)90256-2

Badarinath, K.V.S., Latha, K.M., Chand, T.R.K., Gupta, P.K., 2009. Impact of biomass burning on aerosol properties over tropical wet evergreen forests of Arunachal Pradesh, India. Atmos. Res. 91, 87–93. https://doi.org/10.1016/j.atmosres.2008.03.023

Bai, P., Zhang, H., Zhang, X., Wang, Y., Zhang, L., Nagao, S., Chen, B., Tang, N., 2022. Chemical Characteristics of Water-Soluble Inorganic Ions in Different Types of Asian Dust in Wajima, a Background Site in Japan. Atmosphere (Basel). 13. https://doi.org/10.3390/atmos13081210

Bali, K., Banerji, S., Campbell, J.R., Vallabhbhai, A., Chen, L.A., Holmes, C.D., Mao, J., 2024. Measurements of brown carbon and its optical properties from boreal forest fires in Alaska summer. Atmos. Environ. 324, 120436. https://doi.org/10.1016/j.atmosenv.2024.120436

Barrett, S.R.H., Britter, R.E., Waitz, I.A., 2010. Global mortality attributable to aircraft cruise emissions. Environ. Sci. Technol. 44, 7736–7742. https://doi.org/10.1021/es101325r

Bartley, D.L., Martinez, A.B., Baron, P.A., Secker, D.R., Hirst, E., 2000. Droplet distortion in accelerating flow. J. Aerosol Sci. 31, 1447–1460. https://doi.org/10.1016/S0021-8502(00)00042-2

Bauer, H., Claeys, M., Vermeylen, R., Schueller, E., Weinke, G., Berger, A., Puxbaum, H., 2008. Arabitol and mannitol as tracers for the quantification of airborne fungal spores. Atmos. Environ. 42, 588–593. https://doi.org/10.1016/j.atmosenv.2007.10.013

Bauer, S.E., Koch, D., Unger, N., Metzger, S.M., Shindell, D.T., Streets, D.G., 2007. Nitrate aerosols today and in 2030: A global simulation including aerosols and tropospheric ozone. Atmos. Chem. Phys. 7, 5043–5059. https://doi.org/10.5194/acp-7-5043-2007

Bebkiewicz, K., Chłopek, Z., Sar, H., Szczepański, K., Zimakowska-Laskowska, M., 2021. Assessment of environmental risks of particulate matter emissions from road transport based on the emission inventory. Appl. Sci. 11. https://doi.org/10.3390/app11136123

Bisht, D.S., Dumka, U.C., Kaskaoutis, D.G., Pipal, A.S., Srivastava, A.K., Soni, V.K., Attri, S.D., Sateesh, M., Tiwari, S., 2015. Carbonaceous aerosols and pollutants over Delhi urban environment: Temporal evolution, source apportionment and radiative forcing. Sci. Total Environ. 521–522, 431–445.

https://doi.org/10.1016/j.scitotenv.2015.03.083

Bilal, M., Ali, M.A., Nichol, J.E., Bleiweiss, M.P., de Leeuw, G., Mhawish, A., Shi, Y., Mazhar, U., Mehmood, T., Kim, J., Qiu, Z., Qin, W., & Nazeer, M. (2022). AEROsol generic classification using a novel Satellite remote sensing Approach (AEROSA). *Front. Environ. Sci.*,10:981522. https://doi.org/10.3389/fenvs.2022.981522.

Blanco, A. E., Calvo, A.I., Fraile, R., Castro, A., 2012. The influence of wildfires on aerosol size distributions in rural areas. Sci. World J. 2012. https://doi.org/10.1100/2012/735697

Bock, J., Michou, M., Nabat, P., Abe, M., Mulcahy, J.P., Olivié, D.J.L., Schwinger, J., Suntharalingam, P., Tjiputra, J., Van Hulten, M., Watanabe, M., Yool, A., Séférian, R., 2021. Evaluation of ocean dimethylsulfide concentration and emission in CMIP6 models. Biogeosciences 18, 3823–3860. https://doi.org/10.5194/bg-18-3823-2021

Brooks, S.D., Thornton, D.C.O., 2018. Marine aerosols and clouds. Ann. Rev. Mar. Sci. 10, 289–313. https://doi.org/10.1146/annurev-marine-121916-063148

Bukowiecki, N., Lienemann, P., Hill, M., Furger, M., Richard, A., Amato, F., Prévôt, A.S.H., Baltensperger, U., Buchmann, B., Gehrig, R., 2010. PM10 emission factors for non-exhaust particles generated by road traffic in an urban street canyon and along a freeway in Switzerland. Atmos. Environ. 44, 2330–2340. https://doi.org/10.1016/j.atmosenv.2010.03.039

Buonanno, G., Morawska, L., Stabile, L., 2009. Particle emission factors during cooking activities. Atmos. Environ. 43, 3235–3242. https://doi.org/10.1016/j.atmosenv.2009.03.044

Byčenkienė, S., Gill, T., Khan, A., Kalinauskaitė, A., Ulevicius, V., Plauškaitė, K., 2023. Estimation of Carbonaceous Aerosol Sources under Extremely Cold Weather Conditions in an Urban Environment. Atmosphere (Basel). 14. https://doi.org/10.3390/atmos14020310

Cadondon, J., Caido, N.G., Galvez, M.C., Rempillo, O., Esmeria Jr., J., Vallar, E. (2024). Black carbon and PM0.49 characterization in Manila North Harbour Port, Metro Manila, Philippines. *Environmental Advances*, 16, 100526. https://doi.org/10.1016/j.envadv.2024.100526.

Calvo, A.I., Alves, C., Castro, A., Pont, V., Vicente, A.M., Fraile, R., 2013. Research on aerosol sources and chemical composition: Past, current and emerging issues. Atmos. Res. 120–121, 1–28. https://doi.org/10.1016/j.atmosres.2012.09.021

Calvo, A.I., Castro, A., Pont, V., Cuetos, M.J., Sánchez, M.E., Fraile, R., 2011. Aerosol size distribution and gaseous products from the oven-controlled combustion of straw materials. Aerosol Air Qual. Res. 11, 616–629. https://doi.org/10.4209/aaqr.2011.02.0015

Canonaco, F., Crippa, M., Slowik, J.G., Baltensperger, U., Prévôt, A.S.H., 2013. SoFi, an IGOR-based interface for the efficient use of the generalized multilinear engine (ME-2) for the source apportionment: ME-2 application to aerosol mass spectrometer data. Atmos. Meas. Tech. 6, 3649–3661. https://doi.org/10.5194/amt-6-3649-2013

Cao, J.J., Lee, S.C., Ho, K.F., Zhang, X.Y., Zou, S.C., Fung, K., Chow, J.C., Watson, J.G., 2003. Characteristics of carbonaceous aerosol in Pearl River Delta Region, China during 2001 winter period. Atmos. Environ. 37, 1451–1460. https://doi.org/10.1016/S1352-2310(02)01002-6

Castro, A., Alonso-Blanco, E., González-Colino, M., Calvo, A.I., Fernández-Raga, M., Fraile, R., 2010. Aerosol size distribution in precipitation events in León, Spain. Atmos. Res. 96, 421–435. https://doi.org/10.1016/j.atmosres.2010.01.014

Chahine, T., Schultz, B., Zartarian, V., Subramanian, S. V., Spengler, J., Hammitt, J., Levy, J.I., 2011. Modeling geographic and demographic variability in residential concentrations of environmental tobacco smoke using national data sets. J. Expo. Sci. Environ. Epidemiol. 21, 646–655. https://doi.org/10.1038/jes.2011.12

Chen, Y., Zhi, G., Feng, Y., Liu, D., Zhang, G., Li, J., Sheng, G., Fu, J., 2009. Measurements of black and organic carbon emission factors for household coal combustion in China: Implication for emission reduction. Environ. Sci. Technol. 43, 9495–9500. https://doi.org/10.1021/es9021766

Chen, X., Zhang, Z., Engling, G., Zhang, R., Tao, J., Lin, M., Sang, X., Chan, C., Li, S., Li, Y., 2014. Characterization of fine particulate black carbon in Guangzhou, a megacity of south China. Atmos. Pollut. Res. 5, 361–370. https://doi.org/10.5094/APR.2014.042.

Chien, S.M., Huang, Y.J., Chuang, S.C., Yang, H.H., 2009. Effects of biodiesel blending on particulate and polycyclic aromatic hydrocarbon emissions in Nano/Ultrafine/Fine/Coarse ranges from diesel engine. Aerosol Air Qual. Res. 9, 18–31. https://doi.org/10.4209/aaqr.2008.09.0040

Chirico, R., Decarlo, P.F., Heringa, M.F., Tritscher, T., Richter, R., Prévôt, A.S.H., Dommen, J., Weingartner, E., Wehrle, G., Gysel, M., Laborde, M., Baltensperger, U., 2010. Impact of aftertreatment devices on primary emissions and secondary organic aerosol formation potential from in-use diesel vehicles: Results from smog chamber experiments. Atmos. Chem. Phys. 10, 11545–11563. https://doi.org/10.5194/acp-10-11545-2010

Choël, M., Deboudt, K., Flament, P., 2010. Development of time-resolved description of aerosol properties at the particle scale during an episode of industrial pollution plume. Water. Air. Soil Pollut. 209, 93–107. https://doi.org/10.1007/s11270-009-0183-9

Christian, T.J., Yokelson, R.J., Cárdenas, B., Molina, L.T., Engling, G., Hsu, S.C., 2010. Trace gas and particle emissions from domestic and industrial biofuel use and garbage burning in central Mexico. Atmos. Chem. Phys. 10, 565–584. https://doi.org/10.5194/acp-10-565-2010

Ciarelli, G., Theobald, M.R., Vivanco, M.G., Beekmann, M., Aas, W., Andersson, C., Bergström, R., Manders-Groot, A., Couvidat, F., Mircea, M., Tsyro, S., Fagerli, H., Mar, K., Raffort, V., Roustan, Y., Pay, M.T., Schaap, M., Kranenburg, R., Adani, M., Briganti, G., Cappelletti, A., D'Isidoro, M., Cuvelier, C., Cholakian, A., Bessagnet, B., Wind, P., Colette, A., 2019. Trends of inorganic and organic aerosols and precursor gases in Europe: Insights from the EURODELTA multi-model experiment over the 1990-2010 period. Geosci. Model Dev. 12, 4923–4954. https://doi.org/10.5194/gmd-12-4923-2019

Claeys, M., Wang, W., Vermeylen, R., Kourtchev, I., Chi, X., Farhat, Y., Surratt, J.D., Gómez-González, Y., Sciare, J., Maenhaut, W., 2010. Chemical characterisation of marine aerosol at Amsterdam Island during the austral summer of 2006-2007. J. Aerosol Sci. 41, 13–22. https://doi.org/10.1016/j.jaerosci.2009.08.003

Corbett, J.J., Winebrake, J.J., Green, E.H., Kasibhatla, P., Eyring, V., Lauer, A., 2007. Mortality from ship emissions: A global assessment. Environ. Sci. Technol. 41, 8512–8518. https://doi.org/10.1021/es071686z

Colbeck, I., Lazardis, M., (2014) Aerosol science technology and applications. John Wiley & Sons Ltd. ISBN: 978-1-119-97792-6

Costa, E.A.L., Campos, V.P., da Silva Filho, L.C.P., Greven, H.A., 2009. Evaluation of the aggressive potential of marine chloride and sulfate salts on mortars applied as renders in the Metropolitan Region of Salvador - Bahia, Brazil. J. Environ. Manage. 90, 1060–1068. https://doi.org/10.1016/j.jenvman.2008.04.006

Crippa, M., Canonaco, F., Lanz, V.A., Äijälä, M., Allan, J.D., Carbone, S., Capes, G., Ceburnis, D., Dall'Osto, M., Day, D.A., DeCarlo, P.F., Ehn, M., Eriksson, A., Freney, E., Ruiz, L.H., Hillamo, R., Jimenez, J.L., Junninen, H., Kiendler-Scharr, A., Kortelainen, A.M., Kulmala, M., Laaksonen, A., Mensah, A.A., Mohr, C., Nemitz, E., O'Dowd, C., Ovadnevaite, J., Pandis, S.N., Petäjä, T., Poulain, L., Saarikoski, S., Sellegri, K., Swietlicki, E., Tiitta, P., Worsnop, D.R., Baltensperger, U., Prévôt, A.S.H., 2014. Organic aerosol components derived from 25 AMS data sets across Europe using a consistent ME-2 based source apportionment approach. Atmos. Chem. Phys. 14, 6159–6176. https://doi.org/10.5194/acp-14-6159-2014

Crippa, M., Decarlo, P.F., Slowik, J.G., Mohr, C., Heringa, M.F., Chirico, R., Poulain, L., Freutel, F., Sciare, J., Cozic, J., Di Marco, C.F., Elsasser, M.,

Nicolas, J.B., Marchand, N., Abidi, E., Wiedensohler, A., Drewnick, F., Schneider, J., Borrmann, S., Nemitz, E., Zimmermann, R., Jaffrezo, J.L., Prévôt, A.S.H., Baltensperger, U., 2013. Wintertime aerosol chemical composition and source apportionment of the organic fraction in the metropolitan area of Paris. Atmos. Chem. Phys. 13, 961–981. https://doi.org/10.5194/acp-13-961-2013

Cui, S., Xian, J., Shen, F., Zhang, L., Deng, B., Zhang, Y., Ge, X., 2021. One year real time measurement of black carbon in the rural area of Qingado, Northen China: seasonal variations, meterological effects, and the COVID-19 case analyisi. Atmosphere 12 (3), 394. https://doi.org/10.3390/atmos12030394.

De Sa, S.S., Rizzo, L.V., Palm, B.B., Campuzano-Jost, P., Day, D.A., Yee, L.D., Wernis, R., Isaacman-VanWertz, G., Brito, J., Carbone, S., Liu, Y.J., Sedlacek, A., Springston, S., Goldstein, A.H., Barbosa, H.M.J., Alexander, M.L., Artaxo, P., Jimenez, J.L., Martin, S.T. (2019). Contributions of biomass-burning, urban, and biogenic emissions to the concentrations and light-absorbing properties of particulate matter in central Amazonia during the dry season. *Atmos. Chem. Phys.*, 19, 7973–8001. https://doi.org/10.5194/acp-19-7973-2019.

Di Ianni, A., Costabile, F., Barnaba, F., Di Liberto, L., Weinhold, K., Wiedensohler, A., Struckmeier, C., Drewnick, F., Gobbi, G., 2018. Black Carbon Aerosol in Rome (Italy): Inference of a Long-Term (2001–2017) Record and Related Trends from AERONET Sun-Photometry Data. Atmosphere 9, 81. https://doi.org/10.3390/atmos9030081

Dowd, O., C.D., De Leeuw, G., 2007. Marine aerosol production: A review of the current knowledge. Philos. Trans. R. Soc. A Math. Phys. Eng. Sci. 365, 1753–1774. https://doi.org/10.1098/rsta.2007.2043

Draxler, R.R., Hess, G.D., 1998. An overview of the HYSPLIT_4 modelling system for trajectories, dispersion and deposition. Aust. Meteorol. Mag. 47, 295–308.

Drewnicki, P., Luft, R., Wójtowicz, Ł., 2024. Evolution and Impact of the European Union's Energy Policy: From Fossil Fuels to Renewable Energy and Greenhouse Gas Emissions Reduction. Eur. Res. Stud. J. 27(1), 114-126. https://doi.org/10.35808/ersj/3352.

Drugé, T., Nabat, P., Mallet, M., Somot, S., 2019. Model simulation of ammonium and nitrate aerosols distribution in the Euro-Mediterranean region and their radiative and climatic effects over 1979-2016. Atmos. Chem. Phys. 19, 3707–3731. https://doi.org/10.5194/acp-19-3707-2019

Duong, T.T.T., Lee, B.K., 2011. Determining contamination level of heavy metals in road dust from busy traffic areas with different characteristics. J. Environ. Manage. 92, 554–562. https://doi.org/10.1016/j.jenvman.2010.09.010

Dumka, U.C., Kaskaoutis, D.G., Devara, P.C.S., Kumar, R., Kumar, S., Tiwari, S.,

Gerasopoulos, E., & Mihalopoulos, N. (2019). Year-long variability of the fossil fuel and wood burning black carbon components at a rural site in southern Delhi outskirts. *Atmospheric Research*, 216, 11–25. https://doi.org/10.1016/j.atmosres.2018.09.016.

Dumka, U.C., Tiwari, S., Kaskaoutis, D.G., Soni, V.K., Safai, P.D., Attri, S.D. (2019). Aerosol and pollutant characteristics in Delhi during a winter research campaign. *Environmental Science and Pollution Research*, 26, 3771–3794. https://doi.org/10.1007/s11356-018-3885-y.

Egen, P.N.C., 1835. Der Haarrauch. Essen.

Elbert, W., Taylor, P.E., Andreae, M.O., Pöschl, U., 2007. Contribution of fungi to primary biogenic aerosols in the atmosphere: Wet and dry discharged spores, carbohydrates, and inorganic ions. Atmos. Chem. Phys. 7, 4569–4588. https://doi.org/10.5194/acp-7-4569-2007

European Environment Agency. (2023). Lithuania - Climate-ADAPT. https://climate-adapt.eea.europa.eu/en/countries-regions/countries/lithuania 13 June 2023.

Fang, G.C., Wu, Y.S., Rau, J.Y., Huang, S.H., 2006. Traffic aerosols (18 nm ≦ particle size ≦ 18 μm) source apportionment during the winter period. Atmos. Res. 80, 294–308. https://doi.org/10.1016/j.atmosres.2005.10.001

Feng, J., Zhang, Y., Li, S., Mao, J., Patton, A., Zhou, Y., Ma, W., Liu, C., Kan, H., Huang, C., An, J., Li, L., Shen, Y., Fu, Q., Wang, X., Liu, J., Wang, S., Ding, D., Cheng, J., Ge, W., Zhu, H., Walker, K., 2019. The influence of spatiality on shipping emissions, air quality and potential human exposure in the Yangtze River Delta/Shanghai, China. Atmos. Chem. Phys. 19, 6167–6183. https://doi.org/10.5194/acp-19-6167-2019

Finessi, E., Decesari, S., Paglione, M., Giulianelli, L., Carbone, C., Gilardoni, S., Fuzzi, S., Saarikoski, S., Raatikainen, T., Hillamo, R., Allan, J., Mentel, T.F., Tiitta, P., Laaksonen, A., Petäjä, T., Kulmala, M., Worsnop, D.R., Facchini, M.C., 2012. Determination of the biogenic secondary organic aerosol fraction in the boreal forest by NMR spectroscopy. Atmos. Chem. Phys. 12, 941–959. https://doi.org/10.5194/acp-12-941-2012

Gani, S., Bhandari, S., Seraj, S., Wang, D.S., Patel, K., Soni, P., Arub, Z., Habib, G., Hildebrandt Ruiz, L., Apte, J.S., 2019. Submicron aerosol composition in the world's most polluted megacity: The Delhi Aerosol Supersite study. Atmos. Chem. Phys. 19, 6843–6859. https://doi.org/10.5194/acp-19-6843-2019.

Geng, X., Li, J., Zhong, G., Zhao, S., Tian, C., Zhang, Y.-L., & Zhang, G. (2024). Ship Emissions as the Largest Contributor to Coastal Atmospheric Black Carbon at a Receptor Island in Southern China. *Environ. Sci. Technol. Lett.*, 11, 723−729. https://doi.org/10.1021/acs.estlett.4c00362.

Geels, C., Winther, M., Andersson, C., Jalkanen, J.P., Brandt, J., Frohn, L.M., Im, U., Leung, W., Christensen, J.H., 2021. Projections of shipping emissions and the related impact on air pollution and human health in the Nordic region. Atmos. Chem. Phys. 21, 12495–12519. https://doi.org/10.5194/acp-21-12495-2021

Gonçalves, C., Alves, C., Evtyugina, M., Mirante, F., Pio, C., Caseiro, A., Schmidl, C., Bauer, H., Carvalho, F., 2010. Characterisation of PM10 emissions from woodstove combustion of common woods grown in Portugal. Atmos. Environ. 44, 4474–4480. https://doi.org/10.1016/j.atmosenv.2010.07.026

Guenther, A., Karl, T., Harley, P., Weidinmyer, C., Palmer, P.I., Geron, C., 2006. Edinburgh Research Explorer Estimates of global terrestrial isoprene emissions using MEGAN (Model of Emissions of Gases and Aerosols from Nature) and Physics Estimates of global terrestrial isoprene emissions using MEGAN (Model of Emissions of Gases an. Atmos. Chem. Phys. 3181–3210.

Guo, S., Hu, M., Peng, J., Wu, Z., Zamora, M.L., Shang, D., Du, Z., Zheng, J., Fang, X., Tang, R., Wu, Y., Zeng, L., Shuai, S., Zhang, W., Wang, Y., Ji, Y., Li, Y., Zhang, A.L., Wang, W., Zhang, F., Zhao, J., Gong, X., Wang, C., Molina, M.J., Zhang, R., 2020. Remarkable nucleation and growth of ultrafine particles from vehicular exhaust. Proc. Natl. Acad. Sci. U. S. A. 117, 3427–3432. https://doi.org/10.1073/pnas.1916366117

Guo, Y., Lin, C., Li, J., Wei, L., Ma, Y., Yang, Q., Li, D., Wang, H., Shen, J., 2021. Persistent pollution episodes, transport pathways, and potential sources of air pollution during the heating season of 2016–2017 in Lanzhou, China. Environ. Monit. Assess. 193. https://doi.org/10.1007/s10661-021-09597-8

Guoliang, C., Xiaoye, Z., Sunling, G., Fangcheng, Z., 2008. Investigation on emission factors of particulate matter and gaseous pollutants from crop residue burning. J. Environ. Sci. 20, 50–55. https://doi.org/10.1016/S1001-0742(08)60007-8

Hallquist, M., Wenger, J.C., Baltensperger, U., Rudich, Y., Simpson, D., Claeys, M., Dommen, J., 2009. Atmos. Chem. Phys. 9, 5155–5236.

Hao, L.Q., Kortelainen, A., Romakkaniemi, S., Portin, H., Jaatinen, A., Leskinen, A., Komppula, M., Miettinen, P., Sueper, D., Pajunoja, A., Smith, J.N., Lehtinen, K.E.J., Worsnop, D.R., Laaksonen, A., Virtanen, A., 2014. Atmospheric submicron aerosol composition and particulate organic nitrate formation in a boreal forestland-urban mixed region. Atmos. Chem. Phys. 14, 13483–13495. https://doi.org/10.5194/acp-14-13483-2014

Hao, Y., Meng, X., Yu, X., Lei, M., Li, W., Yang, W., Shi, F., Xie, S., 2020. Chemical characteristics and health risks of trace metals in PM2.5 from firework/firecracker burning during the Spring Festival in North China. IOP Conf. Ser. Earth Environ. Sci. 489. https://doi.org/10.1088/1755-

1315/489/1/012002

Heikkinen, L., Äijälä, M., Riva, M., Luoma, K., Dällenbach, K., Aalto, J., Aalto, P., Aliaga, D., Aurela, M., Keskinen, H., Makkonen, U., Rantala, P., Kulmala, M., Petäjä, T., Worsnop, D., Ehn, M., 2020. Long-term sub-micrometer aerosol chemical composition in the boreal forest: Inter- And intra-annual variability. Atmos. Chem. Phys. 20, 3151–3180. https://doi.org/10.5194/acp-20-3151-2020

Hinds, W.C. (1998) Aerosol Technology: Properties, Behavior and Measurement of Airborne Particles. John Wiley & Sons, Hoboken.

Hjortenkrans, D.S.T., Bergbäck, B.G., Häggerud, A. V., 2008. Response to comment on "Metal emissions from brake linings and tires: Case studies of Stockholm, Sweden 1995/1998 and 2005." Environ. Sci. Technol. 42, 2710. https://doi.org/10.1021/es7028069

Holden, A.S., Sullivan, A.P., Munchak, L.A., Kreidenweis, S.M., Schichtel, B.A., Malm, W.C., Collett, J.L., 2011. Determining contributions of biomass burning and other sources to fine particle contemporary carbon in the western United States. Atmos. Environ. 45, 1986–1993. https://doi.org/10.1016/j.atmosenv.2011.01.021

Hsu, Y.K., Holsen, T.M., Hopke, P.K., 2003. Comparison of hybrid receptor models to locate PCB sources in Chicago. Atmos. Environ. 37, 545–562. https://doi.org/10.1016/S1352-2310(02)00886-5

Huang, R.J., Duan, J., Li, Y., Chen, Q., Chen, Y., Tang, M., Yang, L., Ni, H., Lin, C., Xu, W., Liu, Y., Chen, C., Yan, Z., Ovadnevaite, J., Ceburnis, D., Dusek, U., Cao, J., Hoffmann, T., O'Dowd, C.D., 2020. Effects of NH3 and alkaline metals on the formation of particulate sulfate and nitrate in wintertime Beijing. Sci. Total Environ. 717, 137190. https://doi.org/10.1016/j.scitotenv.2020.137190

Huang, W., Yang, Y., Wang, Yonghong, Gao, W., Li, H., Zhang, Y., Li, J., Zhao, S., Yan, Y., Ji, D., Tang, G., Liu, Z., Wang, L., Zhang, R., Wang, Yuesi, 2021. Exploring the inorganic and organic nitrate aerosol formation regimes at a suburban site on the North China Plain. Sci. Total Environ. 768. https://doi.org/10.1016/j.scitotenv.2020.144538

Hungershoefer, K., Zeromskiene, K., Iinuma, Y., Helas, G., Trentmann, J., Trautmann, T., Parmar, R.S., Wiedensohler, A., Andreae, M.O., Schmid, O., 2008. Modelling the optical properties of fresh biomass burning aerosol produced in a smoke chamber: Results from the EFEU campaign. Atmos. Chem. Phys. 8, 3427–3439. https://doi.org/10.5194/acp-8-3427-2008

Hyvärinen, A.P., Vakkari, V., Laakso, L., Hooda, R.K., Sharma, V.P., Panwar, T.S., Beukes, J.P., Van Zyl, P.G., Josipovic, M., Garland, R.M., Andreae, M.O., Pöschl, U., Petzold, A., 2013. Correction for a measurement artifact of the

Multi-Angle Absorption Photometer (MAAP) at high black carbon mass concentration levels. Atmos. Meas. Tech. 6, 81–90. https://doi.org/10.5194/amt-6-81-2013

IMO, 2018. MEPC.304(72) - Initial IMO strategy on reduction of GHG emissions from ships. IMO Publ. 304, 1–11.

Jaenicke, R., 2005. Abundance of cellular material and proteins in the atmosphere. Science (80-.). 308, 73. https://doi.org/10.1126/science.1106335

Janẗall, S., Andreae, M.O., Pöschl, U., 2010. Biomass burning aerosol emissions from vegetation fires: Particle number and mass emission factors and size distributions. Atmos. Chem. Phys. 10, 1427–1439. https://doi.org/10.5194/acp-10-1427-2010

Jiang, F., Liu, F., Lin, Q., Fu, Y., Yang, Y., Peng, L., Lian, X., Zhang, G., Bi, X., Wang, X., Sheng, G., 2019. Characteristics and formation mechanisms of sulfate and nitrate in size-segregated atmospheric particles from Urban Guangzhou, China. Aerosol Air Qual. Res. 19, 1284–1293. https://doi.org/10.4209/aaqr.2018.07.0251

Jiang, M., Marr, L.C., Dunlea, E.J., Herndon, S.C., Jayne, J.T., Kolb, C.E., Knighton, W.B., Rogers, T.M., Zavala, M., Molina, L.T., Molina, M.J., 2005. Vehicle fleet emissions of black carbon, polycyclic aromatic hydrocarbons, and other pollutants measured by a mobile laboratory in Mexico City. Atmos. Chem. Phys. 5, 3377–3387. https://doi.org/10.5194/acp-5-3377-2005

Jimenez, J.L., Canagaratna, M.R., Donahue, N.M., Prevot, A.S.H., Zhang, Q., Kroll, J.H., DeCarlo, P.F., Allan, J.D., Coe, H., Ng, N.L., Aiken, A.C., Docherty, K.S., Ulbrich, I.M., Grieshop, A.P., Robinson, A.L., Duplissy, J., Smith, J.D., Wilson, K.R., Lanz, V.A., Hueglin, C., Sun, Y.L., Tian, J., Laaksonen, A., Raatikainen, T., Rautiainen, J., Vaattovaara, P., Ehn, M., Kulmala, M., Tomlinson, J.M., Collins, D.R., Cubison, M.J., Dunlea, E.J., Huffman, J.A., Onasch, T.B., Alfarra, M.R., Williams, P.I., Bower, K., Kondo, Y., Schneider, J., Drewnick, F., Borrmann, S., Weimer, S., Demerjian, K., Salcedo, D., Cottrell, L., Griffin, R., Takami, A., Miyoshi, T., Hatakeyama, S., Shimono, A., Sun, J.Y., Zhang, Y.M., Dzepina, K., Kimmel, J.R., Sueper, D., Jayne, J.T., Herndon, S.C., Trimborn, A.M., Williams, L.R., Wood, E.C., Middlebrook, A.M., Kolb, C.E., Baltensperger, U., Worsnop, D.R., 2009. Evolution of organic aerosols in the atmosphere. Science (80-.). 326, 1525–1529. https://doi.org/10.1126/science.1180353

Jo, D.S., Park, R.J., Lee, S., Kim, S.W., Zhang, X., 2016. A global simulation of brown carbon: Implications for photochemistry and direct radiative effect. Atmos. Chem. Phys. 16, 3413–3432. https://doi.org/10.5194/acp-16-3413-2016

Johansson, L.S., Tullin, C., Leckner, B., Sjövall, P., 2003. Particle emissions from

biomass combustion in small combustors. Biomass and Bioenergy 25, 435–446. https://doi.org/10.1016/S0961-9534(03)00036-9

Kanawade, V.P., Tripathi, S.N., Chakraborty, A., Yu, H., 2020. Chemical characterization of sub-micron aerosols during new particle formation in an urban atmosphere. Aerosol Air Qual. Res. 20, 1294–1305. https://doi.org/10.4209/aaqr.2019.04.0196

Kasthuriarachchi, N.Y., Rivellini, L.H., Adam, M.G., Lee, A.K.Y. (2020). Light absorbing properties of primary and secondary brown carbon in a tropical urban environment. *Environ. Sci. Technol.*, 54, 10808–10819. https://doi.org/10.1021/acs.est.0c02414.

Katul, G.G., Grönholm, T., Launiainen, S., Vesala, T., 2011. The effects of the canopy medium on dry deposition velocities of aerosol particles in the canopy sub-layer above forested ecosystems. Atmos. Environ. 45, 1203–1212. https://doi.org/10.1016/j.atmosenv.2010.06.032

Keskinen, H.-M., Ylivinkka, I., Heikkinen, L., Aalto, P., Nieminen, T., Lehtipalo, K., Aalto, J., Levula, J., Kesti, J., Ahonen, L., Ezhova, E., Kulmala, M., Petäjä, T., 2020. Long-term aerosol mass concentrations in southern Finland: instrument validation, seasonal variation and trends. Atmos. Meas. Tech. Discuss. 2005, 1–27.

Kecorius, S., Madueño, L., Vallar, E., Alas, H., Betito, G., Birmili, W., Cambaliza, M.O., Catipay, G., Gonzaga-Cayetano, M., Galvez, M.C., Lorenzo, G., Müller, T., Simpas, J.B., Tamayo, E.G., Wiedensohler, A., 2017. Aerosol particle mixing state, refractory particle number size distributions and emission factors in a polluted urban environment: Case study of Metro Manila, Philippines. Atmos. Environ. 170, 169–183. https://doi.org/10.1016/j.atmosenv.2017.09.037.

Kecorius, S., Madueño, L., Löndahl, J., Vallar, E., Cecilia, M., Idolor, L.F., Gonzaga-cayetano, M., Müller, T., Birmili, W., Wiedensohler, A., 2019. Science of the Total Environment Respiratory tract deposition of inhaled roadside ultra fi ne refractory particles in a polluted megacity of South-East Asia. Sci. Total Environ. 663, 265–274. https://doi.org/10.1016/j.scitotenv.2019.01.338.

Khaparde, V. V., Pipalatkar, P.P., Pustode, T., Rao, C.V.C., Gajghate, D.G., 2012. Influence of burning of fireworks on particle size distribution of PM 10 and associated barium at Nagpur. Environ. Monit. Assess. 184, 903–911. https://doi.org/10.1007/s10661-011-2008-8

Khabarova, M.A., Novikova, O.V., Khabarov, A.A., 2019. State and Perspectives of Power and Industry Applications of Coal. Presented at the IEEE International Conference. ISBN 978-1-7281-0339-6.

Kim, H., Collier, S., Ge, X., Xu, J., Sun, Y., Jiang, W., Wang, Y., Herckes, P.,

Zhang, Q., 2019. Chemical processing of water-soluble species and formation of secondary organic aerosol in fogs. Atmos. Environ. 200, 158–166. https://doi.org/10.1016/j.atmosenv.2018.11.062

Kim, S.W., Cho, C., Rupakheti, M. (2021). Estimating contributions of black and brown carbon to solar absorption from aethalometer and AERONET measurements in the highly polluted Kathmandu Valley, Nepal. *Atmos. Res.*, 247, 105164. https://doi.org/10.1016/j.atmosres.2020.105164.

Kleindienst, T.E., Jaoui, M., Lewandowski, M., Offenberg, J.H., Lewis, C.W., Bhave, P. V., Edney, E.O., 2007. Estimates of the contributions of biogenic and anthropogenic hydrocarbons to secondary organic aerosol at a southeastern US location. Atmos. Environ. 41, 8288–8300. https://doi.org/10.1016/j.atmosenv.2007.06.045

Knobelspiesse, K., Cairns, B., Ottaviani, M., Ferrare, R., Hair, J., Hostetler, C., Obland, M., Rogers, R., Redemann, J., Shinozuka, Y., Clarke, A., Freitag, S., Howell, S., Kapustin, V., McNaughton, C., 2011. Combined retrievals of boreal forest fire aerosol properties with a polarimeter and lidar. Atmos. Chem. Phys. 11, 7045–7067. https://doi.org/10.5194/acp-11-7045-2011

Koppmann, R., Von Czapiewski, K., Reid, J.S., 2005. A review of biomass burning emissions, part I: gaseous emissions of carbon monoxide, methane, volatile organic compounds, and nitrogen containing compounds. Atmos. Chem. Phys. Discuss. 5, 10455–10516. https://doi.org/10.5194/acpd-5-10455-2005

Kroll, J.H., Ng, N.L., Murphy, S.M., Flagan, R.C., Seinfeld, J.H., 2006. Secondary organic aerosol formation from isoprene photooxidation. Environ. Sci. Technol. 40, 1869–1877. https://doi.org/10.1021/es0524301

Krzywański, J., Rajczyk, R., Nowak, W., 2014. Model research of gas emissions from lignite and biomass co-combustion in a large scale cfb boiler. Chem. Process Eng. - Inz. Chem. i Proces. 35, 217–231. https://doi.org/10.2478/cpe-2014-0017

Kumar, R., Verma, V., Thakur, M., Singh, G., Bhargava, B., 2023. A systematic review on mitigation of common indoor air pollutants using plant-based methods: a phytoremediation approach. Air Qual. Atmos. Heal. 16, 1501–1527. https://doi.org/10.1007/s11869-023-01326-z

Kumar, R.R., Soni, V.K., Jain, M.K. (2020). Evaluation of spatial and temporal heterogeneity of black carbon aerosol mass concentration over India using three-year measurements from IMD BC observation network. *Science of the Total Environment*, 723, 138060. https://doi.org/10.1016/j.scitotenv.2020.138060.

Lai, A.C.K., Chen, F.Z., 2007. Modeling of cooking-emitted particle dispersion and deposition in a residential flat: A real room application. Build. Environ. 42, 3253–3260. https://doi.org/10.1016/j.buildenv.2006.08.015

Lau, A.P.S., Lee, A.K.Y., Chan, C.K., Fang, M., 2006. Ergosterol as a biomarker for the quantification of the fungal biomass in atmospheric aerosols. Atmos. Environ. 40, 249–259. https://doi.org/10.1016/j.atmosenv.2005.09.048

Lee, A.K.Y., Chen, C.L., Liu, J., Price, D.J., Betha, R., Russell, L.M., Zhang, X., Cappa, C.D., 2017. Formation of secondary organic aerosol coating on black carbon particles near vehicular emissions. Atmos. Chem. Phys. 17, 15055–15067. https://doi.org/10.5194/acp-17-15055-2017

Lee, B.H., Mohr, C., Lopez-Hilfiker, F.D., Lutz, A., Hallquist, M., Lee, L., Romer, P., Cohen, R.C., Iyer, S., Kurtén, T., Hu, W., Day, D.A., Campuzano-Jost, P., Jimenez, J.L., Xu, L., Ng, N.L., Guo, H., Weber, R.J., Wild, R.J., Brown, S.S., Koss, A., De Gouw, J., Olson, K., Goldstein, A.H., Seco, R., Kim, S., McAvey, K., Shepson, P.B., Starn, T., Baumann, K., Edgerton, E.S., Liu, J., Shilling, J.E., Miller, D.O., Brune, W., Schobesberger, S., D'Ambro, E.L., Thornton, J.A., 2016. Highly functionalized organic nitrates in the southeast United States: Contribution to secondary organic aerosol and reactive nitrogen budgets. Proc. Natl. Acad. Sci. U. S. A. 113, 1516–1521. https://doi.org/10.1073/pnas.1508108113

Li, Q.Q., Guo, Y.T., Yang, J.Y., Liang, C.S., 2023. Review on main sources and impacts of urban ultrafine particles: Traffic emissions, nucleation, and climate modulation. Atmos. Environ. X 19, 100221. https://doi.org/10.1016/j.aeaoa.2023.100221

Li, Y., Xu, H., Wang, J., Ho, S.S.H., He, K., Shen, Z., Ning, Z., Sun, J., Li, L., Lei, R., Zhang, T., Lei, Y., Yang, L., Cao, Y., Cao, J., 2019. Personal exposure to PM2.5-bound organic species from domestic solid fuel combustion in rural Guanzhong Basin, China: Characteristics and health implication. Chemosphere 227, 53–62. https://doi.org/10.1016/j.chemosphere.2019.04.010

Li, Z., Tan, H., Zheng, J., Liu, L., Qin, Y., Wang, N., Li, F., Li, Y., Cai, M., Ma, Y., Chan, C.K. (2019). Light absorption properties and potential sources of particulate brown carbon in the Pearl River Delta region of China. *Atmos. Chem. Phys.*, 19, 11669–11685. https://doi.org/10.5194/acp-19-11669-2019.

Liakakou, E., Kaskaoutis, D.G., Grivas, G., Stavroulas, I., Tsagkaraki, M., Paraskevopoulou, D., Bougiatioti, A., Dumka, U.C., Gerasopoulos, E., Mihalopoulos, N. (2020). Long-term brown carbon spectral characteristics in a Mediterranean city (Athens). *Sci. Total Environ.*, 708, 135019. https://doi.org/10.1016/j.scitotenv.2019.135019.

Lin, W., Dai, J., Liu, R., Zhai, Y., Yue, D., Hu, Q., 2019. Integrated assessment of health risk and climate effects of black carbon in the Pearl River Delta region, China. Environ. Res. 176, 108522. https://doi.org/10.1016/j.envres.2019.06.003

Liu, C., Chung, C.E., Yin, Y., Schnaiter, M., 2018. The absorption Ångström

exponent of black carbon: From numerical aspects. Atmos. Chem. Phys. 18, 6259–6273. https://doi.org/10.5194/acp-18-6259-2018

Liu, Z., Ge, Y., Johnson, K.C., Shah, A.N., Tan, J., Wang, C., Yu, L., 2011. Real-world operation conditions and on-road emissions of Beijing diesel buses measured by using portable emission measurement system and electric low-pressure impactor. Sci. Total Environ. 409, 1476–1480. https://doi.org/10.1016/j.scitotenv.2010.12.042

Lushnikov, A.A., 2010. Introduction to Aerosols, Aerosols - Science and Technology. https://doi.org/10.1002/9783527630134.ch1

Luo, L., , Zhang, Y.Y., Xiao, H.Y., Xiao, H. W., Zheng, N. J., Zhang, Z. Y., Xie, Y. J., Liu, C., 2018. Spatial Distributions and Sources of Inorganic Chlorine in PM2.5 across China in Winter. Atmos, 10, 505; doi:10.3390/atmos10090505

Manisalidis, I., Stavropoulou, E., Stavropoulos, A., Bezirtzoglou, E., 2020. Environmental and Health Impacts of Air Pollution: A Review. Front. Public Heal. 8, 1–13. https://doi.org/10.3389/fpubh.2020.00014

Marković, B. J.Z., Marinković, A.D., Savić, J.Z., Mladenović, M.R., Erić, M.D., Marković, Z.J., Ristić, M. n., 2023. Risk Evaluation of Pollutants Emission from Coal and Coal Waste Combustion Plants and Environmental Impact of Fly Ash Landfilling. Toxics 11. https://doi.org/10.3390/toxics11040396

Mărmureanu, L., Vasilescu, J., Slowik, J., Prévôt, A.S.H., Marin, C.A., Antonescu, B., Vlachou, A., Nemuc, A., Dandocsi, A., Szidat, S., 2020. Online chemical characterization and source identification of summer and winter aerosols in Magurele, Romania. Atmosphere (Basel). 11. https://doi.org/10.3390/ATMOS11040385

Martuzevicius, D., Grinshpun, S.A., Lee, T., Hu, S., Biswas, P., Reponen, T., LeMasters, G., 2008. Traffic-related PM2.5 aerosol in residential houses located near major highways: Indoor versus outdoor concentrations. Atmos. Environ. 42, 6575–6585. https://doi.org/10.1016/j.atmosenv.2008.05.009

Meskhidze, N., Nenes, A., 2006. Phytoplankton and cloudiness in the southern ocean. Science (80-.). 314, 1419–1423. https://doi.org/10.1126/science.1131779

Masalaite, A., Holzinger, R., Remeikis, V., Röckmann, T., Dusek, U., 2017. Characteristics, sources and evolution of fine aerosol (PM1) at urban, coastal and forest background sites in Lithuania. Atmos. Environ. 148, 62–76. https://doi.org/10.1016/j.atmosenv.2016.10.038

Masalaite, A., Remeikis, V., Zenker, K., Westra, I., Meijer, H.A.J., Dusek, U., 2020. Seasonal changes of sources and volatility of carbonaceous aerosol at urban, coastal and forest sites in Eastern Europe (Lithuania). Atmos. Environ. 225, 117374. https://doi.org/10.1016/j.atmosenv.2020.117374

Minderytė, A., Pauraite, J., Dudoitis, V., Plauškaitė, K., Kilikevičius, A., Matijošius,

J., Rimkus, A., Kilikevičienė, K., Vainorius, D., Byčenkienė, S., 2022. Carbonaceous aerosol source apportionment and assessment of transport-related pollution. Atmos. Environ. 279. https://doi.org/10.1016/j.atmosenv.2022.119043

Mohanty, B., Mohanty, S., Sahoo, J., Anil, 2010. Climate Change: Impacts on Fisheries and Aquaculture. Clim. Chang. Var. https://doi.org/10.5772/9805

Mohr, C., Huffman, J.A., Cubison, M.J., Aiken, A.C., Docherty, K.S., Kimmel, J.R., Ulbrich, I.M., Hannigan, M., Jimenez, J.L., 2009. Characterization of primary organic aerosol emissions from meat cooking, trash burning, and motor vehicles with high-resolution aerosol mass spectrometry and comparison with ambient and chamber observations. Environ. Sci. Technol. 43, 2443–2449. https://doi.org/10.1021/es8011518

Morris, L., 2022. Spatio-Temporal Modelling for Nonstationary Point Referenced Data. Bull. Aust. Math. Soc. 105, 518–519. https://doi.org/10.1017/S0004972722000272

Ng, N.L., Canagaratna, M.R., Jimenez, J.L., Zhang, Q., Ulbrich, I.M., Worsnop, D.R., 2011. Real-time methods for estimating organic component mass concentrations from aerosol mass spectrometer data. Environ. Sci. Technol. 45, 910–916. https://doi.org/10.1021/es102951k

Oh, H.J., Ma, Y., Kim, J., 2020. Human inhalation exposure to aerosol and health effect: Aerosol monitoring and modelling regional deposited doses. Int. J. Environ. Res. Public Health 17, 1–2. https://doi.org/10.3390/ijerph17061923

Oros, D.R., Simoneit, B.R.T., 2001. Identification and emission factors of molecular tracers in organic aerosols from biomass burning Part 1. Temperate climate conifers. Appl. Geochemistry 16, 1513–1544. https://doi.org/10.1016/S0883-2927(01)00021-X

Osto, D., M., Harrison, R.M., Coe, H., Williams, P.I., Allan, J.D., 2009. Real time chemical characterization of local and regional nitrate aerosols. Atmos. Chem. Phys. 9, 3709–3720. https://doi.org/10.5194/acp-9-3709-2009

Osto, D., M., Ovadnevaite, J., Paglione, M., Beddows, D.C.S., Ceburnis, D., Cree, C., Cortés, P., Zamanillo, M., Nunes, S.O., Pérez, G.L., Ortega-Retuerta, E., Emelianov, M., Vaqué, D., Marrasé, C., Estrada, M., Sala, M.M., Vidal, M., Fitzsimons, M.F., Beale, R., Airs, R., Rinaldi, M., Decesari, S., Facchini, M.C., Harrison, R.M., O'Dowd, C., Simó, R., 2017. Antarctic sea ice region as a source of biogenic organic nitrogen in aerosols. Sci. Rep. 7, 1–10. https://doi.org/10.1038/s41598-017-06188-x

Ouidir, M., Seyve, E., Rivière, E., Bernard, J., Cheminat, M., Cortinovis, J., Ducroz, F., Dugay, F., Hulin, A., Kloog, I., Laborie, A., Launay, L., Malherbe, L., Robic, P.Y., Schwartz, J., Siroux, V., Virga, J., Zaros, C., Charles, M.A., Slama, R., Lepeule, J., 2021. Maternal ambient exposure to atmospheric

pollutants during pregnancy and offspring term birth weight in the nationwide ELFE cohort. Int. J. Environ. Res. Public Health 18, 1–17. https://doi.org/10.3390/ijerph18115806

Pabroa, P.C.B., Racho, J.M.D., Jagonoy, A.M., Valdez, J.D.G., Bautista VII, A.T., Yee, J.R., Pineda, R., Manlapaz, J., Atanacio, A.J., Coronel, I.C. V., Salvador, C.M.G., Cohen, D.D., 2022. Characterization, source apportionment and associated health risk assessment of respirable air particulates in Metro Manila, Philippines. Atmos. Pollut. Res. 13, 101379. https://doi.org/10.1016/j.apr.2022.101379.

Pachauri, T., Singla, V., Satsangi, A., Lakhani, A., Kumari, K.M., 2013. Characterization of carbonaceous aerosols with special reference to episodic events at Agra, India. Atmos. Res. 128, 98–110. https://doi.org/10.1016/j.atmosres.2013.03.010

Paglione, M., Gilardoni, S., Rinaldi, M., Decesari, S., Zanca, N., Sandrini, S., Giulianelli, L., Bacco, D., Ferrari, S., Poluzzi, V., Scotto, F., Trentini, A., Poulain, L., Herrmann, H., Wiedensohler, A., Canonaco, F., Prévôt, A.S.H., Massoli, P., Carbone, C., Facchini, M.C., Fuzzi, S., 2020. The impact of biomass burning and aqueous-phase processing on air quality: A multi-year source apportionment study in the Po Valley, Italy. Atmos. Chem. Phys. 20, 1233–1254. https://doi.org/10.5194/acp-20-1233-2020

Pani, S.K., Wang, S.H., Lin, N.H., Chantara, S., Lee, C. Te, Thepnuan, D., 2020. Black carbon over an urban atmosphere in northern peninsular Southeast Asia: Characteristics, source apportionment, and associated health risks. Environ. Pollut. 259, 113871. https://doi.org/10.1016/j.envpol.2019.113871

Pani, S.K., Lin, N.-H., Griffith, S.M., Chantara, S., Lee, C.-T., Thepnuan, D., Tsai, Y.I. (2021). Brown carbon light absorption over an urban environment in northern peninsular Southeast Asia. *Environmental Pollution*, 276, 116735. https://doi.org/10.1016/j.envpol.2021.116735.

Papa, G., Capitani, G., Capri, E., Pellecchia, M., Negri, I., 2021. Vehicle-derived ultrafine particulate contaminating bees and bee products. Sci. Total Environ. 750, 141700. https://doi.org/10.1016/j.scitotenv.2020.141700

Park, K., Kittelson, D.B., McMurry, P.H., 2004. Structural properties of diesel exhaust particles measured by Transmission Electron Microscopy (TEM): Relationships to particle mass and mobility. Aerosol Sci. Technol. 38, 881–889. https://doi.org/10.1080/027868290505189

Park, S.S., Hansen, A.D.A., Cho, S.Y., 2010. Measurement of real-time black carbon for investigating spot loading effects of Aethalometer data. Atmos. Environ. 44, 1449–1455. https://doi.org/10.1016/j.atmosenv.2010.01.025

Patel, K., Bhandari, S., Gani, S., Campmier, M.J., Kumar, P., Habib, G., Apte, J., Hildebrandt Ruiz, L., 2021. Sources and Dynamics of Submicron Aerosol

during the Autumn Onset of the Air Pollution Season in Delhi, India. ACS Earth Sp. Chem. 5, 118–128. https://doi.org/10.1021/acsearthspacechem.0c00340.

Pauraite, J., Mordas, G., Byčenkiene, S., Ulevicius, V., 2015. Spatial and temporal analysis of organic and black carbon mass concentrations in Lithuania. Atmosphere (Basel). 6, 1229–1242. https://doi.org/10.3390/atmos6081229

Pauraite, J., Mainelis, G., Kecorius, S., Minderytė, A., Dudoitis, V., Garbarienė, I., Plauškaitė, K., Ovadnevaite, J., Byčenkienė, S., 2021. Office indoor PM and BC level in Lithuania: The role of a long-range smoke transport event. Atmosphere (Basel). 12. https://doi.org/10.3390/atmos12081047

Peñuelas, J., Llusià, J., 2001. Complexity of factors driving VOC emissions from plants. Biol. Plant. BIOLOGIA PLANTARUM 4 (4): 481-487, 201.

Peters, T.M., Ott, D., O'Shaughnessy, P.T., 2006. Comparison of the Grimm 1.108 and 1.109 portable aerosol spectrometer to the TSI 3321 aerodynamic particle sizer for dry particles. Ann. Occup. Hyg. 50, 843–850. https://doi.org/10.1093/annhyg/mel067

Petzold, A., Schönlinner, M., 2004. Multi-angle absorption photometry - A new method for the measurement of aerosol light absorption and atmospheric black carbon. J. Aerosol Sci. 35, 421–441. https://doi.org/10.1016/j.jaerosci.2003.09.005

Pfeifer, S., Müller, T., Weinhold, K., Zikova, N., Dos Santos, S.M., Marinoni, A., Bischof, O.F., Kykal, C., Ries, L., Meinhardt, F., Aalto, P., Mihalopoulos, N., Wiedensohler, A., 2016. Intercomparison of 15 aerodynamic particle size spectrometers (APS 3321): Uncertainties in particle sizing and number size distribution. Atmos. Meas. Tech. 9, 1545–1551. https://doi.org/10.5194/amt-9-1545-2016

Pillar-Little, E.A., Guzman, M.I., 2018. An overview of dynamic heterogeneous oxidations in the troposphere. Environ. - MDPI 5, 1–23. https://doi.org/10.3390/environments5090104

Pöschl, U., 2005. Atmospheric aerosols: Composition, transformation, climate and health effects. Angew. Chemie - Int. Ed. 44, 7520–7540. https://doi.org/10.1002/anie.200501122

Presto, A.A., Saha, P.K., Robinson, A.L., 2021. Past, present, and future of ultrafine particle exposures in North America. Atmos. Environ. X 10, 100109. https://doi.org/10.1016/j.aeaoa.2021.100109

Prichard, H.M., Fisher, P.C., 2012. Identification of platinum and palladium particles emitted from vehicles and dispersed into the surface environment. Environ. Sci. Technol. 46, 3149–3154. https://doi.org/10.1021/es203666h

Prospero, J.M., Blades, E., Mathison, G., Naidu, R., 2005. Interhemispheric transport of viable fungi and bacteria from Africa to the Caribbean with soil

dust. Aerobiologia (Bologna). 21, 1–19. https://doi.org/10.1007/s10453-004-5872-7

Qin, Y.M., Bo Tan, H., Li, Y.J., Jie Li, Z., Schurman, M.I., Liu, L., Wu, C., Chan, C.K., 2018. Chemical characteristics of brown carbon in atmospheric particles at a suburban site near Guangzhou, China. Atmos. Chem. Phys. 18, 16409–16418. https://doi.org/10.5194/acp-18-16409-2018

Querol, X., Alastuey, A., Ruiz, C.R., Artiñano, B., Hansson, H.C., Harrison, R.M., Buringh, E., Ten Brink, H.M., Lutz, M., Bruckmann, P., Straehl, P., Schneider, J., 2004. Speciation and origin of PM10 and PM2.5 in selected European cities. Atmos. Environ. 38, 6547–6555. https://doi.org/10.1016/j.atmosenv.2004.08.037

Quang, T.N., Hue, N.T., Dat, M. Van, Tran, L.K., Phi, T.H., Morawska, L., Thai, P.K., 2021. Motorcyclists have much higher exposure to black carbon compared to other commuters in traffic of Hanoi, Vietnam. Atmos. Environ. 245, 118029. https://doi.org/10.1016/j.atmosenv.2020.118029.

Rabbi, M.F.; Popp, J.; Máté, D.; Kovács, S., 2022. Energy Security and Energy Transition to Achieve Carbon Neutrality. Energies, 15, 8126. https://doi.org/10.3390/en15218126.

Radovanović, M., Filipović, S., Vukadinović, S., Trbojević, M., & Podbregar, I. (2022). Decarbonisation of eastern European economies: monitoring, economic, social and security concerns. Energy, Sustainability and Society,12(16). https://doi.org/10.1186/s13705-022-00342-8.

Rahman, M.M., Mazaheri, M., Clifford, S., Morawska, L., 2017. Estimate of main local sources to ambient ultrafine particle number concentrations in an urban area. Atmos. Res. 194, 178–189. https://doi.org/10.1016/j.atmosres.2017.04.036

Ramacher, M.O.P., Tang, L., Moldanová, J., Matthias, V., Karl, M., Fridell, E., Johansson, L., 2020. The impact of ship emissions on air quality and human health in the Gothenburg area - Part II: Scenarios for 2040. Atmos. Chem. Phys. 20, 10667–10686. https://doi.org/10.5194/acp-20-10667-2020

Reid, J.S., Eck, T.F., Christopher, S.A., Koppman, R., Dubovik, O., Eleuterio, D.P., Holben, B.N., Reid, E.A., Zhang, J., 2005. A review of biomass burning emissions part III: Intensive optical properties of biomass burning particles. Atmos. Chem. Phys. 5, 827–849. https://doi.org/10.5194/acp-5-827-2005

Retama, A., Neria-Hernández, A., Jaimes-Palomera, M., Rivera-Hernández, O., Sánchez-Rodríguez, M., López-Medina, A., Velasco, E., 2019. Fireworks: A major source of inorganic and organic aerosols during Christmas and New Year in Mexico city. Atmos. Environ. X 2, 100013. https://doi.org/10.1016/j.aeaoa.2019.100013

Rivas, I., Vicens, L., Basagaña, X., Tobías, A., Katsouyanni, K., Walton, H., Hüglin,

C., Alastuey, A., Kulmala, M., Harrison, R.M., Pekkanen, J., Querol, X., Sunyer, J., Kelly, F.J., 2021. Associations between sources of particle number and mortality in four European cities. Environ. Int. 155. https://doi.org/10.1016/j.envint.2021.106662

Robinson, A.L., Subramanian, R., Donahue, N.M., Bernardo-Bricker, A., Rogge, W.F., 2006. Source apportionment of molecular markers and organic aerosol. 3. Food cooking emissions. Environ. Sci. Technol. 40, 7820–7827. https://doi.org/10.1021/es060781p

Russo, M., Carvalho, D., Jalkanen, J.P., Monteiro, A., 2023. The Future Impact of Shipping Emissions on Air Quality in Europe under Climate Change. Atmosphere (Basel). 14, 1–14. https://doi.org/10.3390/atmos14071126

Ryu, S.Y., Kwon, B.G., Kim, Y.J., Kim, H.H., Chun, K.J., 2007. Characteristics of biomass burning aerosol and its impact on regional air quality in the summer of 2003 at Gwangju, Korea. Atmos. Res. 84, 362–373. https://doi.org/10.1016/j.atmosres.2006.09.007

Safai, P.D., Raju, M.P., Rao, P.S.P., Pandithurai, G., 2014. Characterization of carbonaceous aerosols over the urban tropical location and a new approach to evaluate their climatic importance. Atmos. Environ. 92, 493–500. https://doi.org/10.1016/j.atmosenv.2014.04.055

Salcedo, D., Onasch, T.B., Dzepina, K., Canagaratna, M.R., Zhang, Q., Huffmann, J.A., DeCarlo, P.F., Jayne, J.T., Mortimer, P., Worsnop, D.R., Kolb, C.E., Johnson, K.S., Zuberi, B., Marr, L.C., Volkamer, R., Molina, L.T., Molina, M.J., Cardenas, B., Bernabé, R.M., Márquez, C., Gaffney, J.S., Marley, N.A., Laskin, A., Shutthanandan, V., Xie, Y., Brune, W., Lesher, R., Shirley, T., Jimenez, J.L., 2006. Characterization of ambient aerosols in Mexico City during the MCMA-2003 campaign with Aerosol Mass Spectrometry: Results from the CENICA Supersite. Atmos. Chem. Phys. 6, 925–946. https://doi.org/10.5194/acp-6-925-2006

Saleh, R., M. Marks, J. Heo, P. J. Adams, N. M. Donahue, and A. L. Robinson (2015), Contribution of brown carbon and lensing to the direct radiative effect of carbonaceous aerosols from biomass and biofuel burning emissions, J. Geophys. Res. Atmos., 120, 10,285–10,296, doi:10.1002/ 2015JD023697.

Saliba, G., Sanchez, K.J., Russell, L.M., Twohy, C.H., Roberts, G.C., Lewis, S., Dedrick, J., McCluskey, C.S., Moore, K., DeMott, P.J., Toohey, D.W., 2020. Organic composition of three different size ranges of aerosol particles over the Southern Ocean. Aerosol Sci. Technol. 55, 268–288. https://doi.org/10.1080/02786826.2020.1845296

Saliba, M., Azzopardi, F., Muscat, R., Grima, M., Smyth, A., Jalkanen, J.P., Johansson, L., Deidun, A., Gauci, A., Galdies, C., Caruana, T., Ellul, R., 2021. Trends in vessel atmospheric emissions in the central mediterranean over the

last 10 years and during the covid-19 outbreak. J. Mar. Sci. Eng. 9. https://doi.org/10.3390/jmse9070762

Sánchez, J.E. C., González Chávez, M. del C.A., Carrillo González, R., Scheckel, K., Tapia Maruri, D., García Cue, J.L., 2021. Metal(loid) bioaccessibility of atmospheric particulate matter from mine tailings at Zimapan, Mexico. Environ. Sci. Pollut. Res. 28, 19458–19472. https://doi.org/10.1007/s11356-020-11887-6

Sandradewi, J., Prévôt, A.S.H., Weingartner, E., Schmidhauser, R., Gysel, M., Baltensperger, U., 2008. A study of wood burning and traffic aerosols in an Alpine valley using a multi-wavelength Aethalometer. Atmos. Environ. 42, 101–112. https://doi.org/10.1016/j.atmosenv.2007.09.034

Salvador, C.M.G., Yee, J.R. dR., Coronel, I.C. V., Bautista VII, A.T., Sugcang, R.J., Lavapie, M.A.M., Capangpangan, R.Y., Pabroa, P.C.B., 2022. Variability and Source Characterization of Regional PM of Two Urban Areas Dominated by Biomass Burning and Anthropogenic Emission. Aerosol Air Qual. Res. 22, 220026. https://doi.org/10.4209/aaqr.220026.

Schleicher, N.J., Norra, S., Chai, F., Chen, Y., Wang, S., Cen, K., Yu, Y., Stüben, D., 2011. Temporal variability of trace metal mobility of urban particulate matter from Beijing - A contribution to health impact assessments of aerosols. Atmos. Environ. 45, 7248–7265. https://doi.org/10.1016/j.atmosenv.2011.08.067

Scharr, K., A., Mensah, A.A., Friese, E., Topping, D., Nemitz, E., Prevot, A.S.H., Äijälä, M., Allan, J., Canonaco, F., Canagaratna, M., Carbone, S., Crippa, M., Dall Osto, M., Day, D.A., De Carlo, P., Di Marco, C.F., Elbern, H., Eriksson, A., Freney, E., Hao, L., Herrmann, H., Hildebrandt, L., Hillamo, R., Jimenez, J.L., Laaksonen, A., McFiggans, G., Mohr, C., O'Dowd, C., Otjes, R., Ovadnevaite, J., Pandis, S.N., Poulain, L., Schlag, P., Sellegri, K., Swietlicki, E., Tiitta, P., Vermeulen, A., Wahner, A., Worsnop, D., Wu, H.C., 2016. Ubiquity of organic nitrates from nighttime chemistry in the European submicron aerosol. Geophys. Res. Lett. 43, 7735–7744. https://doi.org/10.1002/2016GL069239

Schmidl, C., Marr, I.L., Caseiro, A., Kotianová, P., Berner, A., Bauer, H., Kasper-Giebl, A., Puxbaum, H., 2008. Chemical characterisation of fine particle emissions from wood stove combustion of common woods growing in mid-European Alpine regions. Atmos. Environ. 42, 126–141. https://doi.org/10.1016/j.atmosenv.2007.09.028

See, S.W., Balasubramanian, R., 2008. Chemical characteristics of fine particles emitted from different gas cooking methods. Atmos. Environ. 42, 8852–8862. https://doi.org/10.1016/j.atmosenv.2008.09.011

Seinfeld, J.H., Pandis, S.N., 2012. Atmospheric Chemistry and Physics: from Air

Pollution to Climate Change. John Wiley & Sons, New York, USA, p. 1326.
Shank, L.M., Howell, S., Clarke, A.D., Freitag, S., Brekhovskikh, V., Kapustin, V., McNaughton, C., Campos, T., Wood, R., 2012. Organic matter and non-refractory aerosol over the remote Southeast Pacific: Oceanic and combustion sources. Atmos. Chem. Phys. 12, 557–576. https://doi.org/10.5194/acp-12-557-2012
Shen, G., Wang, W., Yang, Y., Zhu, C., Min, Y., Xue, M., Ding, J., 2013. HHS Public Access 44, 5737–5743. https://doi.org/10.1016/j.atmosenv.2010.08.042.Shen
Shetty, S.S., D, D., S, H., Sonkusare, S., Naik, P.B., Kumari N, S., Madhyastha, H., 2023. Environmental pollutants and their effects on human health. Heliyon 9, e19496. https://doi.org/10.1016/j.heliyon.2023.e19496
Shindell, D., Faluvegi, G., 2010. The net climate impact of coal-fired power plant emissions. Atmos. Chem. Phys. 10, 3247–3260. https://doi.org/10.5194/acp-10-3247-2010
Shakya, K.M., Peltier, R.E., Shrestha, H., Byanju, R.M., 2017. Measurements of TSP, PM10, PM2.5, BC, and PM chemical composition from an urban residential location in Nepal. Atmos. Pollut. Res. 8, 1123–1131. https://doi.org/10.1016/j.apr.2017.05.002.
Singh, R.B., Sloan, J.J., 2006. A high-resolution NOx emission factor model for North American motor vehicles. Atmos. Environ. 40, 5214–5223. https://doi.org/10.1016/j.atmosenv.2006.04.012
Smith, S.J., Van Aardenne, J., Klimont, Z., Andres, R.J., Volke, A., Delgado Arias, S., 2011. Anthropogenic sulfur dioxide emissions: 1850-2005. Atmos. Chem. Phys. 11, 1101–1116. https://doi.org/10.5194/acp-11-1101-2011
Sobanski, N., Thieser, J., Schuladen, J., Sauvage, C., Song, W., Williams, J., Lelieveld, J., Crowley, J.N., 2017. Day and night-time formation of organic nitrates at a forested mountain site in south-west Germany. Atmos. Chem. Phys. 17, 4115–4130. https://doi.org/10.5194/acp-17-4115-2017
Sofia, D., Gioiella, F., Lotrecchiano, N., Giuliano, A., 2020. Mitigation strategies for reducing air pollution. Environ. Sci. Pollut. Res. 27, 19226–19235. https://doi.org/10.1007/s11356-020-08647-x
Stavroulas, I., Grivas, G., Liakakou, E., Kalkavouras, P., Bougiatioti, A., Kaskaoutis, D.G., Lianou, M., Papoutsidaki, K., Tsagkaraki, M., Zarmpas, P., Gerasopoulos, E., Mihalopoulos, N. (2021). Online Chemical Characterization and Sources of Submicron Aerosol in the Major Mediterranean Port City of Piraeus, Greece. *Atmosphere*, 12, 1686. https://doi.org/10.3390/atmos12121686.
Sühring, N., Chambers, C., Koenigk, T., Kruschke, T., Einarsson, N., Ogilvie, A.E.J., 2023. Effects of storms on fisheries and aquaculture: An Icelandic case

study on climate change adaptation. Arctic, Antarct. Alp. Res. 55. https://doi.org/10.1080/15230430.2023.2269689

Surratt, J.D., Murphy, S.M., Kroll, J.H., Ng, N.L., Hildebrandt, L., Sorooshian, A., Szmigielski, R., Vermeylen, R., Maenhaut, W., Claeys, M., Flagan, R.C., Seinfeld, J.H., 2006. Chemical composition of secondary organic aerosol formed from the photooxidation of isoprene. J. Phys. Chem. A 110, 9665–9690. https://doi.org/10.1021/jp061734m

Thorpe, A., Harrison, R.M., 2008. Sources and properties of non-exhaust particulate matter from road traffic: A review. Sci. Total Environ. 400, 270–282. https://doi.org/10.1016/j.scitotenv.2008.06.007

Tohka, A., Karvosenoja, N., 2006. Fine particle emissions and emission reduction potential in Finnish industrial processes.

Tun, M.M., Juchelkova, D., Win, M.M., Thu, A.M., Puchor, T., 2019. Biomass energy: An overview of biomass sources, energy potential, and management in Southeast Asian countries. Resources 8. https://doi.org/10.3390/resources8020081.

Uddin, S., Sarker, S.C., Mondal, D.K., 2018. Health risk from contaminated aquaculture fish, International Journal of Natural and Social Sciences, 1–16. ISSN: 2313-4461

Ulevičius, V., Byčenkienė, S., Špirkauskaitė, N., Kecorius, S., 2010. Biomass burning impact on black carbon aerosol mass concentration at a coastal site: Case studies. Lithuanian J. Phys. 50, 335–344. https://doi.org/10.3952/lithjphys.50304

Urbanski, S.P., Hao, W.M., Nordgren, B., 2011. The wildland fire emission inventory: Western United States emission estimates and an evaluation of uncertainty. Atmos. Chem. Phys. 11, 12973–13000. https://doi.org/10.5194/acp-11-12973-2011

Vera, C. J.A., Lyamani, H., Titos, G., Minguillón, M.C., Dada, L., Alastuey, A., Querol, X., Petäjä, T., Olmo, F.J., Alados-Arboledas, L., 2021. Quantifying traffic, biomass burning and secondary source contributions to atmospheric particle number concentrations at urban and suburban sites. Sci. Total Environ. 768. https://doi.org/10.1016/j.scitotenv.2021.145282

Vieno, M., Heal, M.R., Hallsworth, S., Famulari, D., Doherty, R.M., Dore, A.J., Tang, Y.S., Braban, C.F., Leaver, D., Sutton, M.A., Reis, S., 2014. The role of long-range transport and domestic emissions in determining atmospheric secondary inorganic particle concentrations across the UK. Atmos. Chem. Phys. 14, 8435–8447. https://doi.org/10.5194/acp-14-8435-2014

Wainwright, M., Wickramasinghe, N.C., Narlikar, J. V., Rajaratnam, P., 2003. Microorganisms cultured from stratospheric air samples obtained at 41 km. FEMS Microbiol. Lett. 218, 161–165. https://doi.org/10.1016/S0378-

1097(02)01138-2

Wang, G., Zhang, R., Gomez, M.E., Yang, L., Zamora, M.L., Hu, M., Lin, Y., Peng, J., Guo, S., Meng, J., Li, J., Cheng, C., Hu, T., Ren, Y., Wang, Yuesi, Gao, J., Cao, J., An, Z., Zhou, W., Li, G., Wang, J., Tian, P., Marrero-Ortiz, W., Secrest, J., Du, Z., Zheng, J., Shang, D., Zeng, L., Shao, M., Wang, W., Huang, Y., Wang, Yuan, Zhu, Y., Li, Y., Hu, J., Pan, B., Cai, L., Cheng, Y., Ji, Y., Zhang, F., Rosenfeld, D., Liss, P.S., Duce, R.A., Kolb, C.E., Molina, M.J., 2016. Persistent sulfate formation from London Fog to Chinese haze. Proc. Natl. Acad. Sci. U. S. A. 113, 13630–13635. https://doi.org/10.1073/pnas.1616540113

Wang, H., Wang, X., Yang, X., Li, W., Xue, L., Wang, T., Chen, J., Wang, W., 2017. Mixed chloride aerosols and their atmospheric implications: A review. Aerosol Air Qual. Res. 17, 878–887. https://doi.org/10.4209/aaqr.2016.09.0383

Wang, J., Nie, W., Cheng, Y., Shen, Y., Chi, X., Wang, J., Huang, X., Xie, Y., Sun, P., Xu, Z., Qi, X., Su, H., Ding, A. (2018). Light absorption of brown carbon in eastern China based on 3-year multi-wavelength aerosol optical property observations and an improved absorption Ångström exponent segregation method. *Atmos. Chem. Phys.*, 18, 9061–9074. https://doi.org/10.5194/acp-18-9061-2018.

Wang, Q., Han, Yongming, Ye, J., Liu, S., Pongpiachan, S., Zhang, N., Han, Yuemei, Tian, J., Wu, C., Long, X., Zhang, Q., Zhang, W., Zhao, Z., Cao, J., 2019. High Contribution of Secondary Brown Carbon to Aerosol Light Absorption in the Southeastern Margin of Tibetan Plateau. Geophys. Res. Lett. 46, 4962–4970. https://doi.org/10.1029/2019GL082731

Wang, Y., Zheng, X., Dong, X., Xi, B., Wu, P., Logan, T., Yung, Y.L., 2020. Impacts of long-range transport of aerosols on marine-boundary-layer clouds in the eastern North Atlantic. Atmos. Chem. Phys. 20, 14741–14755. https://doi.org/10.5194/acp-20-14741-2020

Wang, Y.Q., Zhang, X.Y., Draxler, R.R., 2009. TrajStat: GIS-based software that uses various trajectory statistical analysis methods to identify potential sources from long-term air pollution measurement data. Environ. Model. Softw. 24, 938–939. https://doi.org/10.1016/j.envsoft.2009.01.004

Warneke, C., De Gouw, J.A., Del Negro, L., Brioude, J., McKeen, S., Stark, H., Kuster, W.C., Goldan, P.D., Trainer, M., Fehsenfeld, F.C., Wiedinmyer, C., Guenther, A.B., Hansel, A., Wisthaler, A., Atlas, E., Holloway, J.S., Ryerson, T.B., Peischl, J., Huey, L.G., Hanks, A.T.C., 2010. Biogenic emission measurement and inventories determination of biogenic emissions in the eastern United States and Texas and comparison with biogenic emission inventories. J. Geophys. Res. Atmos. 115, 1–21.

https://doi.org/10.1029/2009JD012445
Werden, B.S., Giordano, M.R., Goetz, J.D., Islam, M.R., Bhave, P. V., Puppala, S.P., Rupakheti, M., Saikawa, E., Panday, A.K., Yokelson, R.J., Stone, E.A., DeCarlo, P.F., 2022. Pre-monsoon submicron aerosol composition and source contribution in the Kathmandu Valley, Nepal. Environ. Sci. Atmos. 2, 978–999. https://doi.org/10.1039/d2ea00008c.
Weimer, S., Alfarra, M.R., Schreiber, D., Mohr, M., Prévôt, A.S.H., Baltensperger, U., 2008. Organic aerosol mass spectral signatures from wood-burning emissions: Influence of burning conditions and type. J. Geophys. Res. Atmos. 113, 1–10. https://doi.org/10.1029/2007JD009309
Weingartner, E., Saathoff, H., Schnaiter, M., Streit, N., Bitnar, B., Baltensperger, U., 2003. Absorption of light by soot particles: Determination of the absorption coefficient by means of aethalometers. J. Aerosol Sci. 34, 1445–1463. https://doi.org/10.1016/S0021-8502(03)00359-8
Werf, G. R. V. D., Randerson, J.T., Giglio, L., Collatz, G.J., Mu, M., Kasibhatla, P.S., Morton, D.C., Defries, R.S., Jin, Y., Van Leeuwen, T.T., 2010. Global fire emissions and the contribution of deforestation, savanna, forest, agricultural, and peat fires (1997-2009). Atmos. Chem. Phys. 10, 11707–11735. https://doi.org/10.5194/acp-10-11707-2010
Winiwarter, W., Bauer, H., Caseiro, A., Puxbaum, H., 2009. Quantifying emissions of primary biological aerosol particle mass in Europe. Atmos. Environ. 43, 1403–1409. https://doi.org/10.1016/j.atmosenv.2008.01.037
Wu, C., Wang, G., Li, Jin, Li, Jianjun, Cao, C., Ge, S., Xie, Y., Chen, J., Li, X., Xue, G., Wang, X., Zhao, Z., Cao, F., 2020. The characteristics of atmospheric brown carbon in Xi'an, inland China: Sources, size distributions and optical properties. Atmos. Chem. Phys. 20, 2017–2030. https://doi.org/10.5194/acp-20-2017-2020
Wu, Y., Zhao, Y., Qi, Y., Li, J., Hou, Y., Hao, H., Xiao, N., Zhi, Q., 2023. Characteristics, Source and Risk Assessment of Soil Polycyclic Aromatic Hydrocarbons around Oil Wells in the Yellow River Delta, China. Water (Switzerland) 15. https://doi.org/10.3390/w15183324
Xie, C., Xu, W., Wang, J., Wang, Q., Liu, D., Tang, G., Chen, P., Du, W., Zhao, J., Zhang, Y., Zhou, W., Han, T., Bian, Q., Li, J., Fu, P., Wang, Z., Ge, X., Allan, J., Coe, H., Sun, Y. (2019). Vertical characterization of aerosol optical properties and brown carbon in winter in urban Beijing. *Atmos. Chem. Phys.*, 19, 165–179. https://doi.org/10.5194/acp-19-165-2019.
Xu, M., Yu, D., Yao, H., Liu, X., Qiao, Y., 2011. Coal combustion-generated aerosols: Formation and properties. Proc. Combust. Inst. 33, 1681–1697. https://doi.org/10.1016/j.proci.2010.09.014
Yan, J., Wang, X., Gong, P., Wang, C., Cong, Z., 2018. Review of brown carbon

aerosols: Recent progress and perspectives. Sci. Total Environ. 634, 1475–1485. https://doi.org/10.1016/j.scitotenv.2018.04.083

Yang, M., Howell, S.G., Zhuang, J., Huebert, B.J. (2009). Attribution of aerosol light absorption to black carbon, brown carbon, and dust in China. *Atmos. Chem. Phys.*, 9, 2035–2050. https://doi.org/10.5194/acp-9-2035-2009.

Yazdi, D.S. khoshnevis, Shakouri, D.B., 2010. The Effects of Climate Change on Aquaculture. Int. J. Environ. Sci. Dev. 1, 378–382. https://doi.org/10.7763/ijesd.2010.v1.73

Yoo, H., Wu, L., Geng, H., Ro, C.U., 2024. Physicochemical and temporal characteristics of individual atmospheric aerosol particles in urban Seoul during KORUS-AQ campaign: insights from single-particle analysis. Atmos. Chem. Phys. 24, 853–867. https://doi.org/10.5194/acp-24-853-2024

Yuan, T., Remer, L.A., Pickering, K.E., Yu, H., 2011. Observational evidence of aerosol enhancement of lightning activity and convective invigoration. Geophys. Res. Lett. 38. https://doi.org/10.1029/2010GL046052

Zárate, .D.O. I., Ezcurra, A., Lacaux, J.P., Van Dinh, P., Díaz de Argandoña, J.D., 2005. Pollution by cereal waste burning in Spain. Atmos. Res. 73, 161–170. https://doi.org/10.1016/j.atmosres.2004.07.006

Zeuthen, J.H., Pedersen, A.J., Hansen, J., Frandsen, F.J., Livbjerg, H., Riber, C., Astrup, T., 2007. Combustion aerosols from municipal waste incineration - Effect of fuel feedstock and plant operation. Combust. Sci. Technol. 179, 2171–2198. https://doi.org/10.1080/00102200701386180

Zhang, A., Wang, Y., Zhang, Y., Weber, R.J., Song, Y., Ke, Z., Zou, Y., 2020. Modeling the global radiative effect of brown carbon: A potentially larger heating source in the tropical free troposphere than black carbon. Atmos. Chem. Phys. 20, 1901–1920. https://doi.org/10.5194/acp-20-1901-2020

Zhang, Q., Jimenez, J.L., Canagaratna, M.R., Ulbrich, I.M., Ng, N.L., Worsnop, D.R., Sun, Y., 2011. Understanding atmospheric organic aerosols via factor analysis of aerosol mass spectrometry: A review. Anal. Bioanal. Chem. 401, 3045–3067. https://doi.org/10.1007/s00216-011-5355-y

Zhang, X., Yang, Y., Huang, G., Chen, B., Chen, Y., Zhao, J.R., Sun, H.J., 2022. of China.

Zhang, Y., Wang, X., Chen, H., Yang, X., Chen, J., Allen, J.O., 2009. Source apportionment of lead-containing aerosol particles in Shanghai using single particle mass spectrometry. Chemosphere 74, 501–507. https://doi.org/10.1016/j.chemosphere.2008.10.004

Zhang, Y., Albinet, A., Petit, J.E., Jacob, V., Chevrier, F., Gille, G., Pontet, S., Chretien, E., Dominik-Segue, M., Levigoureux, G., Mocnik, G., Gros, V., Jaffrezo, J.L., Favez, O. (2020). Substantial brown carbon emissions from wintertime residential wood burning over France. *Sci. Total Environ.*, 743,

140752. https://doi.org/10.1016/j.scitotenv.2020.140752.

Zhao, H.Y., Zhang, Q., Guan, D.B., Davis, S.J., Liu, Z., Huo, H., Lin, J.T., Liu, W.D., He, K.B., 2015. Assessment of China's virtual air pollution transport embodied in trade by using a consumption-based emission inventory. Atmos. Chem. Phys. 15, 5443–5456. https://doi.org/10.5194/acp-15-5443-2015

Zhao, X., Liu, X., Phillips, V.T.J., Patade, S., 2021. Impacts of secondary ice production on Arctic mixed-phase clouds based on ARM observations and CAM6 single-column model simulations. Atmos. Chem. Phys. 21, 5685–5703. https://doi.org/10.5194/acp-21-5685-2021

Zhou, S., Collier, S., Jaffe, D.A., Briggs, N.L., Hee, J., Iii, A.J.S., Kleinman, L., Onasch, T.B., Zhang, Q., 2017. Regional influence of wildfires on aerosol chemistry in the western US and insights into atmospheric aging of biomass burning organic aerosol. Atmos. Chem. Phys. 17, 2477–2493. https://doi.org/10.5194/acp-17-2477-2017

Zhu, S., Zhou, M., Qiao, L., Huang, D.D., Wang, Qiongqiong, Wang, S., Gao, Y., Jing, S., Wang, Qian, Wang, H., Chen, C., Huang, C., Yu, J.Z., 2023. Evolution and chemical characteristics of organic aerosols during wintertime PM2.5 episodes in Shanghai, China: insights gained from online measurements of organic molecular markers. Atmos. Chem. Phys. 23, 7551–7568. https://doi.org/10.5194/acp-23-7551-2023

Zotter, P., Herich, H., Gysel, M., El-Haddad, I., Zhang, Y., Mocnik, G., Hüglin, C., Baltensperger, U., Szidat, S., Prévôt, A.S.H., 2017. Evaluation of the absorption Ångström exponents for traffic and wood burning in the Aethalometer-based source apportionment using radiocarbon measurements of ambient aerosol. Atmos. Chem. Phys. 17, 4229–4249. https://doi.org/10.5194/acp-17-4229-2017

Zou, C., Wang, J., Hu, K., Li, J., Yu, C., Zhu, F., Huang, H., 2022. Distribution Characteristics and Source Apportionment of Winter Carbonaceous Aerosols in a Rural Area in Shandong, China. Atmosphere (Basel). 13. https://doi.org/10.3390/atmos13111858

ANNEXES /PRIEDAI

ACKNOWLEDGMENTS / PADĖKA

I am very grateful to my doctoral supervisor Dr. Kristina Plauškaitė-Šukienė, for her utmost support at all stages. It has been a very productive experience to work as her team member. She taught me not just new scientific methods but also how to be a good researcher, how to ask questions and how to keep looking for the right answers. I am also grateful to Dr. Steigvilė Byčenkienė for accepting me to join the Department of Environmental Research.

I thank the entire staff at the Department of Environmental Research, particularly Dr. Julija Pauraitė-Dudek and Dr. Vadimas Dudoitis for their help and guidance. I also offer my deepest gratitude to all members of Dissertation Defence Panel: Dr. Evaldas Maceika, Dr. Galina Lujanienė, Dr. Pauli J. Paasonen, Dr. Rita Plukienė, and Dr. Vaida Šerevičienė, for carefully reviewing this thesis and for their valuable suggestions that significantly improved the quality of the work.

I am grateful to Dr. Pauli Paasonen and Prof. Mikael Ehn for their fruitful teaching and supervision during my research visit at INAR, University of Helsinki. I would also like to acknowledge Prof. Tuukka Petäjä and Mr. Sujai Banerji from university of Helsinki for their help and support at, INAR University of Helsinki.

I thank my teammates Dr. Audrė Kalinauskaitė and Kamilė Kandrotaitė for their interest in my research and a dedicated work. It was a team work that enabled a contribution to the field. I also thank Dr. Simonas Kecorius, Dr. Leizel Madueño, Alfred Wiedensohler (TROPOS, Leipzig, Germany), Dr. Edgar A. Vallard, and Dr. Maria Cecilia D. Galvezd (ARCHERS, CENSER, De La Salle University, Philippines) for their support.

I dedicate my thesis to my parents Mr. Pervaiz Gill and Mrs. Agnus Venus, and to all my teachers who educated and inspired me, particularly Prof. Janne Jänis from university of Eastern Finland, Prof. Peter O'Connor from University of Warwick (England), Prof. Peter Novak from Charles university (Czech Republic), Dr. Johann FAR from Liège university (Belgium) and Prof. Christy Munir from Forman Christian University (Pakistan).

I extend my respect and regards to my family, particularly to my elder sisters, Beenish Gill, Munazza Gill, and Saba Gill, who supported me during times of hardship. I am also highly grateful to all my friends and colleagues who are always a great source of encouragement for me.

CURRICULUM VITAE

Touqeer Gill

11-12-1992, Lahore, Pakistan

Education:

Department of Chemistry, *2011-2015*
Forman Christian College, A Chartered University, Lahore, Pakistan

Bachelor of Science in Chemistry

Department of Chemistry *2016-2018*
University of Eastern Finland, Joensuu, Finland

Master's Degree Programme for Research Chemists

Department of Environmental Studies *2020-2024*
Cetner for Physical Sciences and Technology (FTMC), Lithuania

PhD studies

Professional career:

Department of Environmental Studies *2024-2025*
Cetner for Physical Sciences and Technology (FTMC), Lithuania

Junior researcher

FOR NOTES

FOR NOTES

FOR NOTES

FOR NOTES

1. Vilnius University Press
9 Saulėtekio Ave., Building III, LT-10222 Vilnius
Email: info@leidykla.vu.lt, www.leidykla.vu.lt
bookshop.vu.lt, journals.vu.lt
2. Print run copies 22